Lawrence Berkeley National Laboratory
Recent Work

Title
ULTRACENTRIGUGE PHOTOELECTRIC SCANNER, MULTIPLE CELL

Permalink
https://escholarship.org/uc/item/94t2b5d3

Author
Lamers, Kenneth W.

Publication Date
1965-04-01

eScholarship.org Powered by the California Digital Library
University of California

UCRL-11623

University of California

Ernest O. Lawrence Radiation Laboratory

TWO-WEEK LOAN COPY

This is a Library Circulating Copy which may be borrowed for two weeks. For a personal retention copy, call Tech. Info. Division, Ext. 5545

ULTRACENTRIFUGE PHOTOELECTRIC SCANNER, MULTIPLE CELL

Berkeley, California

DISCLAIMER

This document was prepared as an account of work sponsored by the United States Government. While this document is believed to contain correct information, neither the United States Government nor any agency thereof, nor the Regents of the University of California, nor any of their employees, makes any warranty, express or implied, or assumes any legal responsibility for the accuracy, completeness, or usefulness of any information, apparatus, product, or process disclosed, or represents that its use would not infringe privately owned rights. Reference herein to any specific commercial product, process, or service by its trade name, trademark, manufacturer, or otherwise, does not necessarily constitute or imply its endorsement, recommendation, or favoring by the United States Government or any agency thereof, or the Regents of the University of California. The views and opinions of authors expressed herein do not necessarily state or reflect those of the United States Government or any agency thereof or the Regents of the University of California.

Research and Development

UCRL-11623
UC-37 Instruments
TID-4500 (39th Ed.)

UNIVERSITY OF CALIFORNIA

Lawrence Radiation Laboratory
Berkeley, California

AEC Contract No. W-7405-eng-48

ULTRACENTRIFUGE PHOTOELECTRIC SCANNER, MULTIPLE CELL

Kenneth W. Lamers

April 1, 1965

Printed in USA. Price $4.00. Available from the Clearinghouse for Federal Scientific and Technical Information, National Bureau of Standards, U. S. Department of Commerce, Springfield, Virginia.

ULTRACENTRIFUGE PHOTOELECTRIC SCANNER, MULTIPLE CELL

Contents

List of Abbreviated Captions for Illustrations. v

Abstract ix

I. Introduction 1

II. General Considerations 4

III. System Description

A. Switching Relationships 8
1. Two Double-Sector Cells 8
2. One Double-Sector Cell 17
3. Two Single-Sector Cells 17
B. Reference-Pulse Regulator 21
C. Calibrator 21
D. Derivative 24
E. Scan Control 24
F. Recorder 24
G. Illustrations 25

IV. Circuit Description

A. Switching 36
1. Two Double-Sector Cells 36
2. One Double-Sector Cell 36
3. Two Single-Sector Cells 36
B. Gates and Switches 38
C. Holding Circuits 39
D. Bootstrap Amplifiers 40
E. Calibrator 40
F. Reference-Pulse Regulator 40
G. Differentiator 43
H. Set-Pulse Amplifier 43
I. Marker Generator 43
J. Scan Control, Manual 44
K. Scan Control, Automatic 46
L. Scan-Speed Selector 48
M. Galvanometer Selector, Two Ultracentrifuges 48

V. Operation

A. Two Double-Sector Cells 51
B. Double-Sector Operation, One Cell 52
C. Single-Sector Operation, Two Cells 52
D. Calibration 52
E. Derivative Operation 53
F. Crosschecks 53
G. Anomalies 56

VI. Maintenance Adjustments

A. Pair and Cell Gates 60
B. Regulating Gate 60
C. Holding Circuits 60
D. Bootstrap Amplifiers, Bias 61
E. Set-Pulse Adjustments 61

VII. Performance

A. Visicorder Traces 63
B. Oscilloscope Photographs 63
C. Calibration Curves 75
D. Improvements 75
E. Applications 78

VIII. Future Considerations 79

Acknowledgments 80

Appendices

A. Derivations 81
B. Schematics and Index 88
C. Tables of Switching Properties and Frequency Characteristics 107
D. Pulse Relationships Shown by Oscilloscope Photographs . . . 114
1. Two Double-Sector Cells 114
2. Two Single-Sector Cells 117

References and Footnotes 119

LIST OF ABBREVIATED CAPTIONS FOR ILLUSTRATIONS

Fig. 1. Rotor with two double-sector cells.

Fig. 2. Rotor with one double-sector cell.

Fig. 3. Rotor with two single-sector cells.

Fig. 4. Pulse train, two double-sector cells, air space.

Fig. 5. Rotor, one cell masked.

Fig. 6. Pulse train, one cell masked.

Fig. 7. Block diagram, modified system.

Fig. 8. Block diagram, previous to modification.

Fig. 9. Photomultiplier pulses, two double-sector cells, scanner at several positions.

Fig. 10. Photomultiplier pulses, one double-sector cell, scanner at four positions.

Fig. 11. Pulse relationships, two double-sector cells, ideal case.

Fig. 12. Pulse relationships, two double-sector cells, corrective action.

Fig. 13. Pulse relationships, two double-sector cells, radius marker.

Fig. 14. Pulse relationships, one double-sector cell.

Fig. 15. Pulse train, two single-sector cells.

Fig. 16. Pulse relationships, two single-sector cells.

Fig. 17. Pulse relationships, two single-sector cells, radius marker.

Fig. 18. Photograph of ultracentrifuge.

Fig. 19. Scanner and stationary photomultiplier in centrifuge.

Fig. 20. Scanning mechanism removed.

Fig. 21. Scanning mechanism, disassembled.

Fig. 22. Mirror, stationary photomultiplier.

Fig. 23. Set-pulse amplifier.

Fig. 24. Control console.

Fig. 25. Operational unit, front view.

Fig. 26. Operational unit, front view. Top panel off.

Fig. 27. Operational unit, top front view.

Fig. 28. Operational unit, top view.

Fig. 29. Operational unit, rear view.

Fig. 30. Operational unit, bottom view.

Fig. 31. Operational unit, switch and gate modules.

Fig. 32. Functional block diagram.

Fig. 33. Graph, calibrate dial versus optical density.

Fig. 34. Scan control, simplified schematic, manual.

Fig. 35. Scan control, simplified schematic, automatic.

Fig. 36. Transmission, gear arrangements.

Fig. 37. Visicorder traces, derivative.

Fig. 38. Visicorder traces, scattered light.

Fig. 39. Oscilloscope traces, scattered light, log pulses.

Fig. 40. Oscilloscope traces, scattered light, reference hold.

Fig. 41. Visicorder traces, two double-sector cells.

Fig. 42. Visicorder traces, light source pulsing.

Fig. 43. Visicorder traces, compensation, nonuniform illumination.

Fig. 44. Visicorder traces, regulator performance.

Fig. 45. Oscilloscope traces, pulse separation.

Fig. 46. Oscilloscope traces, switching time.

Fig. 47. Oscilloscope traces, reference and sample-pair gates.

Fig. 48. Oscilloscope traces, sample-hold charging time.

Fig. 49. Oscilloscope traces, sample-hold discharge time.

Fig. 50. Oscilloscope traces, log pulses.

Fig. 51. Graph, log-compressor response.

Fig. 52. Graph, Visicorder deflection versus reference amplitude, non switching.

Fig. 53. Graph, Visicorder deflection versus optical density.

Fig. 54. Optical system, simplified diagram for derivation.

Fig. 55. Schematic, operational unit, trouble shooting.

Fig. 56. Schematic, scanning photomultiplier.

Fig. 57. Schematic, linear amplifier and clamp.

Fig. 58. Schematic, log amplifier.

Fig. 59. Schematic, gate drivers and calibrator.

Fig. 60. Schematic, pulse separators.

Fig. 61. Schematic, holding circuits, bootstrap and derivative amplifiers.

Fig. 62. Schematic, gating chain.

Fig. 63. Schematic, reference-pulse regulator.

Fig. 64. Schematic, stationary photomultiplier.

Fig. 65. Schematic, set-pulse amplifier.

Fig. 66. Schematic, marker generator.

Fig. 67. Schematic, scan control.

Fig. 68. Schematic, scan-speed selector.

Fig. 69. Schematic, galvanometer selector, two centrifuges.

Fig. 70. Schematic, operational unit power supply.

Fig. 71. Schematic, log compressor power supply.

Fig. 72. Schematic, scanning-photomultiplier power supply.

Fig. 73. Oscilloscope traces, two double sectors, flip-flop, one-shot, and switches; cell selector at 1.

Fig. 74. Oscilloscope traces, same as Fig. 73 except cell at 2.

Fig. 75. Oscilloscope traces, two double sectors, holding circuits, cell at 1 and 2.

Fig. 76. Oscilloscope traces, two double sectors, delay uni and one-shot versus RPM control setting.

Fig. 77. Oscilloscope traces, two double sectors, scanner at radius marker, flip-flop, one-shot, and switches; cell at 1.

Fig. 78. Oscilloscope traces, same as Fig. 77 except cell at 2.

Fig. 79. Oscilloscope traces, two single-sector cells, flip-flop, one-shot, and holding circuits.

Fig. 80. Oscilloscope traces, two single-sector cells, switches.

Fig. 81. Oscilloscope traces, two single-sector cells, SO-4 and flip-flop.

Fig. 82. Oscilloscope traces, two single-sector cells, linear amplifier, SO-1, and one-shot.

Fig. 83. Oscilloscope traces, two single-sector cells, linear amplifier, SO-1, and delay uni.

Fig. 84. Oscilloscope traces, two single-sector cells, delay uni versus RPM control setting.

ULTRACENTRIFUGE PHOTOELECTRIC SCANNER, MULTIPLE CELL

Kenneth W. Lamers

Lawrence Radiation Laboratory
University of California
Berkeley, California

April 1, 1965

ABSTRACT

This report describes the modifications for conversion of an electromechanical scanner to multiple-cell operation and doubles as an instruction manual. The scanner is used for displaying optical density changes that take place when a light-absorbing material such as virus, protein, or nucleic acid is sedimenting in the centrifugal field of an ultracentrifuge--that is, a high-speed centrifuge employing an optical system. These materials absorb some of the light transmitted by the optical system, thereby projecting a pulsating image that varies in intensity with distance from the center of rotation. This image is scanned by a photomultiplier and compared with the pulsating image of a reference cell in order to compensate for nonuniform illumination and other optical imperfections. Circuitry separates the reference and sample pulses, subtracts their logarithmic equivalents, and displays the subtraction on a chart recorder. The chart moves in synchronism with the scanner, and optical density (concentration) is therefore displayed as a function of radius.

The system includes additional features such as: (a) an internal calibration that permits measurements of absolute density; (b) a monochromator to facilitate spectral analysis, a powerful tool for disclosing the radial distribution of components responsive to different wavelengths; and (c) derivative of the function, which is displayed in time coincidence.

The system described is an improved version of an earlier model in that it is designed (a) for two double-sector cells separated 180 deg, with sector separation 2.5 deg at each cell, or (b) for two single-sector cells, also separated 180 deg. Single-sector cells are 4-deg; this permits longer slits and increases illumination proportionately. Other modifications improve basic performance over that of the earlier version.

I. INTRODUCTION

An ultracentrifuge is a high-speed centrifuge employing an optical system.[1] In our application it is used for displaying optical density changes that take place when light-absorbing material such as virus, protein, or nucleic acid is sedimenting in a centrifugal field.

This paper describes the modifications to an earlier photoelectric scanning system developed for ultracentrifuge studies. In particular, it concerns modifications by which the earlier version[2] is converted to multiple-cell operation; it also describes other improvements. This report doubles as an instruction manual, and for this reason repeats some of the information given in the preceding report.[2] The system described herein is designed for two double-sector cells separated 180 deg, as shown in Fig. 1. Each sector is 2 deg, and is separated approximately 2.5 deg from the other sector in the cell. It is possible to operate with only one double-sector cell, as shown in Fig. 2.

The system is also designed for two cells, each containing one 4-deg sector. The cells are separated 180 deg, as shown in Fig. 3. Larger sectors and greater separation permit use of a longer scanning slit,[3] which provides more illumination and a consequent improvement in the signal-to-noise ratio.

When the instrument is operated double-sector, each cell contains a reference and a sample sector, separated 2.5 deg and enclosed by a common cell window (Fig. 1). The reference sectors compensate for such optical imperfections as nonuniform illumination or dirty lenses. This compensation provides continuous correction, an important feature since the lenses become coated with oil deposits from the centrifuge drive. Cell windows are less susceptible than the lenses to deposits but are cleaned prior to each run, whereas the lenses are not.

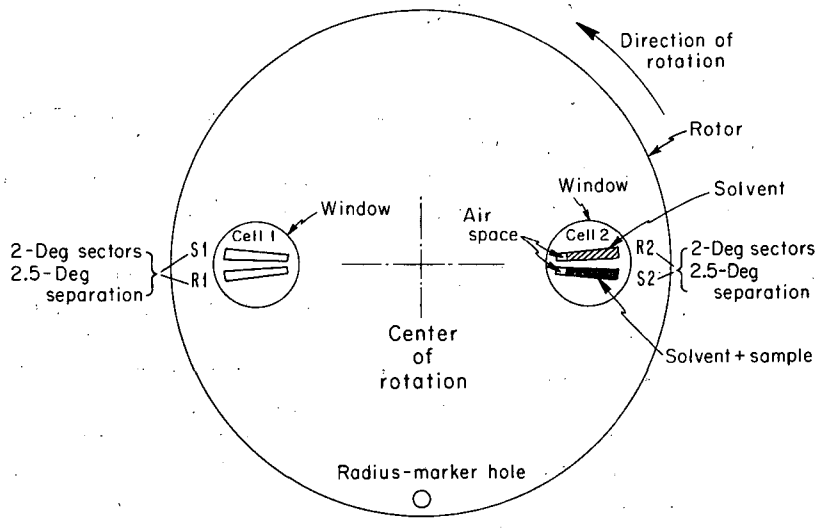

Top view of rotor

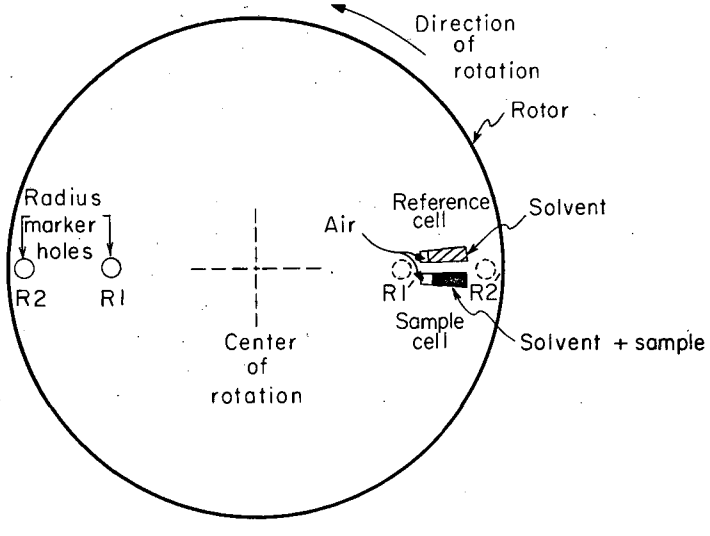

MUB-6301

Fig. 1. Top view of rotor with two double-sector cells. As the cells are not filled completely, an air space forms at the inner radii. Cell 1 is filled in the same manner, usually with a sample of different density. The radius-marker hole is located as shown.

Fig. 2. Top view of rotor with one double-sector cell. The radius-marker hole shown in Fig. 1 is plugged, and one cell is replaced by a counterbalance with two radius-marker holes. (The radius-marker holes are not covered by a window). R1' and R2' are nonexistent; they are included to indicate that the radius-marker images straddle the cell images when the rotor turns one-half revolution.

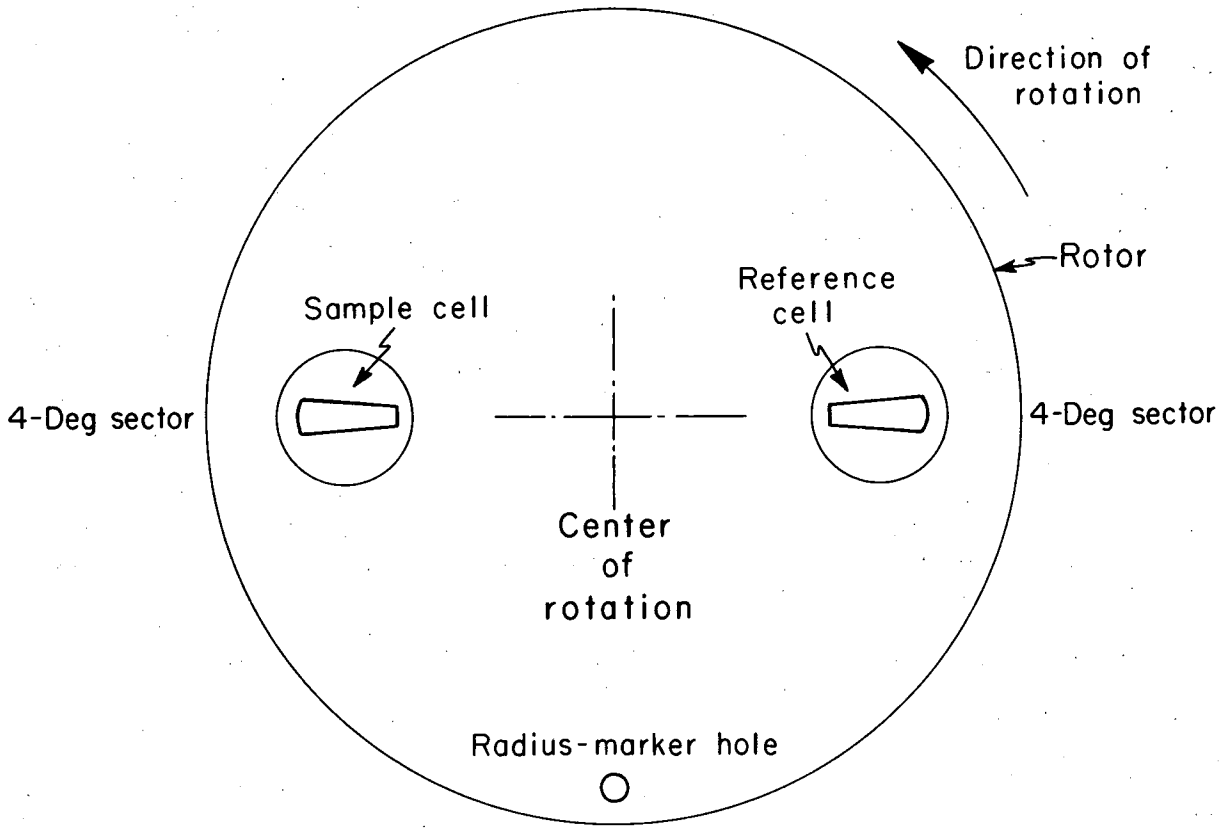

MUB-4723

Fig. 3. Top view of rotor with two single-sector cells. The sectors are large (4 deg instead of 2 deg) and are separated by 180 deg. Each sector enclosed by a different window.

II. GENERAL CONSIDERATIONS

In order for us to understand the requirements for converting from single-cell to multiple-cell operation, it is important that we visualize the images projected by the optical system. Five discrete images are projected; each image is pulsating with time, and time-interlaced with the other four images. The five images represent the four cell sectors and the radius-marker hole, as shown in Fig. 1. Each image, although present less than 1% of the time, must be separated, processed, and recombined with other images to form the profile of interest. A typical pulse train when the air space is scanned (Fig. 1) is shown in Fig. 4. Although nothing in this pulse train distinguishes one pulse pair from another, it is necessary that each pulse be identified with the sector producing it. The earlier system was required to differentiate between reference and sample sectors of only one cell. This was comparatively simple because of asymmetry at the rotor (see Fig. 2).

In contrast, multiple-cell symmetry demands that additional information be supplied to the switching circuits. One approach (not used) is to synchronize the scanning mechanism with the rotor. If the cells are loaded with regard to rotation, it is possible to ascribe each impulse to a given sector. (As shown in Fig. 1, "loaded with respect to rotation" means that the pulse from the solvent precedes the pulse from the solvent-plus-sample.) For example, the first pulse pair would always be due to cell 1, the second to cell 2. On that basis, all odd-numbered pairs could be attributed to the first cell, all even-numbered to the second. The time interval between pulse pairs is very short at high speeds, however (500 μsec at 60 000 rpm), and since the scanner moves very slowly it is not practical to synchronize the scanner with the rotor.

Since scanner-rotor synchronization is impractical, we might consider covering part of the window of one cell as shown in Fig. 5. When this is done the pulse train undergoes predictable changes as the scanner proceeds from the "Start" position. This is best explained by reference to Fig. 6. The initial part of the scan comprises pulse pairs from cell 2 only, so there is only one pair per revolution. As the scanner moves from the masked to the unmasked regions, the appearance of additional pulses from the second cell reduces the time interval between pairs to one-half the initial value. The latter relationship, two pairs per revolution, exists for the major part of the remaining scan. The difference in dimensions between masked and unmasked windows is useful because it creates a transition (single to double pairs of pulses per revolution) that enables the system to determine when the input impulses have changed from cell 2 to cell 1. Synchronization can be derived from this transition, if desired, and offers one advantage: Synchronizing pulses can be derived from a single source, the scanning photomultiplier. Reliance upon the transition has disadvantages as well, the principal one's being the possibility of a totally erroneous scan that might result from a temporary disruption or reduction of pulses when a meniscus or other dark region is scanned. Because synchronization is effected in the transition region only, reliance is placed upon the continued

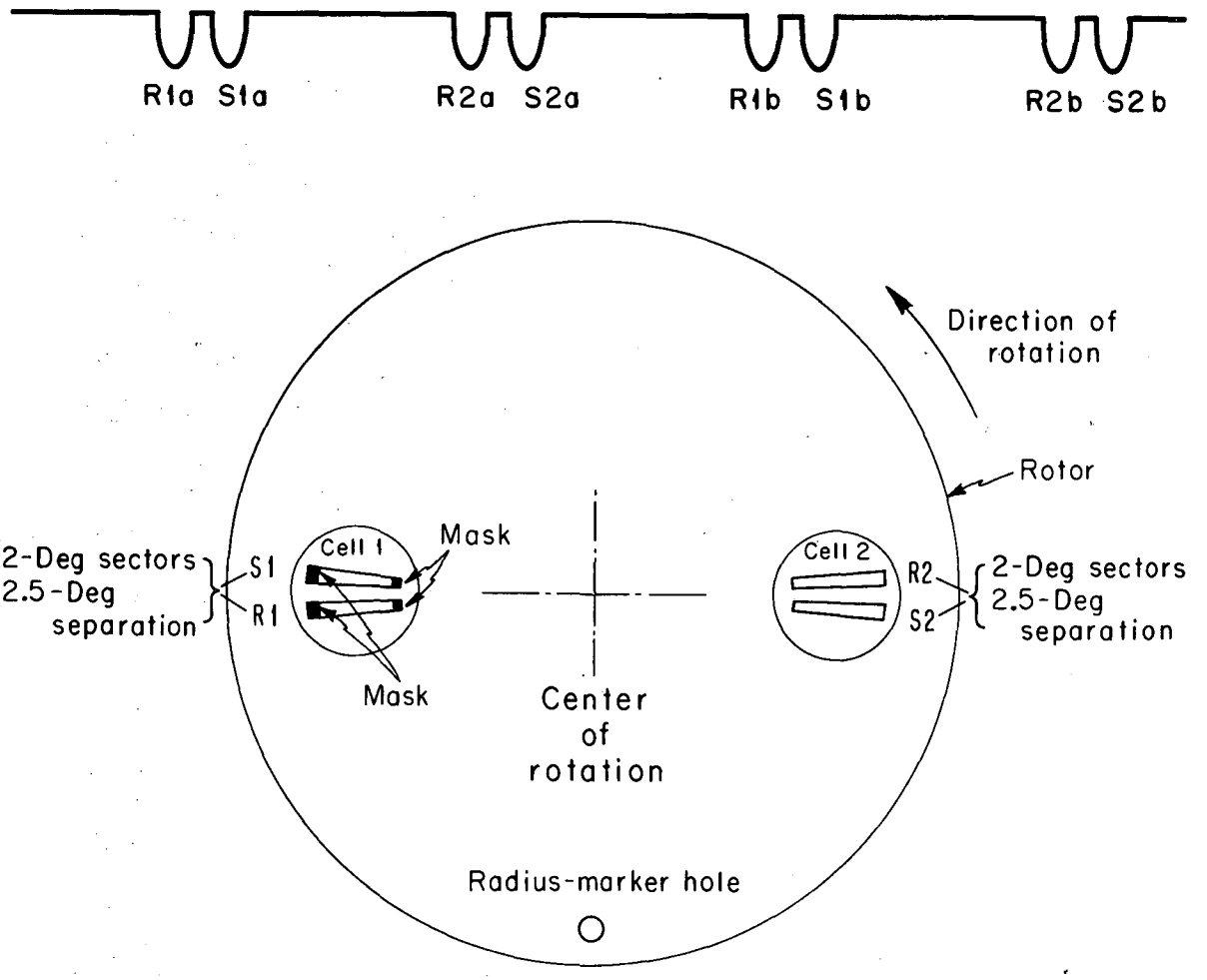

Fig. 4. A typical pulse train when the images projected by the air spaces (all four sectors) of two double-sector cells are scanned.

Fig. 5. Top view of rotor with part of one cell masked. This arrangement was considered, but rejected for reasons described in the text.

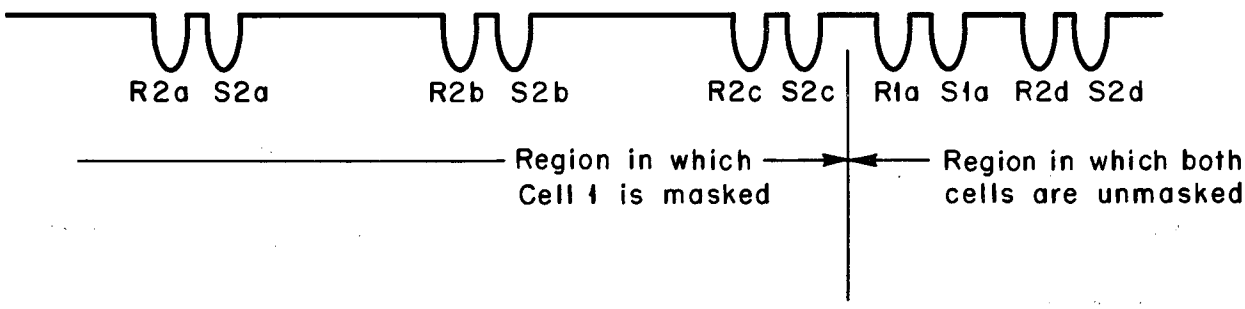

MUB-4726

Fig. 6. The pulse train expected if one were to mask part of Cell 1 as shown in Fig. 5. The masked region permits only one pulse-pair each revolution; the unmasked region permits two pairs.

presence of pulses. Another disadvantage of transition synchronizing is that it requires complex circuit logic.

In view of the above disadvantages, we chose to supplement pulses from the scanner with those from a stationary photomultiplier. The latter intercepts light pulses from a secondary optical system,[4] light that passes through the radius-marker hole in the rotor. These pulses (set pulses) confirm synchronization each revolution. This contrasts with the transition method for which synchronization is confirmed at a check point only.

III. SYSTEM DESCRIPTION

A. Switching Relationships

1. Two Double-Sector Cells

Figure 1 shows cell placement in the rotor when the system employs two double-sector cells. Figure 7 is a simplified diagram of our modified system. When compared to the previous version shown in Fig. 8, many features of the original system are shown to remain unchanged. This report emphasizes those features either unique to the modified system or not discussed in the preceding report. In both systems a photomultiplier with defining slit[5] scans the pulsating images at a constant speed.[6] It accepts light samples as the centrifuge makes them available, generating pulse amplitudes proportional to light intensity and slit area. Pulse duration is related to centrifuge speed, cell angle, and slit length.[7]

Pulses generated at the photomultiplier are shown in Fig. 9. These actual photographs of oscilloscope traces show duration, amplitude, and separation with the scanner stopped at several positions (see Fig. 1). In brief, the photomultiplier generates a pulse when the rotor makes light available. When scanning the cell images, the photomultiplier "sees" two quick light bursts, the first due to the reference sector of a given cell, the second to the sample sector.[8] The light bursts are followed by a quiescent period that is much longer than the time interval between "mates." This quiescent period corresponds to the time required for the rotor to turn 180 deg. At the end of that time two light bursts appear as before, but these are due to the second cell. The net result is alternating pulse pairs, first from one cell, then from the other.

Pulses do not always appear in pairs, however; the rotor includes a radius-marker hole, as shown in Fig. 1. This hole is displaced 90 deg from the center line between cells and is used as a reference for detecting motion within the cells. When the scanner is "observing" the radius-marker image, the rotor allows but one burst per revolution, as shown in Fig. 9(c). If the oscilloscope sweep speed is increased, the pulses due to one cell only are displayed, as illustrated by Fig. 10.

As discussed above, the radius-marker hole also chops a secondary optical system, one that is displaced 180 deg from the principal optical system (absorption). Rotor motion results in light bursts to the stationary photomultiplier (one burst each revolution), bursts that yield synchronizing pulses to supplement those from the scanner.

Assuming that scanner output is a train of pulses, we must decipher which sector is responsible for a given pulse. The first requirement of pulse-separation circuitry is that it route the pulses from each of the four sectors to a different holding circuit.[9] The second requirement is that it route the pulses from a given sector to the same holding circuit every time that the scanner moves across the images.

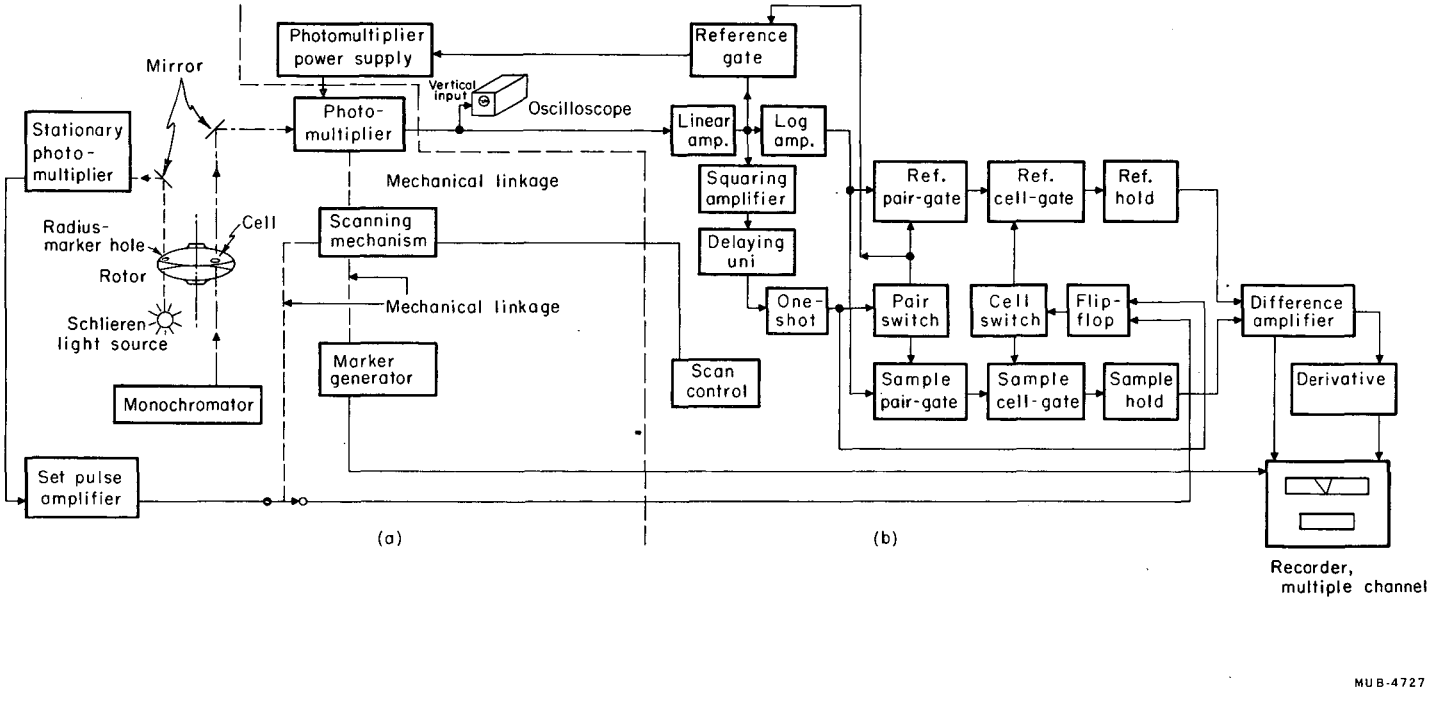

Fig. 7. Block diagram of the modified system showing the important electrical and mechanical components of the photoelectric scanner: (a) ultracentrifuge, and (b) control console. This illustration pertains to operation with two double-sector cells.

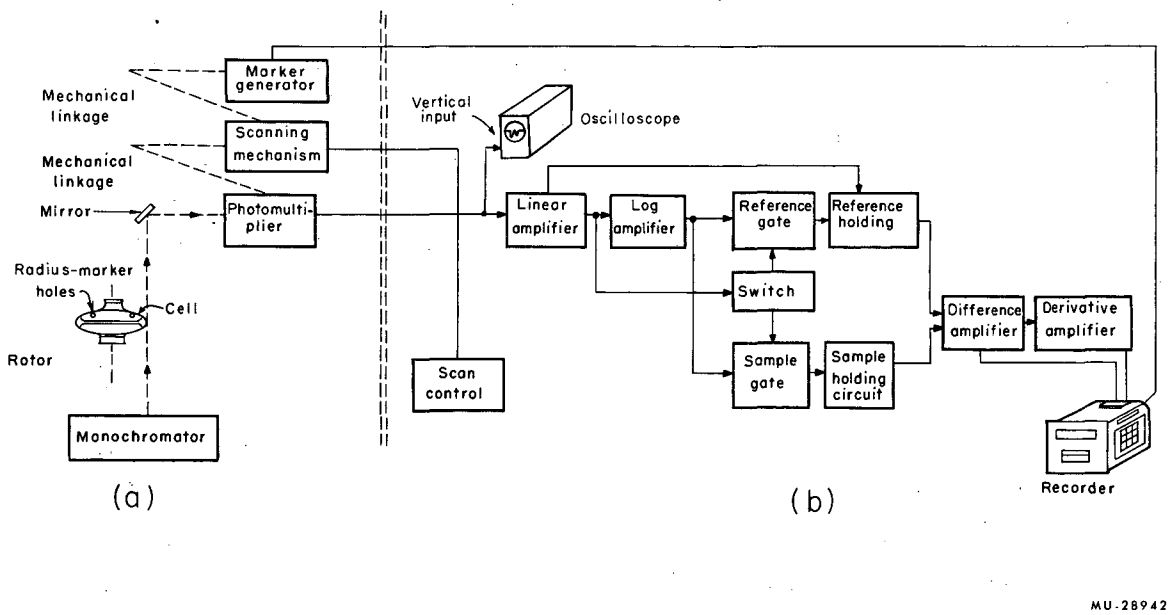

Fig. 8. Block diagram of the system previous to modification (a) ultracentrifuge, and (b) control console.

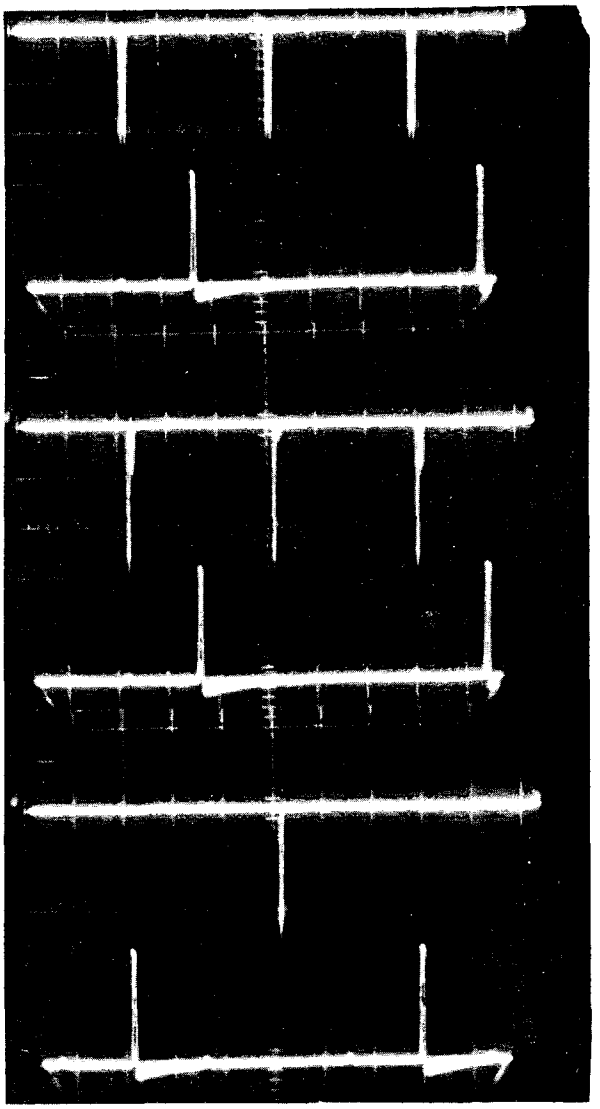

Fig. 9. Oscilloscope traces showing photomultiplier pulses with the scanner stopped at several positions (refer to Fig. 1). The rotor is loaded with two-double sector cells: (a) Scanner positioned to intercept the images projected by the air spaces of all four sectors. The lower pulses are set pulses from the stationary photomultiplier (Fig. 7), and they are due to the radius-marker hole, which permits only one light burst each revolution. (b) Scanner positioned to intercept the images projected by both solutions. One sample sector is filled with a solution of higher density than its counterpart. The lower pulses (set pulses) are for reference only. (c) Scanner positioned to intercept the image projected by the radius-marker hole. The lower pulses are set pulses.

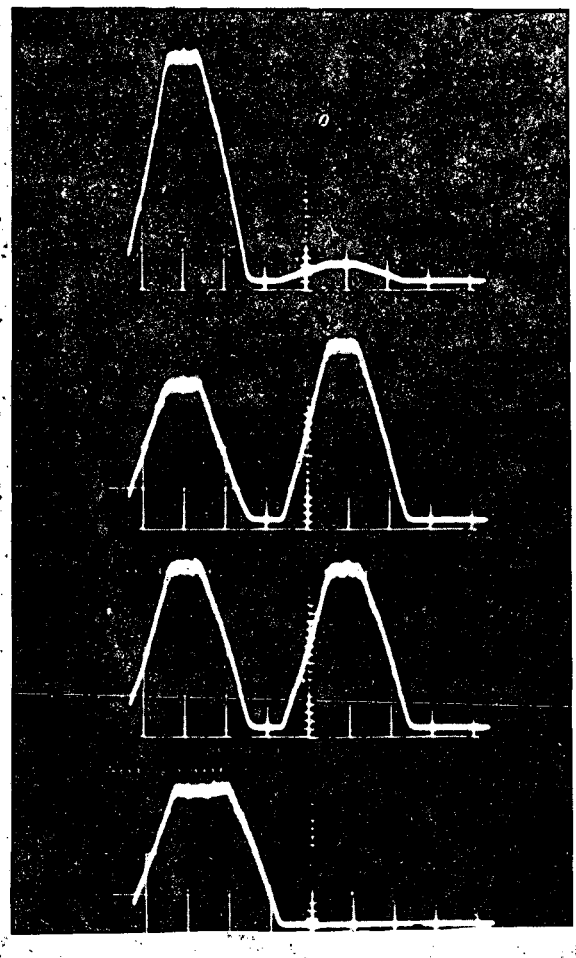

ZN-4849

Fig. 10. Oscilloscope traces (preceding modification) showing photomultiplier pulses (inverted) with the scanner stopped at various positions (Fig. 2). The rotor is loaded with one double-sector cell: (a) Scanner positioned to intercept the image projected by the solution. The first pulse is due to the reference-sector solvent, water; the second to the sample sector. (b) Scanner positioned to intercept the image projectd by the air-solvent boundary within the reference sector. The reference pulse is slightly attenuated by the meniscus. Sample pulse is not attenuated appreciably because light passes through the air space. (c) Scanner positioned to intercept the image projected by the air space of both sectors. As the window is common to both cells, each pulse is the same height. (d) Scanner positioned to intercept the image projected by the radius-marker hole R1. Pulse width is slightly longer and related to the diameter of R1. Photomultiplier "sees" only one light burst per revolution.

Holding circuits are necessary because reference and sample pulses do not occur simultaneously; the reference pulse must be stored for comparison with its "mate." Because the holding circuits are designed to respond to the peak level of each pulse, output levels are high and the effects of drift are minimized.

If the pulses due to each sector are to be routed to the appropriate hold, we need some method for sensing which cell (or the radius-marker hole) is responsible for a given pulse. There are several ways to correlate impulse with rotor position: (a) One is to use extraneous sensing elements for detecting rotor position. (b) Another is to use circuitry that acts upon pulses from the scanning photomultiplier only. The earlier version is based upon (b); the modified version combines both techniques. In short, switching is dictated partly by the scanner, partly by the stationary photomultiplier.

Assume for the moment that only the first requirement is to be satisfied, i. e., pulses from each sector are to be routed to a different hold. Assume further that photomultiplier pulses appear in the sequence indicated by Fig. 11. From previous experience we know that it is practical to separate "mates" by use of a one-shot.[10] The modified system is designed (Figs. 7 and 11) so that the reference-pair gate is open to the first pulse (which is from a reference sector). The trailing edge of each reference pulse activates the one-shot, closing the reference-pair gate for a specified length of time. The transition opens the sample-pair gate (previously closed) for the same period, permitting the following pulse (from the sample sector) to pass through. At normal operating speeds this time interval is comparatively short, permitting only one pulse through the sample-pair gate. Furthermore, the time duration of the one-shot pulse is short enough to ensure that a subsequent pulse passes through the sample-pair gate if, and only if, it is mated to the preceding pulse.

The first pulse is sometimes associated with a sample sector. Since the reference-pair gate is open, the first pulse inadvertently passes through it. This confusing condition is rectified when the one-shot returns to its original state, allows the following pulse to pass through the reference-pair gate. Since that pulse is produced by a reference sector, gating is restored to normal.

The one-shot has particular utility for this application because it has a built-in recovery time (determined by the length of its quasi-stable state) that prevents it from responding to consecutive pulses of a given pulse pair. This recovery time is effective in discriminating between "mates," but it does not discriminate between cells. Additional circuitry is required to ensure that every other pulse pair is routed identically. This indicates the need for a binary device, the flip-flop,[11] that presents a different set of conditions to alternate pulse pairs.

We next consider the gates operated by a one-shot and flip-flop. The system herein is designed so that each pulse must pass through two gates,[12] the first operated by a one-shot (pair gate), the second by a flip-flop (cell gate) as shown in Fig. 7. Either gate can be open or closed, so

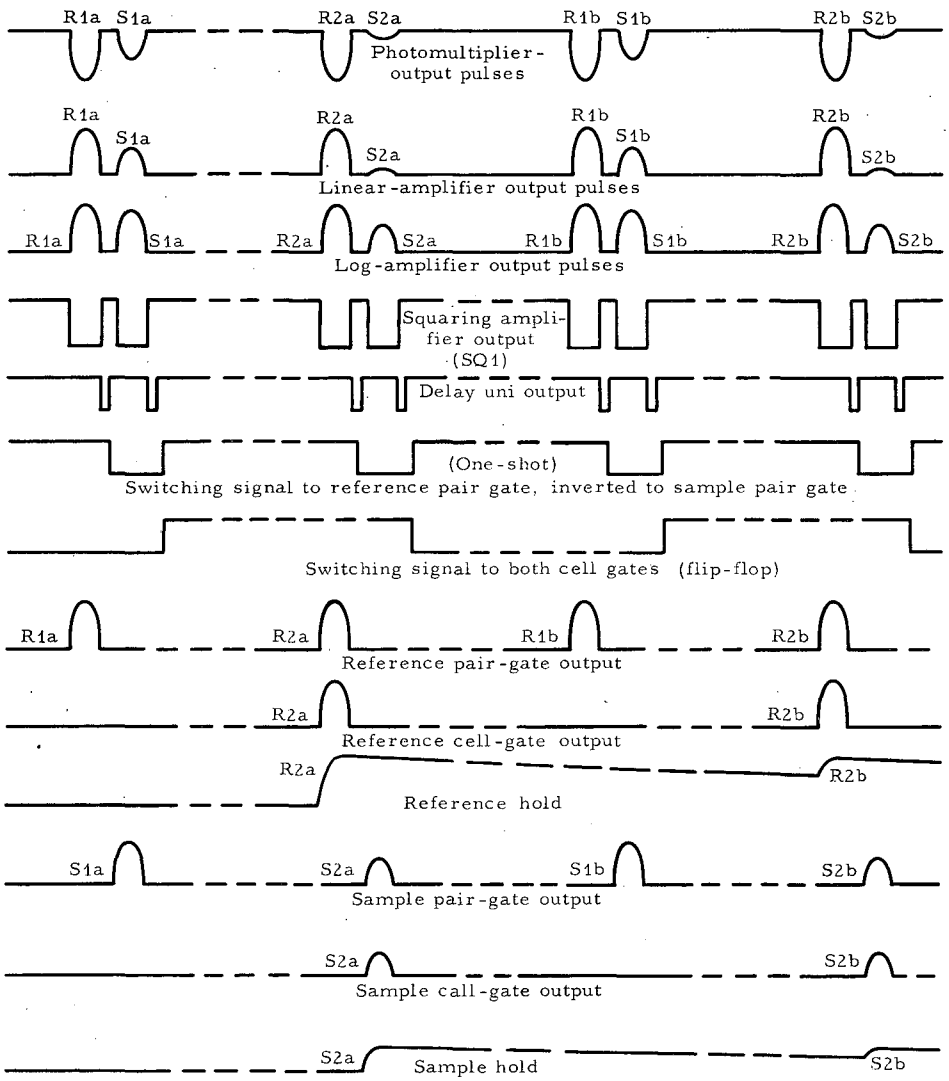

Fig. 11. Pulse relationships for two double-sector cells. The scanner is positioned to intercept the images projected by both solutions (Fig. 1). Each gate is open when its switching signal is at the higher level. This is an idealized case for which set pulses would not be required.

there are four possible states for a given pair of gates (a pair gate plus a cell gate). The trick is to drive each gate with a properly timed signal so that a given pair of gates is open only to the pulse that it is supposed to pass.

The one-shot is triggered by the trailing edge (delayed) of each reference pulse as shown in Fig. 11.[13] The flip-flop, in turn, is triggered by the trailing edge of each one-shot pulse. This triggering mode is important because no reliance is placed upon sample pulses, some of which are highly attenuated at large optical densities.

The pair gates, operated by the one-shot, are driven out of phase so that each input pulse passes through only one pair gate. The cell gates are operated by the flip-flop, which opens them in synchronism so that one cell gate passes the reference pulse and its counterpart passes the "mate."

If one wishes to record the image from the other cell, he changes the cell-selector switch accordingly. This inverts flip-flop phasing to both cell gates so that they transmit the alternate pulse pairs.

Referring again to Fig. 11, we see that the pulse relationship illustrated is a special case, i.e., we assume that the first pulse finds the flip-flop in its low-level state. We further assume that the first pulse pair is due to cell 1. This is not necessarily true in practice. The first pulse can come from any of four sectors--which sector is dependent upon the position of the rotor when the scanner intercepts the first pulse. Because these assumptions are not necessarily true, we may get an erroneous routing. In order to obviate that possibility, synchronizing signals from the stationary photomultiplier (set pulses) are applied to the flip-flop to ensure that it is in the proper state relative to the sector under observation.

Set pulses do not usually change flip-flop status. In most cases they merely confirm it, applying corrective action if necessary. Figure 12 illustrates correction when pulses arrive with the flip-flop in an improper state. The first pulse pair, R2a and S2a, is not permitted through the cell gates even though the cell-selector switch has been set for cell 2. The following pulses, R1a and S1a, pass erroneously through the cell gates (reference and sample). In the absence of set pulses, all subsequent pulses admitted to the holding circuits would be due to cell 1. This erroneous routing would occur even though one had selected cell 2 for observation. This, perhaps, would be tolerable if one could turn the cell-selector switch to cell 1 and record the alternate cell. That, however, is not practical. Subsequent scans sometimes "find" a different pulse relationship, and routing becomes erroneous again. Without set pulses the recorded traces vacillate between cells, recording the desired cell only by chance. For a single scan only, a loss of triggering (due to factors such as meniscus and light fluctuations) could cause the recorded output to switch, some parts of the trace representing one cell, other parts another. Set pulses preclude both possibilities.

Refer again to Fig. 12, for which corrective action is as follows: The first set pulse finds the flip-flop in its low-level state. This is

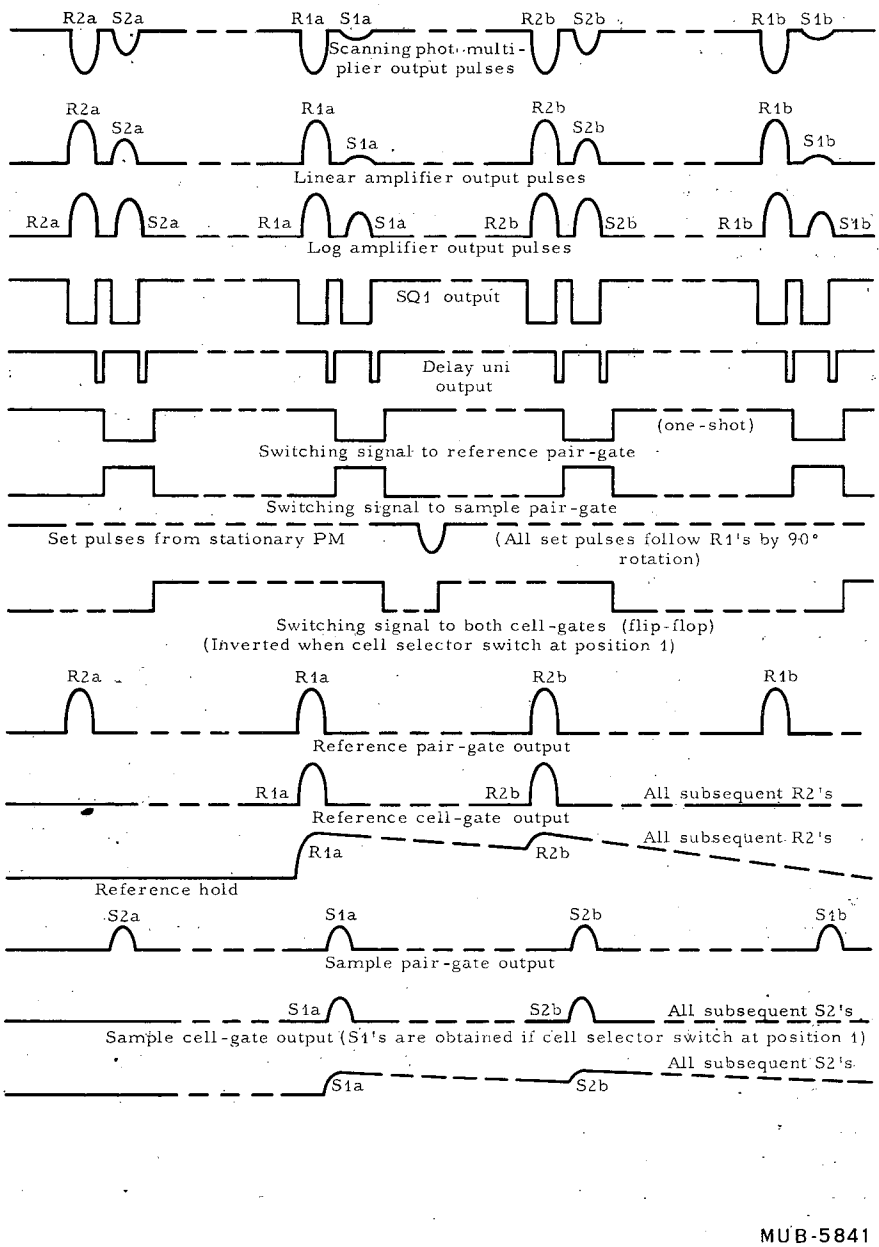

Fig. 12. Pulse relationships for two double-sector cells, illustrating set-pulse corrective action. The scanner is positioned to intercept the images projected by both solutions (Fig. 1). Each gate is open when its switching signal is at the higher level. The set pulse brings the flip-flop "in step," after which the trailing edge of each one-shot pulse dictates switching (unless the flip-flop falls "out of step"). R1a and S1a pass into the holding circuits erroneously, but all subsequent pulses are routed correctly.

improper, and the set pulse promptly shifts the flip-flop to its higher level, at which the cell gates pass cell-2 pulses only (cell selector at 2). Once the system is "back in step," set pulses play no further role because they have no influence when the flip-flop is in its high-level state, one in which all subsequent set pulses find it.

Although it is necessary that both difference traces include the radius-marker image (Fig. 41), they do not do so unless a scanner-activated switch is added to disconnect set pulses when the scanner is at the radius-marker image. Refer to Fig. 13, which shows the switching signal to cell gates when the cell-selector switch is set at 1; here we find that the cell gates are open to every radius-marker pulse. If we changed the selector switch to cell 2 and did nothing to alter the presence of set pulses, the switching signal to the cell gates would be identical (but inverted) from the signal obtained with the cell-selector switch set at 1. This signal would cause the cell gates to restrict passage of the radius-marker pulses in cell-2 position. In order to circumvent this, set pulses are disconnected when the radius marker is being scanned and the cell-selector switch is set at 2.[14] The switching signal to cell gates then corresponds to that shown for cell 2, a relationship that admits every other radius marker to the reference hold. The one-shot restricts radius-marker pulses from the sample hold only so that the radius marker appears in both difference traces.

2. One Double-Sector Cell

Switching for one double-sector cell is different than for two double-sector cells. The radius-marker hole shown in Fig. 1 is plugged and one cell is replaced by a counterbalance with two radius-marker holes as shown in Fig. 2.

The circuitry is modified so that the flip-flop no longer operates the cell switch; thus both cell gates are open continuously. Set pulses are then unnecessary. The pair gates separate the "mates" and every pulse is admitted to the holding circuits. The pulse relationships for one double-sector cell are shown in Fig. 14.

3. Two Single-Sector Cells

Switching for single-sector cells is considerably different than for double sector operation. In order to compensate for the differences, an additional switch, Sector/cell, has been added.

Referring to the photomultiplier pulse train of Fig. 15, we see that the reference and sample pulses are uniformly spaced. This renders the one-shot ineffective as a time discriminator and the flip-flop is used instead.[15] The pair gates are bypassed, and separation is left to the cell gates. In single-sector operation the cell gates are operated out-of-phase and the flip-flop is triggered differently than in double-sector operation.

In single-sector operation the flip-flop is triggered in the "set-reset" mode. When so operated, each set pulse "arms" the flip-flop, placing it in its high-level state. The flip-flop can return to its low-level state only

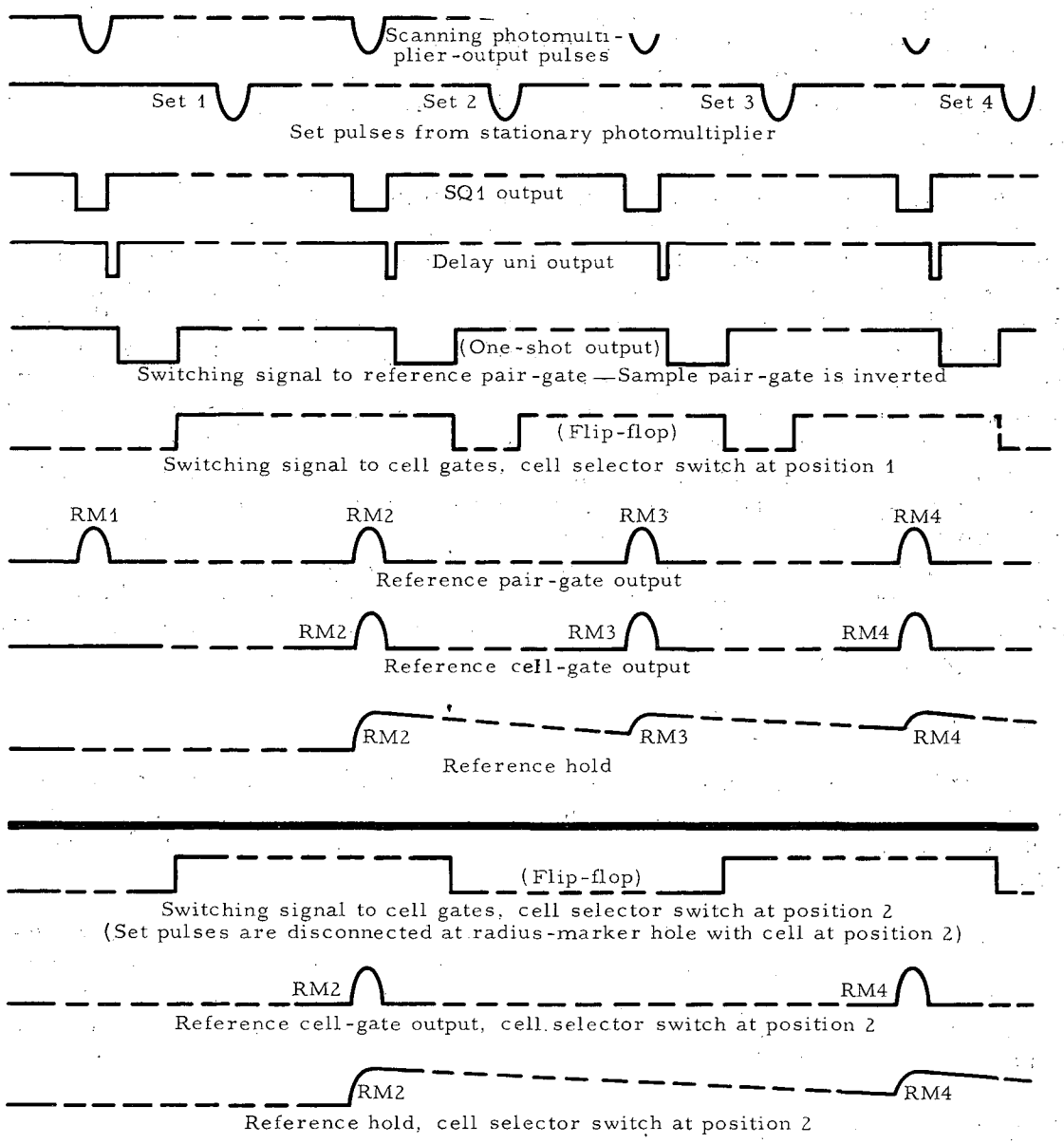

Fig. 13. Pulse relationships for two double-sector cells with the scanner positioned to intercept the image projected by the radius-marker hole (Fig. 1). Each gate is open when its switching signal is at the higher level. The waveforms below the heavy line indicate the significant changes resulting when the cell-selector switch is changed from Cell 1 to Cell 2. Set pulses are disconnected with the cell-selector switch at position 2; the flip-flop spends equal time in each state. Set pulses have no influence when the flip-flop is in the high-level state.

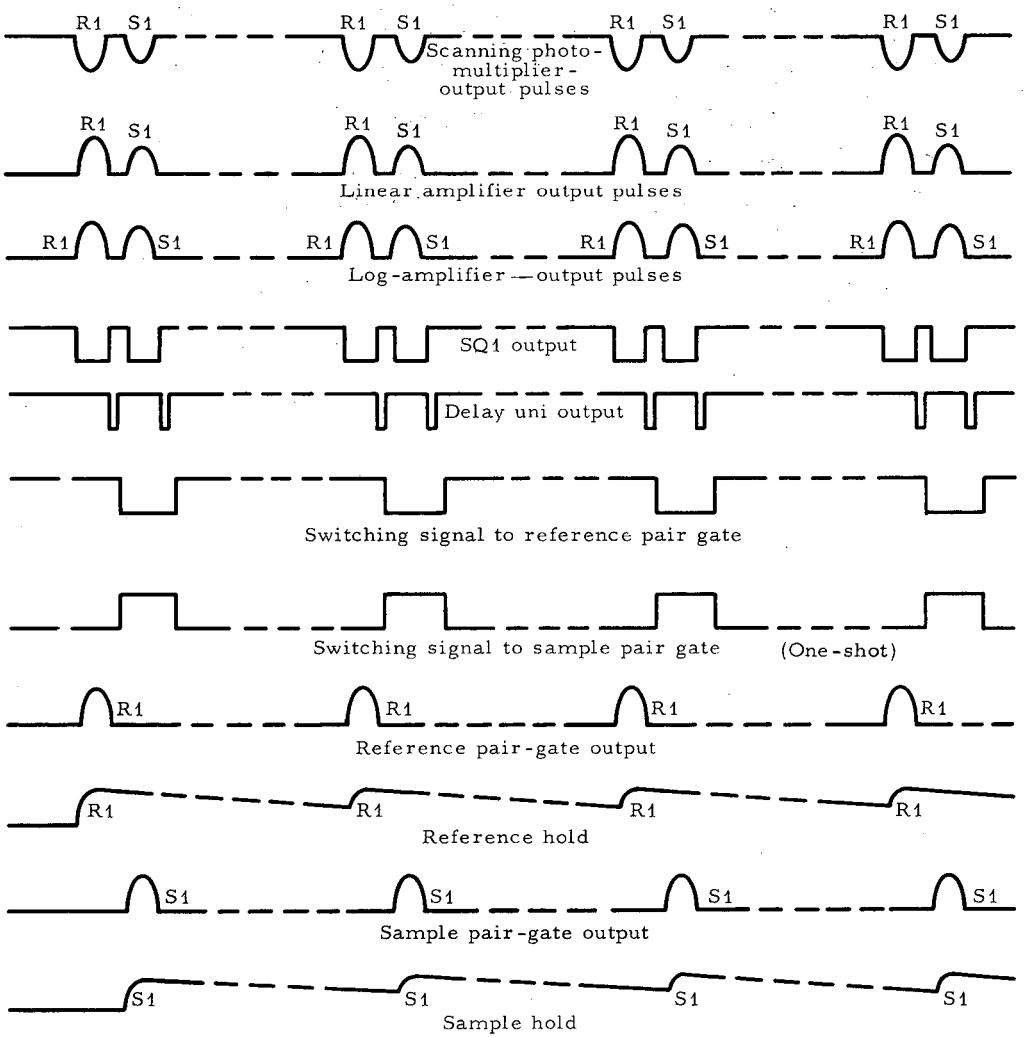

Fig. 14. Pulse relationships for one double-sector cell with the scanner positioned to intercept the image projected by the solution. Each gate is open when its switching signal is at the higher level. The cell gates are open continuously and set pulses are not required.

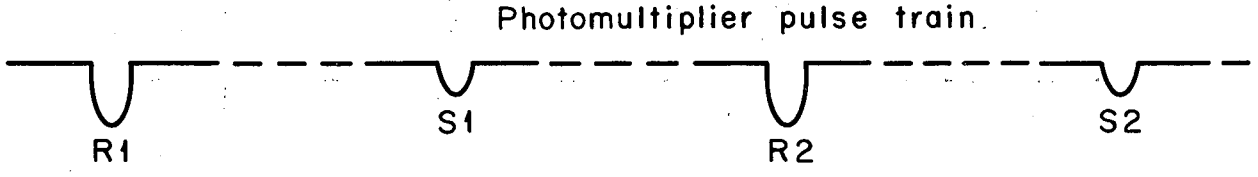

MUB-4728

Fig. 15. A typical pulse train for two single-sector cells, with the scanner positioned to intercept attenuated sample pulses.

if it receives an impulse from the scanner. Cell loading, shown in Fig. 3, ensures that each set pulse is followed by a reference pulse from the scanner. In summary, each set pulse raises the flip-flop to its high-level state; each reference pulse returns it to its low level. In single-cell operation the set pulses effect switching each and every rotor revolution. Pulse relationships when the cell and radius-marker image are being scanned are shown in Figs. 16 and 17, respectively.

B. Reference-Pulse Regulator

The system includes provisions for regulating the reference pulse to an amplitude that remains constant though illumination changes. When so operated, the scanning-photomultiplier supply voltage varies to compensate for changes in illumination, light intensity, linear-amplifier gain, and photomultiplier sensitivity. Such a scheme influences reference and sample pulses proportionately. Regulation (a) ensures that the log compressor operates over a prescribed region, and that none of the compressor's linear region is wasted in compensating for nonuniform illumination; (b) increases accuracy of the calibrating system (the calibration is based upon 25-V reference pulses to the log compressor input. A significant departure from that level results in error); (c) is helpful in sustaining switching when illumination is extremely nonuniform or when a solvent of appreciable optical density is used.

If regulation were perfect one could dispense with the difference system. The sample traces, in that event, would represent the corrected density profile. Regulator performance is very good for illumination profiles of moderate nonuniformity, but subtraction enhances performance even more. Subtraction is also helpful because: (a) It facilitates trace expansion at low optical densities; i.e., recorder deflection per optical density can be increased. The recorded trace need not be displaced when the regions of interest are expanded, and the profile can be recorded in its entirety. (b) It helps discriminate against fluctuations in light intensity, especially those of higher frequency.

C. Calibrator

The system includes an electronic calibrating circuit that permits the measurement of absolute optical density. The measurement is made by comparison of the solution's attenuation (optical effect) with a known electrical attenuation. The electrical attenuator is continuously variable and empirically calibrated in terms of optical density.

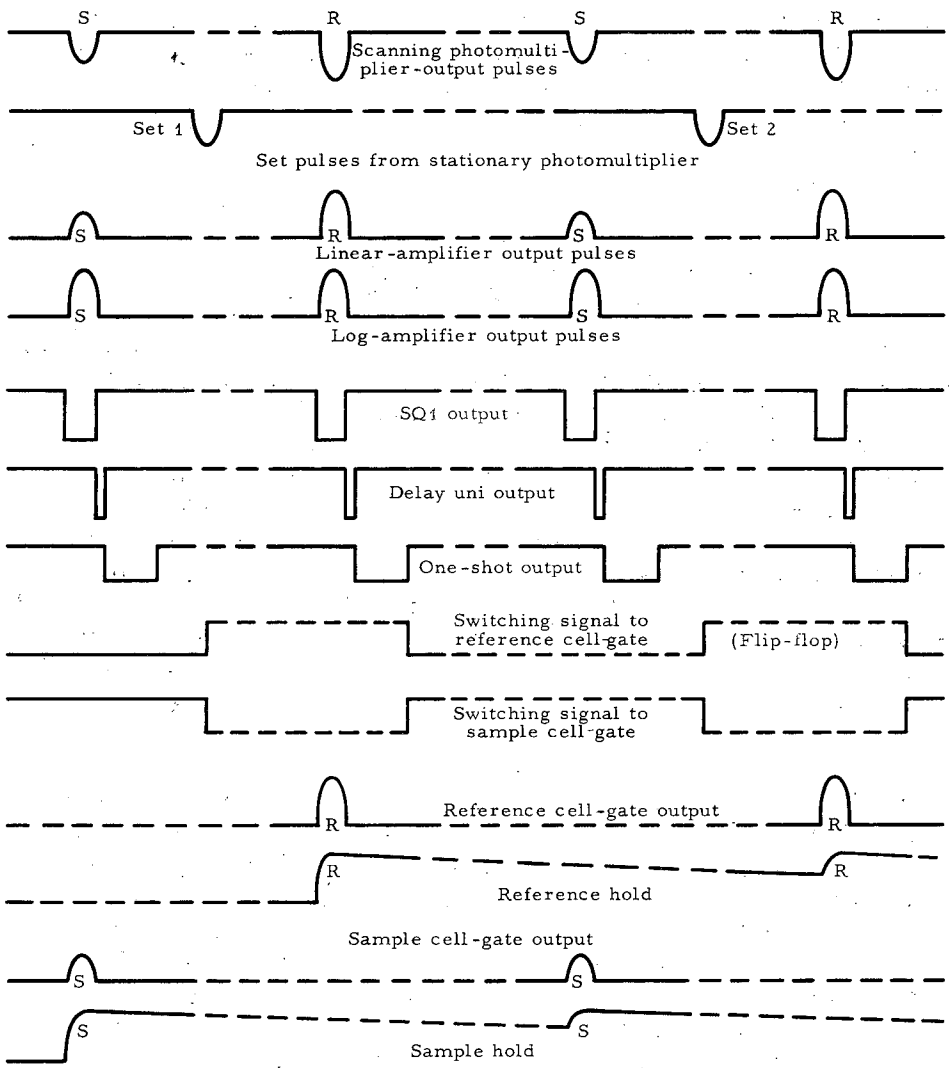

Fig. 16. Pulse relationships for two single-sector cells, with the scanner positioned to intercept attenuated sample pulses. The cells are loaded (Fig. 3) so that each set pulse is followed by a reference pulse from the scanner. The cell gates are operated out-of-phase and the pair gates are bypassed. Each gate is open when its switching signal is at the higher level. One-shot operation is not essential.

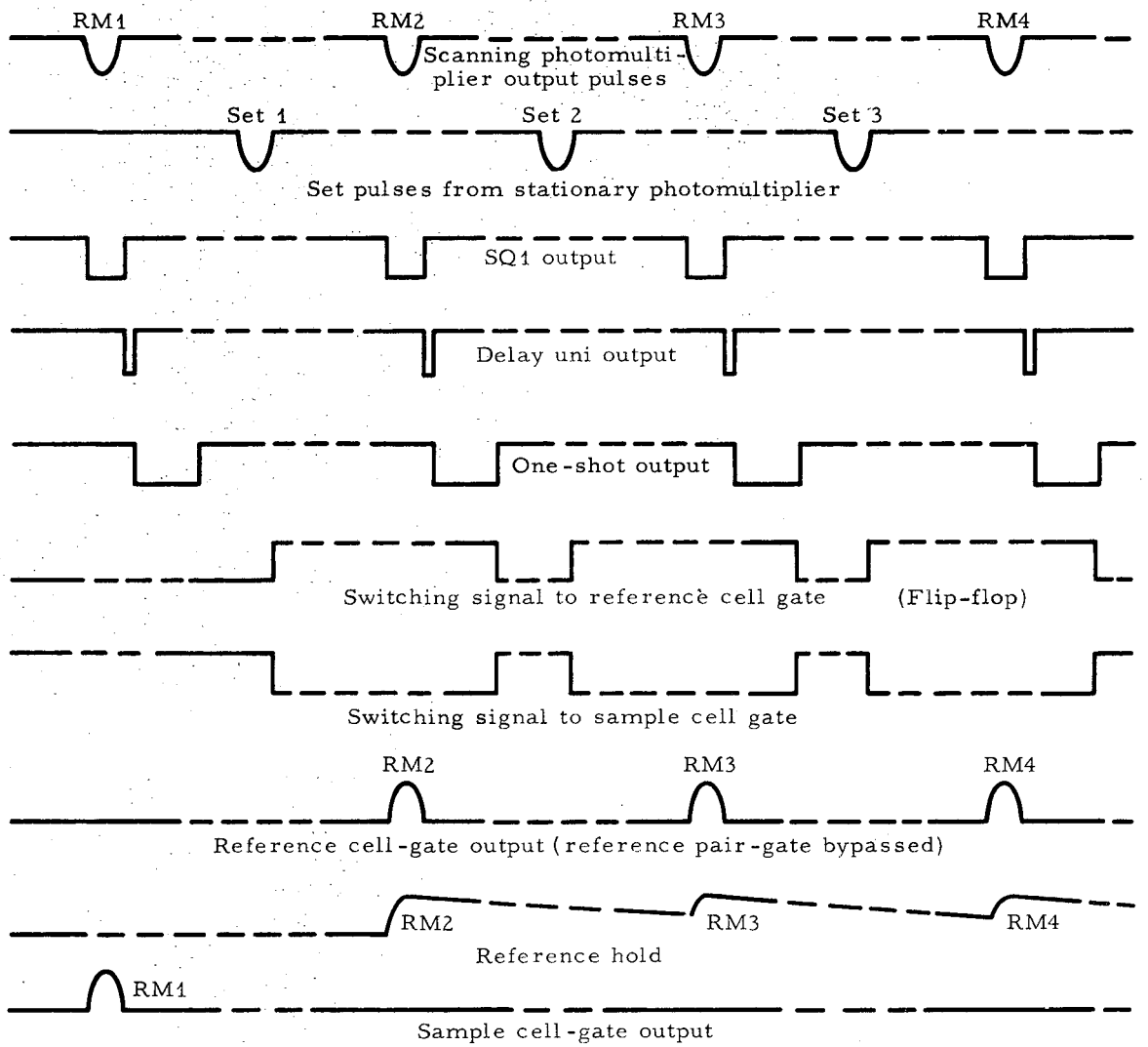

Fig. 17. Pulse relationships for two single-sector cells with the scanner positioned to intercept the image projected by the radius-marker hole (Fig. 3). The cell gates are operated out-of-phase; the pair gates are bypassed. Each gate is open when its switching signal is at the higher level. One-shot operation is not essential. All radius-marker pulses from the scanner (except RM1) pass into the reference hold.

D. Derivative

The function recorded is differentiated electronically, and the derivative applied to another recorder channel. The function and its derivative are recorded in time coincidence.

E. Scan Control

The scan-control is automatic in the sense that it need not be attended once operation has been initiated. The scanning mechanism remains at its start position until it receives an impulse from the ultracentrifuge; after which it moves the photomultiplier across the pulsating images, movement of the carriage being controlled by a synchronous motor driving a lead screw. Mounted on the end of the lead screw is a slotted disk which, in conjunction with a small light and a photosensitive element, generates marker pulses. These marker pulses determine positions of fiducial marks on the recorder chart in terms of distance traversed by the photomultiplier (Fig. 43).

The recorder-chart drive, an independent mechanism, is activated during the forward scan only. When the scanner reaches the end of its travel it actuates a limit switch and returns to its start position where it remains until the centrifuge provides another impulse. Manual scan control is also available.

The scanning mechanism includes a 4-speed transmission operated by solenoid-type clutches. The solenoids permit remote control of scanning speed and facilitate high-speed carriage return; i. e., the scanner automatically returns to the start position at its highest speed (6 seconds) unless the Fast Return is disabled.

F. Recorder

The recorder--Visicorder Model 906B[16]--was selected for a number of reasons, the principal one being that its fast writing speed does not limit resolution. Other reasons were that (a) it permits the function and its derivative to be displayed across the full width of the paper while retaining a common time base and (b) recording is rectilinear. Furthermore, the mutliple-channel arrangement (12 channels plus two timing galvanometers) permits the same recorder to be used simultaneously by two (or more) centrifuges. The additional channels facilitate the recording of more information, if desired.

Also important, the ruling of grid lines on the paper as it issues from the recorder compensates for any lateral paper paper slippage that might occur. Marker pulses from the timing galvanometer provide a check for reproducibility of the mechanically independent scanner and chart drives.

As the Visicorder employs an ultraviolet beam and self-developing paper, inking problems are nonexistent. There is a possibility of lamp

failure, but this has not been a serious limitation.

G. Illustrations

A number of equipment photographs are included here. Figure 18 is an overall view of the ultracentrifuge.[17] Figures 19 through 21 show the scanning mechanism. Figures 19 and 22 show the stationary photomultiplier assembly. Figure 23 illustrates the set-pulse amplifier, and Fig. 24 the control console adapted to include operating controls for two ultracentrifuges. Figures 25 through 31 reveal construction of the operational unit.

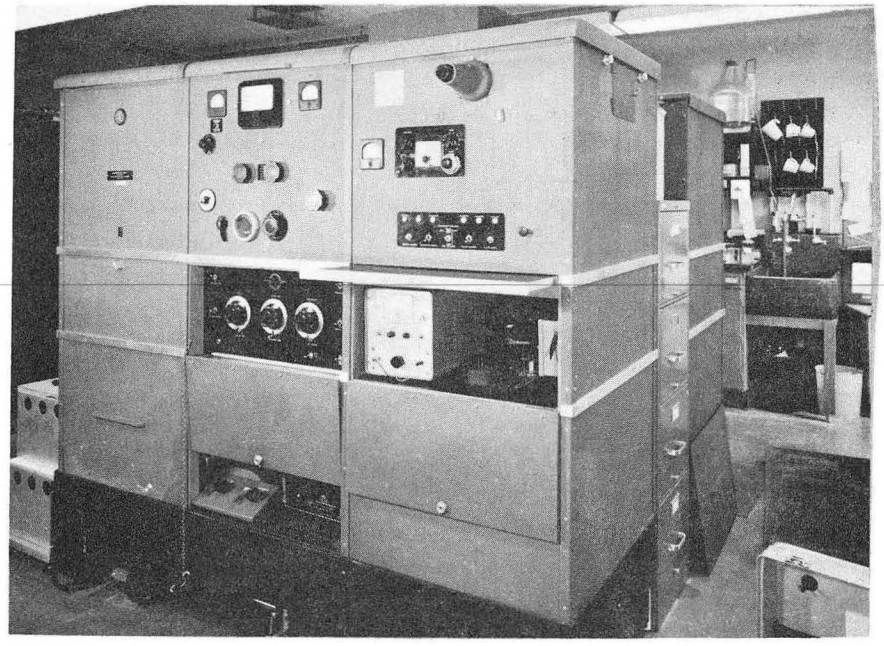

ZN-3502

Fig. 18. An overall view of the ultracentrifuge.

ZN-4851

Fig. 19. Scanning mechanism mounted in the ultracentrifuge. This view shows the upper right-hand end of the centrifuge. The transmission cover plate has been removed to show the clutches (foreground). The micrometer adjustment (lower left) determines the scanner position at which set pulses are disconnected. The stationary-photomultiplier (upper right) straddles the large pipe. The lid of the ultracentrifuge, opened for this picture, clears the scanning mechanism and is normally closed to prevent room light from interfering with its operation.

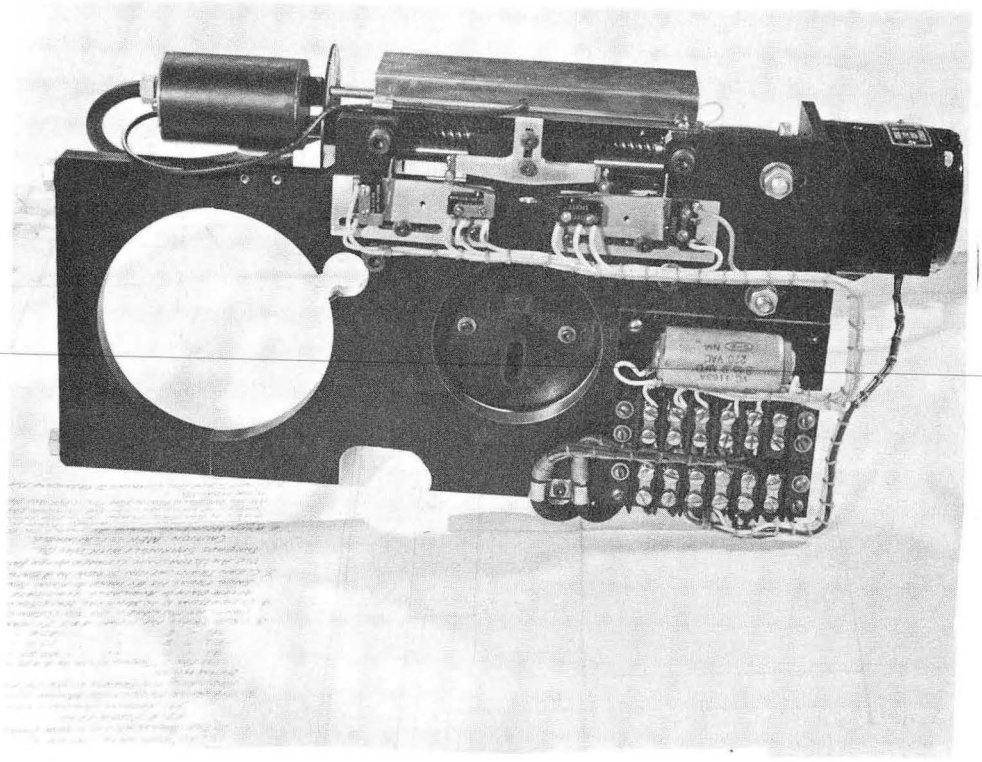

ZN-3570

Fig. 20. A view of an earlier scanning mechanism removed from the ultracentrifuge (prior to addition of the slit selector, the set-pulse disable switch, and the variable-speed transmission). Light rays passing through the optical system (perpendicular to the plane of the photograph) enter the photomultiplier through a narrow vertical slit covered by a small snout that is no longer required.

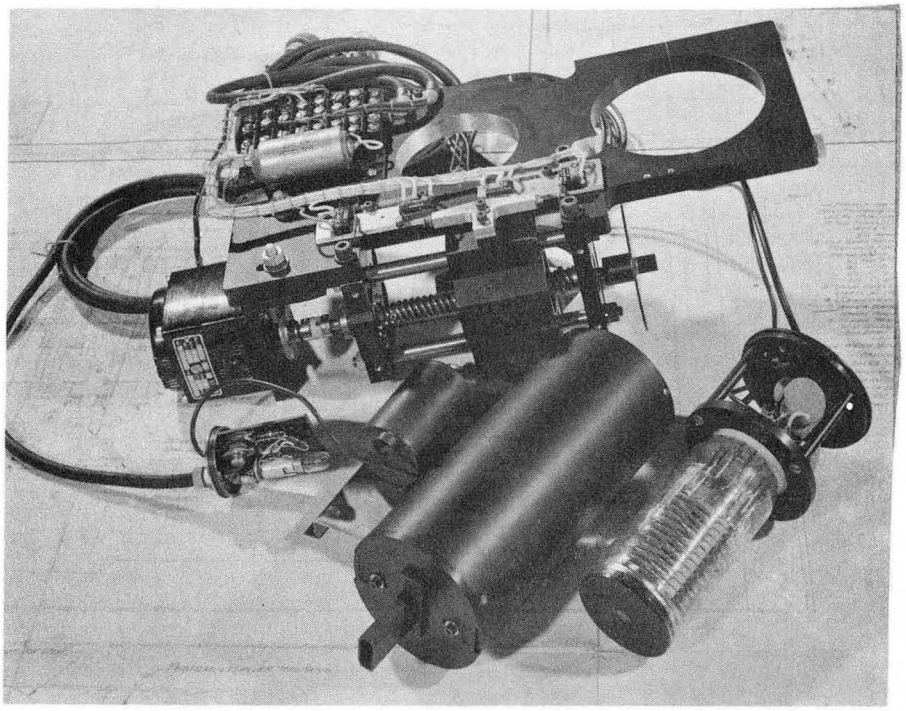

ZN-3499

Fig. 21. An early version of the scanning unit, partially disassembled to show some of the basic components: the photomultiplier and its housing; the light for the marker generator; the lead screw, coupling, and motor; and the cam and safety switches mounted on the support bracket (the slit selector, the set-pulse disable switch, and the variable-speed transmission are not shown). The small snout is unnecessary and is no longer used.

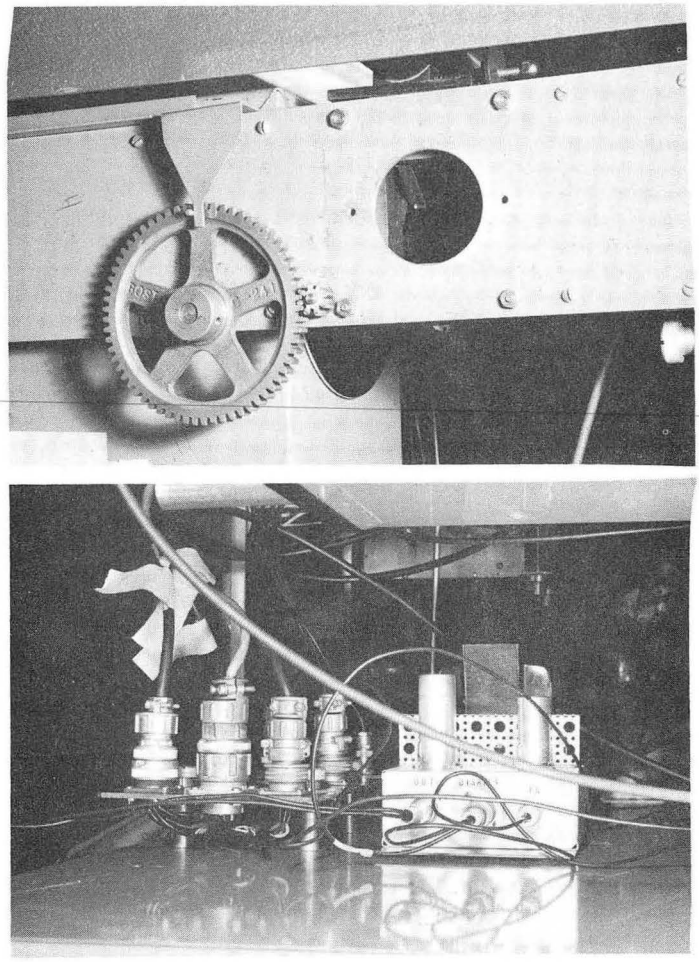

ZN-4844

Fig. 22. Ultracentrifuge with its upper right-hand panel opened. A mirror (within circle) projecting from the stationary photomultiplier (above circle) intercepts light from the Schlieren optical system. The mirror intercepts only the upper third of the radius-marker image, and does not interfere with the Schlieren system. The Schlieren photographic plate does not interfere with set-pulse operation, and both systems can be used simultaneously.

Fig. 23. Ultracentrifuge with its upper right-hand panel opened. Illustrates the set-pulse amplifier and a connector board, the terminal point for all cables connecting to the control console. All connectors are mounted on an insulated plate to minimize the effects of ground loops. The amplifier and connector board are mounted on the centrifuge relay panel (amplifier above the connector board).

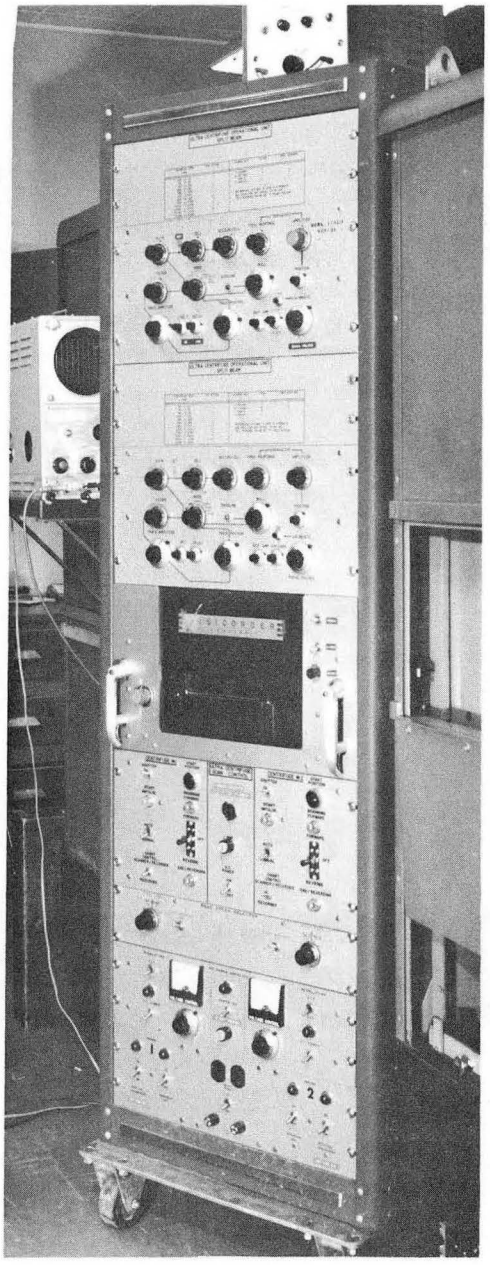

ZN-4852

Fig. 24. Front view of the control console, now adapted to include operating controls for two ultracentrifuges. The top two panels are operational units, one for each machine. Directly below them is the Visicorder. Below the Visicorder, a scan control panel includes separate controls for each scanning mechanism. The bottom panel includes the stationary-photomultiplier power supplies, convenience outlets, and a master power switch for the entire console. Directly above the bottom panel is the photomultiplier power supply which includes separate controls for each scanning photomultiplier.

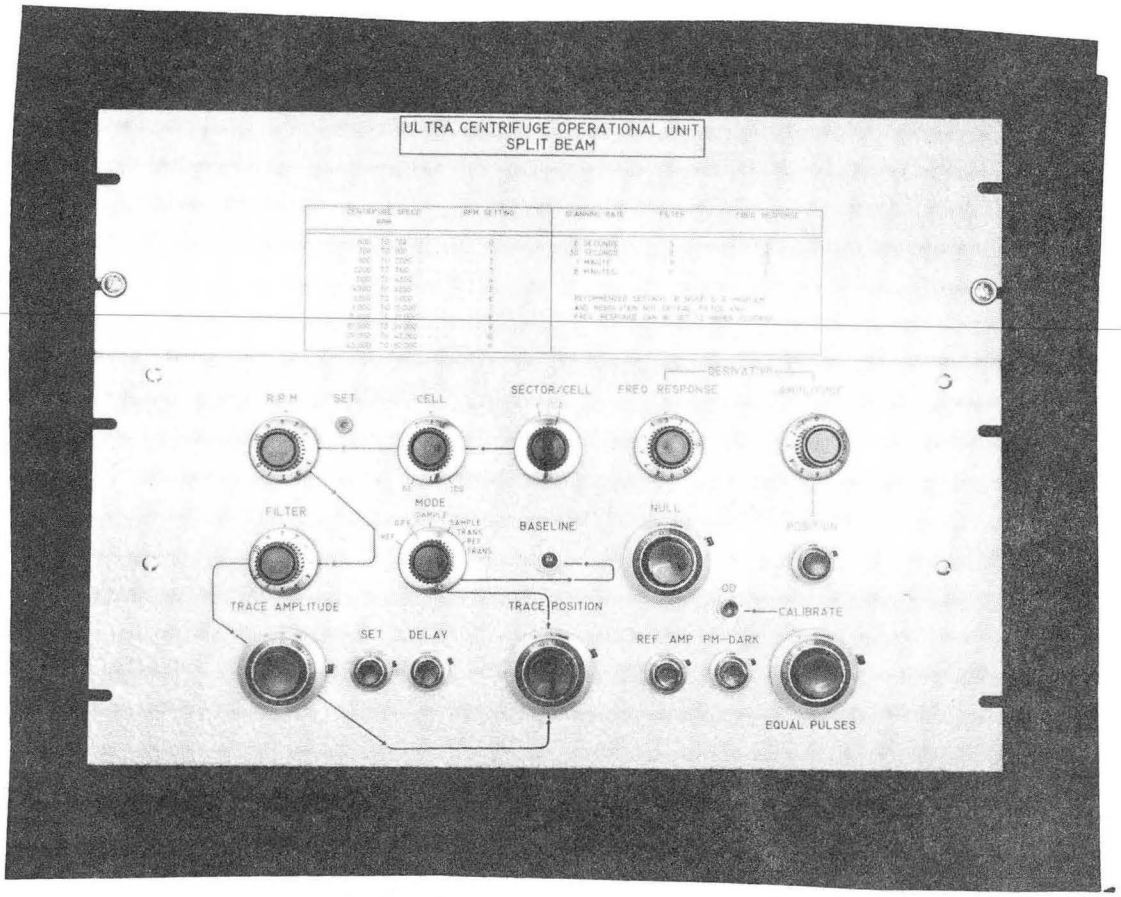

ZN-4727

Fig. 25. Operational unit, front view. The upper panel is removable for easy access to critical circuitry. The controls are arranged according to function with the operating sequence indicated by arrows. The cell-selector knob has marks below to indicate the proper setting for single sector or for one double sector. (SPLIT BEAM nomenclature, upper panel, is misleading).

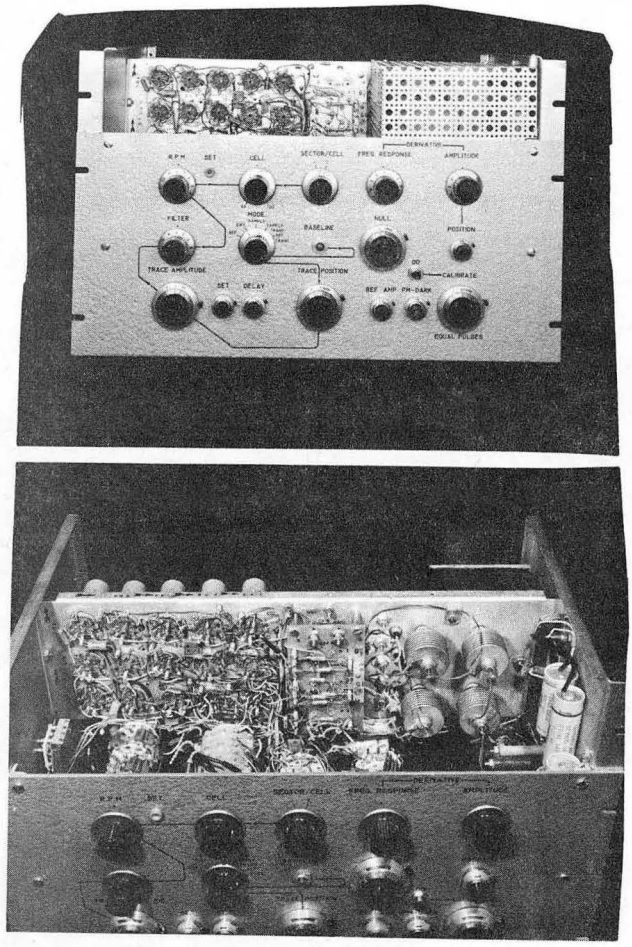

ZN-4845

Fig. 26. Operational unit, front view, top panel removed. The power supply (top right) is covered by a perforated shield. The bootstrap and derivative amplifiers are mounted behind the plate to the left of the perforated shield. Bias and holding-circuit adjustments are mounted on the same plate. Most of the circuitry comprises plug-in modules. Arrows close to each module socket indicate the various switching and signal paths.

Fig. 27. Operational unit, top front view with perforated cover removed from the power supply. Trimpots G1 and G2 are mounted on the plate just to the left of the power supply. Reference Bias and Sample Bias adjustments are mounted on the same plate.

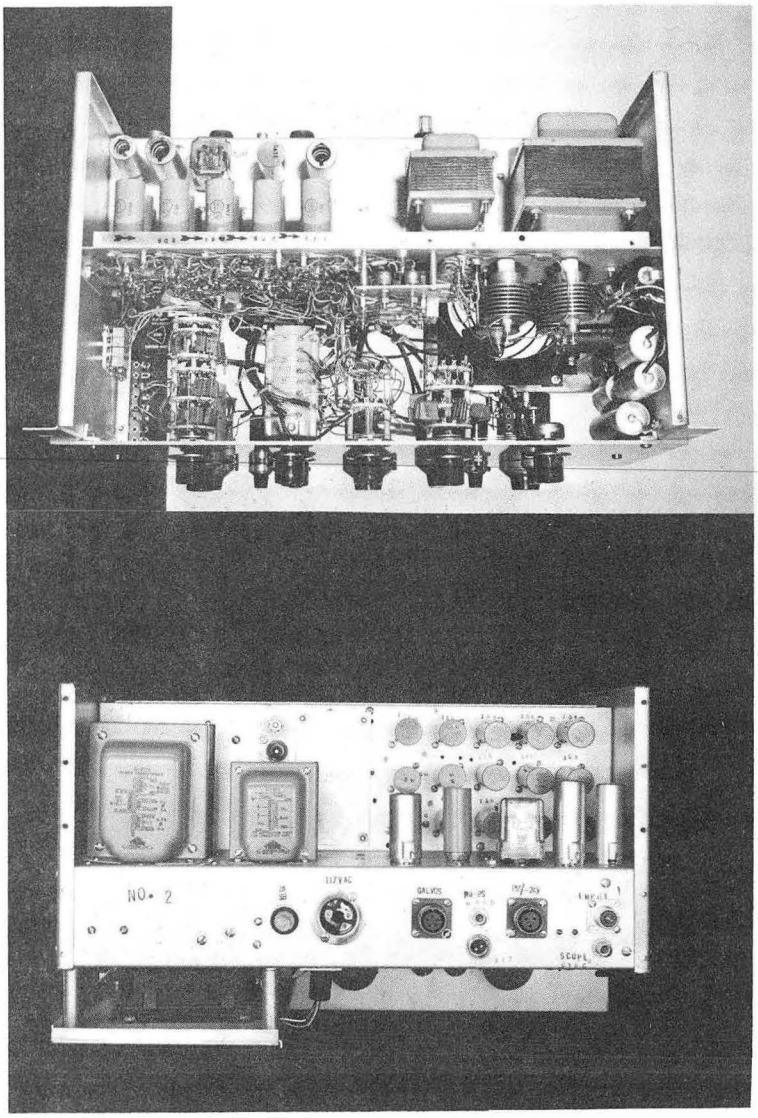

ZN-4962

Fig. 28. Operational unit, top view. The circuit modules are immediately above the arrows. The linear amplifier appears above them and to the left. The reference-pulse regulator is to the right of the linear amplifier, and the gate-adjusting trimpots are mounted on the left-hand panel. The regulator gain adjustment (not visible) is just below the relay to the right of the linear amplifier. The 75-V Zener diodes are mounted on heat sinks (center right), which are fabricated from plate caps.

Fig. 29. Operational unit, rear view. The location and type of modules are more readily apparent than in other views. The reference-pulse regulator relay (rectangle at center right) is a plug-in type. The power supply is cooled by a small blower mounted on the plate at the lower left.

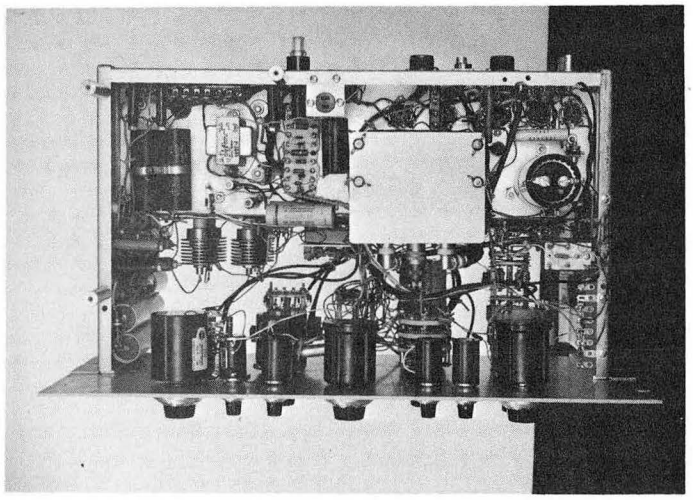

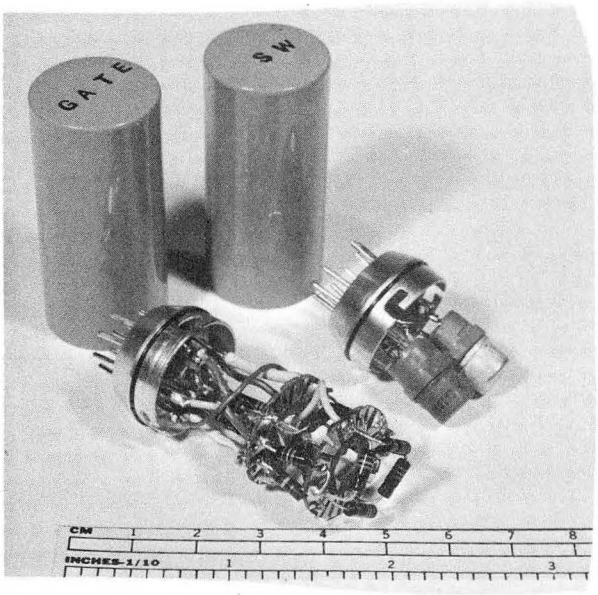

ZN-4847

Fig. 30. Operational unit, bottom view. The blower, normally mounted at the upper left-hand corner, has been removed for clarity. The log compressor is clamped beneath the plate secured by four wing nuts. An additional connector has been added to the log compressor so that it can be operated for an internal power supply to its left. The derivative substraction amplifier (Burr Brown model 1503) extends from the center of the right-hand plate.

Fig. 31. Switches and gates of operational unit. These are fabricated into blank containers supplied by manufacturer.

IV. CIRCUIT DESCRIPTION

A. Switching

1. Two Double-Sector Cells

As shown in the functional block diagram (Fig. 32), the linear amplifier activates a gating chain. At the tail end of that chain are two switches, "Cell" and "Pair," which operate their respective gates so that each pulse is routed to the proper hold. Each switch has two outputs, one inverted in phase. The net result is that all pulses are routed through one pair gate. The pair gates, operated by the one-shot, are gated out of phase so that every pulse passes through one, but not both. The one-shot permits the first pulse of each pair through the reference pair-gate, its mate through the sample pair gate. All reference pulses, independent of cell, pass through the reference-pair gate; all sample pulses pass through the sample-pair gate.

Once a pulse is admitted through either pair-gate, it passes to the following cell-gate. The cell-gates, operated by the flip-flop, permit alternate pulse pairs to charge the holding circuits. Both cell-gates are operated in phase. If one wishes to observe the alternate cell, he changes the cell-selector switch, inverting the phase to both cell gates. This configuration permits the same holding circuits to be used for both cells. Common holding circuits simplify operation and calibration as well as circuitry. Set pulses are not disconnected with the scanner positioned at the radius marker when the cell selector is at "1."

2. One Double-Sector Cell

The cell selector is set to "0," a position that permits the flip-flop to operate but biases the cell switches so that the cell gates are continuously open. Set pulses are unnecessary.

3. Two Single-Sector Cells

The Sector/cell selector is set to "1." This bypasses the pair gates and reverses phasing to the reference-cell gate; the reversal causes the cell gates to be operated out of phase. The Sector/cell switch also changes flip-flop triggering to the "set-reset" mode. When so operated, each set pulse raises the flip-flop to its high-level state; each reference pulse returns it to its lower level. The Sector/cell switch also reconnects the regulating gate so that it is operated by the cell switch, rather than by the pair switch. One-shot operation is not essential to this mode; it remains operative only for expediency.

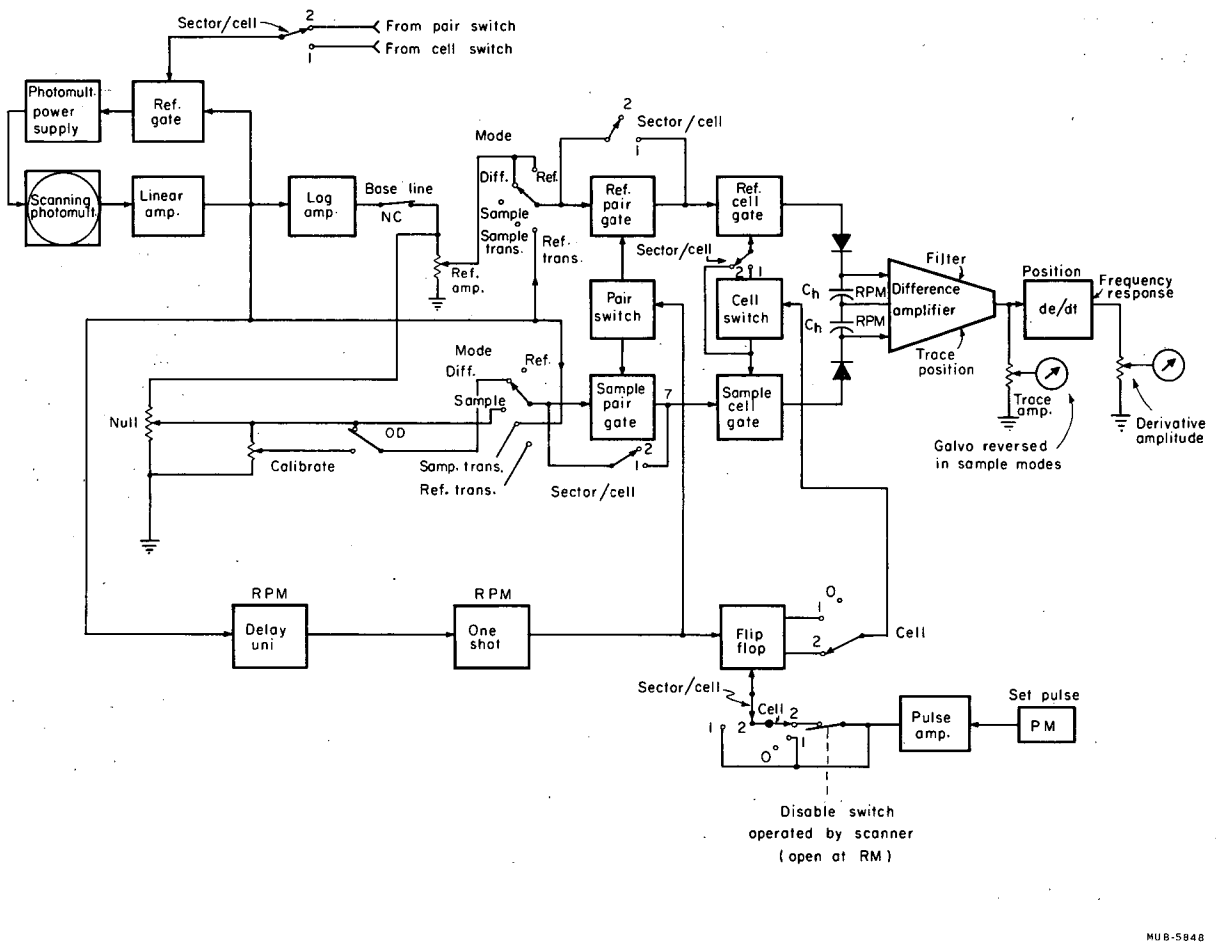

Fig. 32. Functional block diagram of modified system. The controls are set for operation with two double-sector cells, Difference mode.

B. Gates and Switches

The six-diode gate was selected because it has low leakage when the gate is closed (Fig. 60, Appendix B). This characteristic is especially important at high optical densities for which a small leakage introduces a large error. This gate also has other virtues: The switching component does not appear in the output, the gain is close to unity, and the linearity is excellent.[18] The bilateral properties do require a series diode for peak charging, but this is not a serious limitation.

As the gates are operated by bipolar switches, switching spikes must be held to a minimum. If they are not, the spikes charge each holding capacitor to a different level. This, in turn, requires a compensating bias when the instrument is zeroed; i. e., when the Baseline pushbutton is depressed, the gates are switching, but the input pulses are admitted to neither holding circuit. When the system is nulled (reference and sample channels balanced at the air space and base line released), the switching spikes are masked by the signal pulses so that the holding circuits no longer respond to their presence. The compensating bias remains, however, and an erroneous null results. An improper null produces a slight base-line shift (approximately 0.02 OD resulted) if pulse-height changes (because of nonuniform illumination or varying light intensity) reduces accuracy accordingly. Null prevails at only one pulse level, and any departure from that level causes the base line to shift.

Problems due to switching spikes were minimized by the addition of a collector bypass to one transistor of each bipolar switch. This addition compensates for switching disparities between transistors and is very effective in making the null position insensitive to pulse level. The collector-bypass capacitors do not truly eliminate switching spikes—they merely ensure that those spikes most troublesome are negative. Negative spikes are not transmitted by the charging diodes.

Another problem relative to switching was that of cross coupling, i. e., apparent interaction between cells. A high density in the sample sector of cell 1, for example, reflected in the tracing of its counterpart, cell-2 sample.

It was initially believed that this cross-coupling problem was due to faulty clamping at the log compressor input (ac coupling to the log compressor), but subsequent investigation revealed otherwise. The real cause was creation of a small switching pedestal (a fractional percent of gating voltage) with amplitude related to signal-pulse level. Each gate was normally adjusted [R1, R2, S1, and S2 trimpots of pulse-separation circuitry (Fig. 60, Appendix B)] for minimum pedestal in the absence of input pulses (Baseline depressed and switching circuits active). This reduced pedestal amplitude to a negligible value, but when input pulses were admitted (Baseline released) pedestal reappeared with an amplitude related to pulse levels at the gate input. In effect, pulses at the gate input modified bridge balance, permitting the switching circuits to generate a small pedestal. That pedestal charged the gate-input coupling capacitors to a negative level, which they retained until the subsequent switching transient occurred.

The net result was that the transmitted pulses "rode" upon a switching component whose amplitude was related to the number and height of input pulses at each pair gate. Since ac coupling follows the cell gates (reduces drift), changes in the switching component modified the apparent duty cycle, causing a given pulse to have a changing positive component. Since the switching-component duty cycle is much greater than that of the pulses, baseline shift was exaggerated.

The interaction problem was solved by the addition of coupling diodes in series with the coupling capacitor to each pair-gate input (1N904's in Fig. 59 Appendix B). The coupling diodes prevented the negative-going pedestal from charging the coupling capacitors, and the signal pulses no longer rode a switching component. In view of the switching problems we encountered, we might consider using another type of gate.[19]

A study of pulses at the output of both cell gates reveals that clamping immediately previous to each charging diode is unnecessary. This is true despite ac coupling because each cell gate passes only those pulses for which it is responsible. The positive level of each pulse transmitted through the output coupling capacitor is proportional to pulse amplitude, unaffected by other pulses, and clamping is not required.

C. Holding Circuits

Schematics of the holding circuits are shown in Fig. 61, Appendix B. Refer again to Fig. 32; notice that the pulses are separated so that reference pulses pass through one set of gates, sample pulses through another set. The output from each channel charges a holding capacitor through a series diode that is unilateral, and thus permits the capacitor to charge to peak voltage and retain that value with a slowly decaying time constant. Holding capacitors maintain the average output voltage at a high level, minimizing the effects of drift, pickup, and noise. The discharge time constant, determined by the RPM control setting, is a function of holding-capacitor size and its effective shunt resistance.

Figure 32 shows that holding-capacitor size is a function of centrifuge speed. The correct value at any speed is determined by a number of factors but these can be reduced to two discrete effects: (a) the charging-time constant must be short enough to ensure that the capacitor charges to the peak pulse amplitude, and (b) the discharge-time constant must be long enough to maintain the average output voltage at a suitable level without impairing high-frequency performance. In view of these considerations, a selector switch, RPM, is included to ensure that the optimum time constant for each speed is selected.

The optimum holding capacitor was empirically determined at 60 000 rpm; the values for other speeds were calculated on a proportional basis.

D. Bootstrap Amplifiers

The voltage across each holding capacitor is applied to an operational amplifier. The amplifiers, bootstrap type,[20] can be adjusted for infinite input impedance. Bootstrapping permits us to monitor full voltage across each holding capacitor, and minimizes the effects of amplifier drift. The present configuration (Fig. 61, Appendix B) reduces drift to approximately one-hundredth that of the earlier version. Bias to the amplifiers is applied in series with the charging diode to each hold.

The difference output is directed through an adjustable filter to the function galvanometer. An intervening attenuator (Trace Amplitude) controls deflection magnitude at the recorder.

E. Calibrator

The calibrating system (Fig. 59, Appendix B) includes an electronic calibrator that permits the measurement of absolute optical density. The calibrator lowers the pulse amplitude going into the sample channel. The reference channel is unaffected because of the point at which attenuation is introduced.

When using the calibrator to measure optical density, record the difference traces in the conventional manner. Then position the scanner so that reference and sample pulses are of equal height and 2-V amplitude. Depress the optical density (OD) pushbutton and adjust the Calibrate dial to produce the same deflection as that of the desired part of the recorded trace. Note the resulting dial setting and consult the calibration graph (Fig. 33) to find the corresponding optical density. System performance is quite linear up to optical densities greater than 1.5, and so the deflection can be considered proportional to optical density at lesser values.

F. Reference-Pulse Regulator

The scanning-photomultiplier power supply is designed for two modes of regulation, internal and external. When internal regulation is used, the power supply maintains a constant output voltage irrespective of changes in line voltage or load.

In external regulation (Figs. 63 and 72 Appendix B), the reference pulses are maintained at a constant amplitude, because the power-supply voltage varies automatically to compensate for changes in illumination, light intensity, linear-amplifier gain, and photomultiplier sensitivity.

We added an independent gate to the external regulator to isolate the reference pulses (reference gate, Fig. 63) and permit us to bypass the log circuits, thereby increasing loop gain[21] and improving regulation. The regulator gate is actuated by the pair switch with double-sector operation, by the cell switch with single-sector operation.

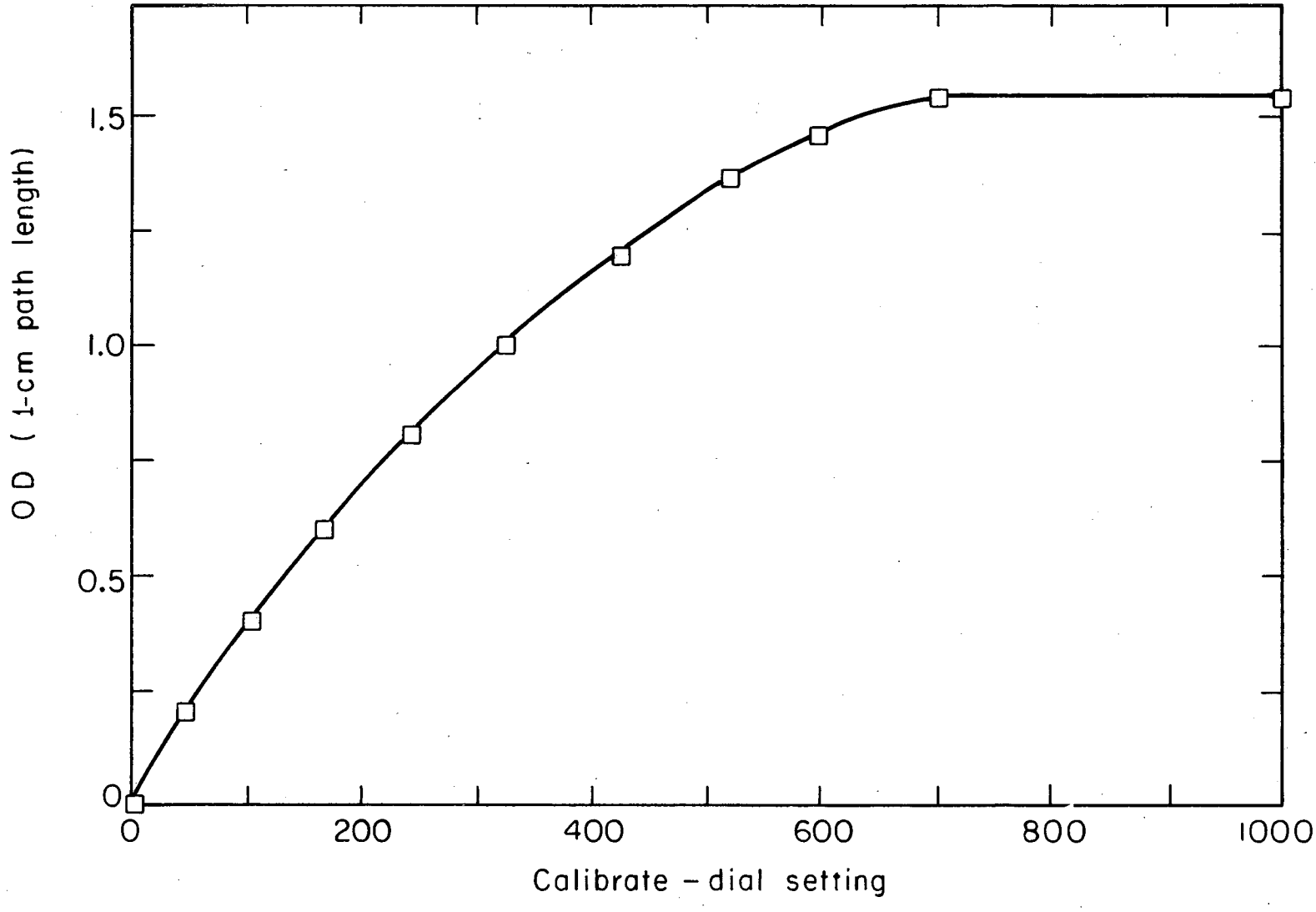

Fig. 33. Calibration graph indicating optical density as a function of the Calibrate dial setting. The curve is nonlinear for reasons described in the text.

The regulator gate does not distinguish between cells (it transmits reference pulses from both cells). This lack of distinction is not important because the illumination profile, the photomultiplier, and the linear amplifier are common to both reference sectors. Regulation with reference pulses from both cells is advantageous in reducing the effect of menisci upon power-supply voltage. The light attenuation from the reference meniscus would normally increase the power-supply voltage and tend to "iron out" the meniscus in the reference trace if the regulating gate passed reference pulses from one cell only. This voltage increase would also reflect the reference meniscus into the sample recording. But if the regulating gate transmits reference pulses from both cells, and if the reference menisci are staggered, the menisci would have little influence on the power-supply voltage.

One could introduce a longer time constant into the regulating loop, but this lengthening would reduce regulator frequency response to changes in light intensity resulting from lamp fluctuations. Furthermore, the time constant might be too long unless adapted to the scanning rate employed.

External regulation creates another problem. When scanning a dark region (unless the regulator is inhibited), the regulator tends to increase photomultiplier-supply voltage to an excessive value. This excessive voltage produces high noise at the photomultiplier output, noise that produces confusing patterns in the recorded traces. Furthermore, if the scanner enters into an illuminated region, the excess voltage produced could damage the photomultiplier.

In order to avoid these regulating problems, we added circuitry that limits the maximum voltage produced by the power supply. Even more, that circuitry ensures that the supply voltage when the scanner is in a dark region is essentially the same as that prevailing when the scanner is in light; this is accomplished with an additional holding circuit that detects light pulses from the scanning photomultiplier. The holding-circuit voltage is amplified to energize a relay that connects the regulating circuit if light is present. If the light falls below a prescribed level the relay de-energizes and substitutes a dc voltage for that normally derived from the regulating hold. This dc voltage is adjustable with a panel control (PM-DARK) and is set so that the power-supply voltage in darkness corresponds to that prevailing with the scanner positioned at the air space. The effects of relay transmit time are minimized by the regulating time constant, and the transition from darkness to light is barely perceptible in the recorded traces. When the scanner passes from dark to light regions (or vice versa), the relay makes a noise that is quite useful in confirming the presence of light. Oscilloscope pulses and the recorded traces provide visual assurance of regulator performance.

G. Differentiator

The recorded function is applied to a differentiator (Fig. 61, Appendix B) that includes an adjustable filter for reducing high-frequency response and associated noise. The differentiated output is applied to another recorder channel, and both outputs, the function and its derivative, are recorded in time coincidence (Fig. 37). Amplitude and positioning controls are provided.

The derivative is inverted in the sample mode because of a reversal of the function galvanometer, which is normally switched to maintain a consistent Visicorder presentation. We didn't bother to reverse the derivative galvanometer because the sample modes are only a crosscheck of system performance.

H. Set-Pulse Amplifier

The set-pulse amplifier (Fig. 65, Appendix B) is conventional, but the manner in which it drives the subsequent squaring amplifier is not. Amplifier-output pulses are positive but triggering is derived from their negative overshoot, useful in discriminating against photomultiplier noise bursts, which are normally positive at the amplifier output. Because some noise bursts are equal in magnitude to the set pulses prevailing when light intensity is minimum, amplitude discrimination is ineffective. Overshoot triggering, on the other hand, is effective because the degree of overshoot is directly proportional to pulse duration. Noise bursts are considerably shorter than set pulses, so the overshoot from noise is practically nil.

The amplifier, driven with negative pulses from the stationary photomultiplier, has a gain of approximately 45. The Schlieren optical system is best operated with the yellow filter removed and with the light aperture adjusted to produce positive pulses of at least 40-V minimum at the amplifier output (Set jack). The requirement for set-pulse amplitude depends upon centrifuge speed. Less light is necessary at slower speeds because set pulses are longer and therefore produce more overshoot.

I. Marker Generator

A schematic of the Marker Generator is given in Fig. 66, Appendix B. Rotation of the slotted disk produces light impulses to the photosensitive element. These impulses are converted to current changes, then amplified to drive the Visicorder timing galvanometers which are connected in series. Two ultracentrifuges share the Visicorder. The timing galvanometers are connected to the marker generator of the machine that is scanning. If both machines scan at the same time, the timing galvonometers are connected to Machine I.

J. Scan Control, Manual

Refer here to Fig. 34 for a simplified schematic of the manual scan control.

1. Scanner is at "Start position". LS-1 is engaged by scanner. Power is disconnected from motor and all relays. ("Start position" light on.)

2. S1 is placed in "Forward" position.

a. S1-A bypasses LS-1. Motor is energized through S1-A, LS-2, and S1-B, advancing scanner to outer radius of image.
b. RE3 is energized through S1-A, LS-2, S1-B, and RE2-3.

(1) RE3-1 connects power to Visicorder chart drive.
(2) RE3-2 connects Visicorder timing galvanometers to Marker Generator of appropriate centrifuge. (Note: The same recorder is used for two separate scanning mechanisms, one in each of two centrifuges. Each scanning mechanism has its own controls, and the schematic nomenclature is the same for both.)

3. Scanner reaches end of travel. LS-2 is engaged by scanner.

a. Motor is de-energized, scanner stops.

b. RE2 is energized through S1-A, LS-2 and S1-D. ("End/reversing" light on.)

RE2-3 disconnects power to RE3.

(1) RE3-1 disconnects power to the recorder-chart drive.
(2) RE3-2 disconnects the timing galvos from the relevant Marker Generator.

4. S1 is placed in "Reverse" position.

a. Motor is energized through LS-1 and S1-C, driving scanner in reverse direction towards "Start position."

b. RE2 is energized through LS-1 and S1-D. RE2-3 disconnects power to RE3.

(1) RE3-1 disconnects power to the recorder-chart drive.
(2) RE3-2 disconnects the timing galvos from the relevant Marker Generator.

5. Scanner reaches "Start position." LS-1 operates, disconnecting power from the motor and all relays.

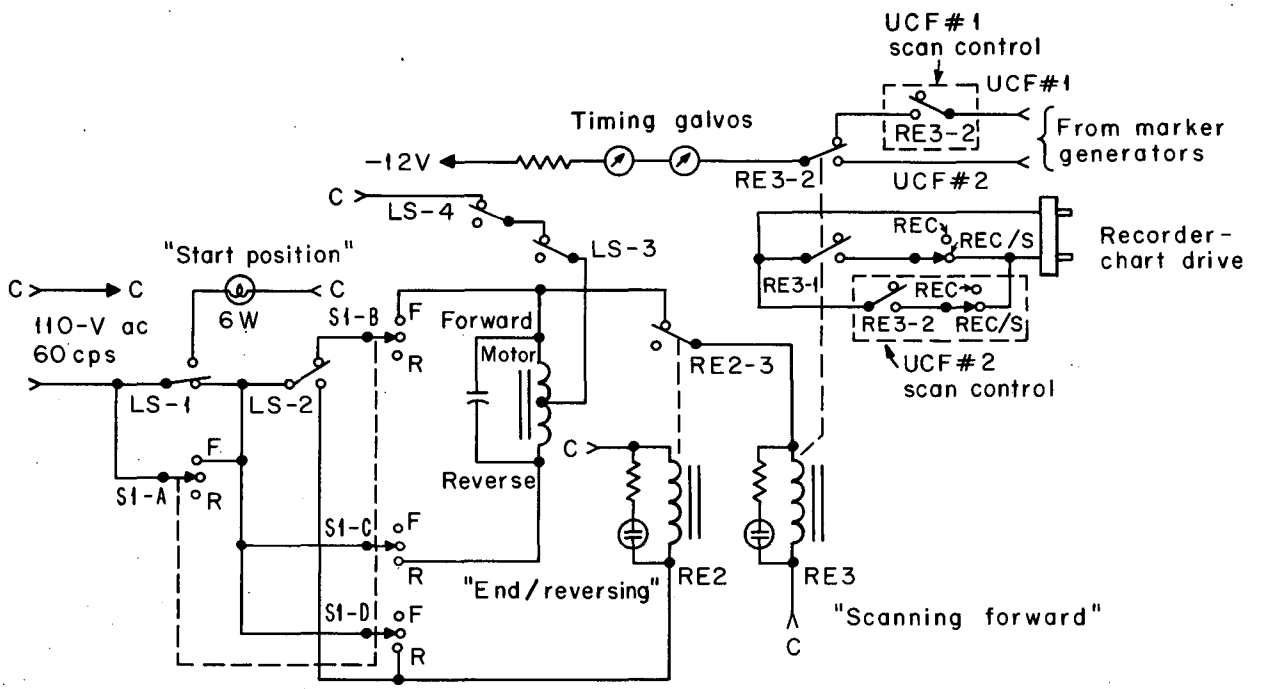

MUB-4729

Fig. 34. Simplified schematic of scan control (manual operation). All relays and limit switches are shown in deactivated position. RE2-3 keeps RE3 from operating through motor capacitor on reverse. LS-3 and LS-4 are safety limit switches. The recorder timing galvanometers and chart drive are operated by two independent scanning mechanisms, one in each of two centrifuges.

K. Scan Control, Automatic

Refer here to Fig. 35 for a schematic of the automatic scan control.

1. Scanner is at "Start position." LS-1 is engaged by scanner. Power is disconnected to motor and all relays ("Start position' light on.)

2. "Start impulse" from centrifuge energizes RE-1.

a. RE-1 bypasses LS-1, energizing motor through RE1-1 and RE2-1 and driving scanner forward to outer radius.

b. RE3 is energized through RE1-1, RE2-1 and RE2-3 ("Scanning forward" light on.)

(1). RE3-1 connects power to Visicorder chart drive.
(2) RE3-2 connects Visicorder timing galvanometers to Marker Generator of appropriate centrifuge. (Note: The same recorder is used for two separate scanning mechanisms, one in each of two centrifuges. Each scanning mechanism has its own controls, and the schematic nomenclature is the same for both.)

3. "Start impulse" terminates. The impulse duration is long enough to disengage LS-1, which bypasses RE1-1 before the impulse terminates. The impulse must be shorter than the time required to scan and return to the "Start position." If not, RE1-1 renders limit switch LS-1 ineffective on the return scan. In practice, the starting impulse also operates the shutter (shutter can be operated manually), exposing the scanner to light, and so impulse duration must be longer than the scan time.

4. Scanner advances to "End" position.

a. Scanner engages LS-2. RE2 is energized through LS-1 and LS-2 (End/reversing" light comes on).

(1) Motor is energized in the reverse direction, receiving power through LS-1 and RE2-1.
(2) RE2-2 are holding contacts for RE2, bypassing LS-2 when the scanner leaves the "End" position.
(3) RE2-3 disconnects power to RE3.

(a) RE3-1 disconnects power to the recorder-chart drive.
(b) RE3-2 disconnects the timing galvos from the relevant Marker Generator.

5. Scanner returns to "Start Positon" and engages LS-1, disconnecting power to the motor and relays. The cycle is complete. The scanner remains at the start position until it receives another start impulse from the centrifuge.

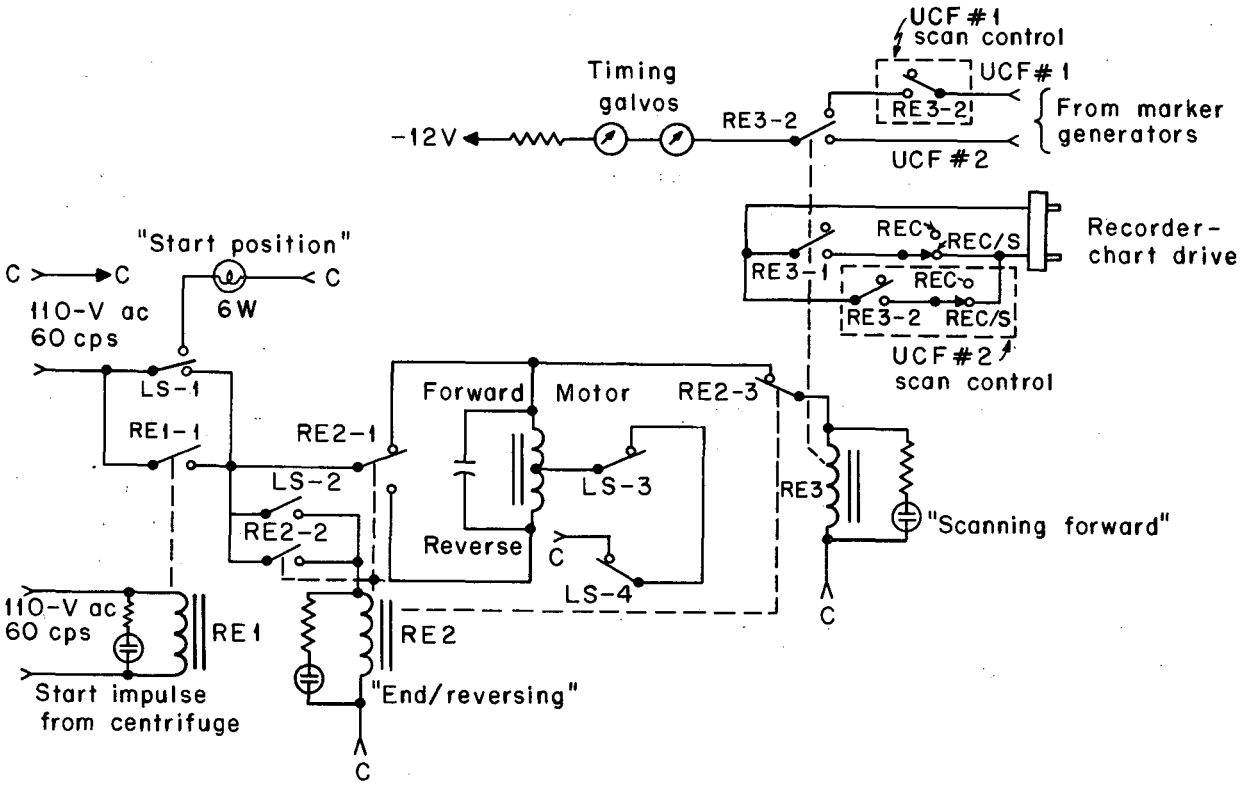

MUB-4730

Fig. 35. Simplified schematic of scan control (automatic operation). All relays and limit switches are shown in deactivated position. RE2-3 keeps RE3 from operating through motor capacitor on reverse. LS-3 and LS-4 are safety limit switches. The recorder timing galvanometers and chart drive are operated by two independent scanning mechanisms, one in each of two centrifuges.

L. Scan-Speed Selector

The scan-speed selector (Fig. 68, Appendix B) comprises circuitry that operates one of four solenoid clutches, each of which moves the scanning photomultiplier at a different rate. The drive motor turns a chain of gears (Fig. 36), the number of which depends upon the scan speed selected. Motor direction, therefore, must be adapted to the number of gears involved. The Scan-Speed Selector includes circuitry for returning the scanner at its fastest speed, but the fast return can be disabled if desirable.

One scanner (Machine I) employs larger clutches than the other. Larger clutches require greater physical separation, and so a 20-tooth spur gear is added as shown in Fig. 36.

M. Galvanometer Selector, Two Ultracentrifuges

The Visicorder, which accommodates as many as 14 channels, records traces from two centrifuges, simultaneously in some cases (Fig. 69, Appendix B). It is generally desirable that a given recording include galvanometer traces from one centrifuge only. Because of this, a displacing circuit has been added to remove tracings from the undesired galvanometers when a given scanner is operating. A selector switch indicates the machine whose galvos are active. The alternate scanner takes precedence during the time that it is scanning forward. The selector switch includes a third position that disables the displacing circuitry.

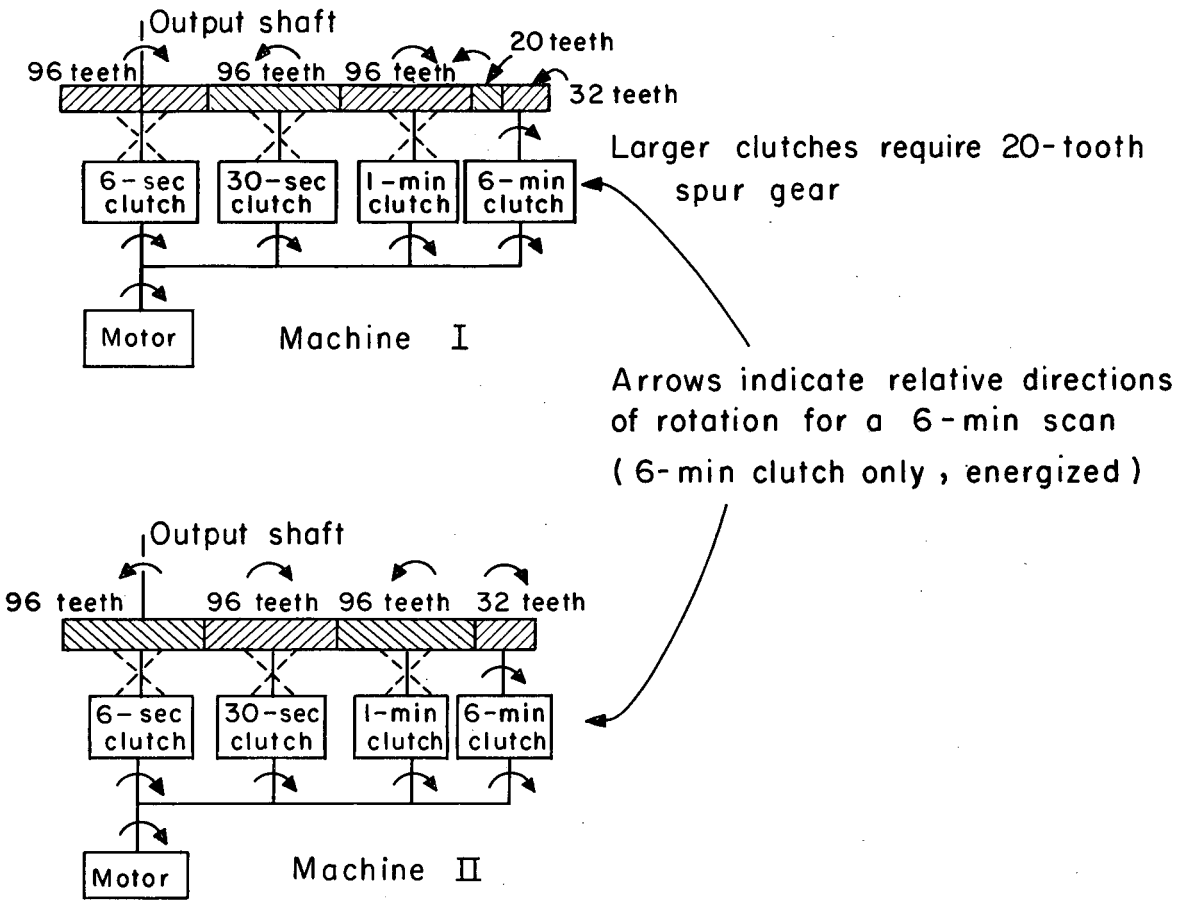

MUB-5839

Fig. 36. Drawings to illustrate transmission design. As Machine I clutches are larger than those of Machine II, the 20-tooth spur gear is added. The spur gear compensates for the greater physical separation demanded by the larger clutches.

Table I. Operational unit, Control Function Chart.[a]

Control	Function
Sector/cell	Adapts circuitry to cell type used--single or double sector.
Cell	Selects the cell to be recorded. Must be set according to the number and type of cell(s). Lower markings indicate proper settings for one double sector or for two single-sector cells.
RPM	Adapts circuitry to centrifuge speed.
Mode	Determines sector(s) recorded. Also determines whether response is linear or logarithmic.
Filter	Selects the function high-frequency response. Set according to scanning rate and noise.
Trace Amplitude	Controls Visicorder deflection for a given optical density change.
Set	Controls set-pulse amplitude to the switching circuits. Adjusted for proper switching when operating with two cells, single or double sector.
Delay	Controls the instant of switching. Adjusted for proper switching.
Trace Position	Determines function trace positioning relative to the Visicorder paper.
Baseline	Depressed to indicate the trace position corresponding to zero optical density.
Null	Attenuates sample pulses preceding subtraction. Balances the reference and sample channels under common density conditions.
Reference Amplitude	Attenuates reference pulses preceding subtraction. Permits balance if Null control does not have sufficient latitude. Should be at highest possible setting that permits a null.
PM/DARK	Determines scanning-photomultiplier power supply voltage in the absence of light. Power supply must be set for external regulation. Must be adjusted subsequent to photomultiplier power supply adjustment.
Derivative Amplitude	Controls Visicorder deflection for a given derivative amplitude.
Frequency Response	Determines derivative high-frequency response. Set according to scanning rate and noise.
Calibrate	Attenuates sample pulses, simulating solutions of various optical densities. Scanner must be at the air space, Mode set to Difference, and OD depressed.
OD	When OD is depressed, the function galvanometer assumes a position determined by Calibrate. When released, the function galvanometer returns to its zero OD position.
Derivative Position	Determines derivative trace positioning relative to the Visicorder paper.

[a] See also Fig. 25.

V. OPERATION

The control function chart of the Operational Unit is shown in Table I.

A. Two Double-Sector Cells

Load the rotor as shown in Fig. 1. Set Sector/cell for double-sector operation and cell selector to position 1 or 2. Position the scanner at the air space (all pulses have the same amplitude) and adjust the photomultiplier supply voltage control (External regulation) for 2-V output pulses. (The oscilloscope is easier to synchronize if triggered externally from the Scope Sync. jack on back of Operational Unit.) This adjustment ensures that the photomultiplier is operated in a linear region, that the switching circuits are triggered with an adequate signal, and that the logarithmic voltage compressor operates at the proper level.[22] Note the photomultiplier supply voltage registered on its meter, close the shutter, and adjust the PM-DARK control for the same voltage. The PM-DARK adjustment ensures that the photomultiplier supply voltage does not rise to excessive values in the absence of light. The dark voltage must not be set too low, however, because if it is the pulses due to an illuminated region are inadequate to operate the relay that connects the regulating circuit.

Set the RPM control according to centrifuge speed, turn on the stationary-photomultiplier power supply,[23] place the Mode switch at Reference, and record a scan. The resulting trace should be flat and include a radius marker. Examine the reference trace, then adjust the Trace Amplitude, Trace Position, and Filter controls accordingly. Filter, which is set according to scanning time (Fig. 25), determines the high-frequency response and influences resolution and output noise. If Filter is used judiciously in combination with slower scanning speeds, a high degree of resolution can be obtained with comparatively noisy photomultiplier pulses.

Change the Mode switch to Difference, return the scanner to the air space, and adjust Null until depressing Baseline does not change the recorded level. This adjustment balances the gates under common optical density conditions, and the function galvanometer assumes a position that corresponds to zero optical density. Subsequent traces in the Difference mode record density difference between reference and sample of the selected cell. (If a calibration is desired, trace amplitude can be adjusted to provide the desired density deflection per optical density, as indicated in Sec. V. D). The Difference traces of both cells should be recorded several times in order to confirm set-pulse performance. Set pulses ensure that the system records the same cell every scan with the cell switch at a given position. If set-pulse amplitude is incorrect, switching becomes erratic and produces inconsistent and/or noisy traces. If the traces are noisy the stationary-photomultiplier supply should be turned off for us to see if noise is reduced; if it is, set pulses are probably responsible. Adjust the Set control until the traces are satisfactory. If this is not possible, it may be necessary to adjust the Schlieren optics as described in Sec. VI. E.

If set-pulse amplitude is satisfactory, a radius marker should appear in the Difference trace of both cells. If it doesn't the scanner-activated switch probably needs adjustment. The adjustment is not routine so is also discussed in Sec. VI. E.

B. Double-Sector Operation, One Cell

Operation with one double-sector cell is essentially the same as with two, the principal exceptions being cell loading (see Fig. 2), and the setting of the cell selector [which is set to "0" (1 DS)]. The "0" position biases the cell switches so that both cell gates are continuously open. Set pulses are unnecessary. The Schlieren light and stationary-photomultiplier supply can be turned off.

C. Single-Sector Operation, Two Cells

The first requirement for this type of operation is that the cells be loaded with regard to rotation as shown in Fig. 3. Sector/cell switch is set at "1", the cell selector at 2 (SS). If the cell selector is set at 1, pulse routing becomes erroneous--the reference pulses are admitted to the sample hold and vice versa, and Visicorder deflection is reversed accordingly. Subsequent operating procedure is the same as with two double-sector cells. Set pulses are necessary throughout the scan; the scanner-activated switch is not permitted to disconnect them when the controls are set as indicated. Set-pulse amplitude is generally more critical with single-sector operation because the set pulses cause switching every rotor revolution.

D. Calibration

To measure optical density, record the Difference traces in the conventional manner, then position the scanner for reference and sample pulses of equal height and 2-V amplitude. Depress the OD pushbutton and adjust the Calibrate dial to produce the same deflection as that of any part of the recorded trace one wishes to measure. Note the resulting dial setting and consult the calibration graph (Fig. 33) to find the corresponding optical density. System performance is quite linear up to optical densities greater than 1.5 so the deflection can be considered proportional to density at lesser values. Optical density in the centrifuge is 1.2 times the value for a 1-cm path length.

Leaky cells are not uncommon. If the measured density differs from the expected value, one should observe the photomultiplier pulse amplitude ratio, reference to sample. The logarithm of that ratio represents optical density for a 1.2-cm path length. Optical density, when a 1-cm path length is used, is 0.833 times that for a 1.2-cm path length.

The calibration graph (Fig. 33) was derived empirically from a single solution of known density. In order to obtain the plot, select a solution with optical density approximating 1. Assuming an arbitrary density of 0.97, adjust the Trace Amplitude control for 97-mm deflection when operating in the Difference mode. With the assumption of linearity, each mm represents an

optical density of 0.01. Depress the OD pushbutton, adjust the Calibrate dial for 97-mm deflection, and record the dial setting required. Choose other dial settings and plot the resulting deflection (each mm represents 0.01 OD). The curve is flat at higher optical densities because the charging diodes require a fractional volt to become conductive. Nonlinearity is due to attenuator loading, and it does not indicate that the system response is nonlinear.

If the calibration is compared with solutions of measured optical density, agreement is excellent over the linear range. The calibration crosscheck is easier if one uses a sample sector with three compartments; each compartment should be filled with a solution of appropriate density.

E. Derivative Operation

If a derivative is required, the related Amplitude, Position, and Frequency Response controls are adjusted to record the derivative simultaneously with the desired function (see Fig. 37). Derivative amplitude is directly proportional to scanning speed, and cleaner traces can be obtained with fast scans. If resolution is inadequate or the derivative waveform distorted, Filter and Frequency Response must be adjusted accordingly--perhaps by slower scanning.

Most noise originates at the scanning photomultiplier; higher dynode voltages increasing noise. It is desirable, therefore, that the photomultiplier operate at the lowest possible voltage that yields 2-Vpulses (below 1000 V is desirable). Light intensity and illumination (related to wavelength, light source, aperture, and photomultiplier-slit area) determine the voltage required, and one or both may be altered for cleaner traces.

It should be emphasized that the derivative responds to the change with time of the recorded function. Steeper boundaries and faster scanning rates, therefore, yield derivative signals of greater amplitude, improving signal/noise ratio accordingly. If one is interested in the derivative of a mildly sloping boundary, he should scan faster. The resulting integral trace will be limited in resolution and some portions of the recorded trace will be a distorted version of the true profile. Even so, the boundary can be recorded with fidelity. Boundary fidelity can be tested by lowering the filter setting until the boundary steepness is unaffected by filter setting. When the optimum integral is obtained, set the Frequency Response control to the highest setting that produces an undistorted derivative. If the radius marker is overly distorted, one can superimpose sequential traces in order to disclose boundary movement. Appendix C includes tables showing frequency characteristics as a function of filter and frequency-response settings.

F. Crosschecks

The system includes a number of crosschecks to provide assurance of satisfactory performance. For example, the Mode-selector switch permits one to record the density profile of every sector. Sector traces in combination with oscilloscope pulses are a powerful tool for detecting switching anomalies. Knowledge of cell contents and menisci location are also helpful.

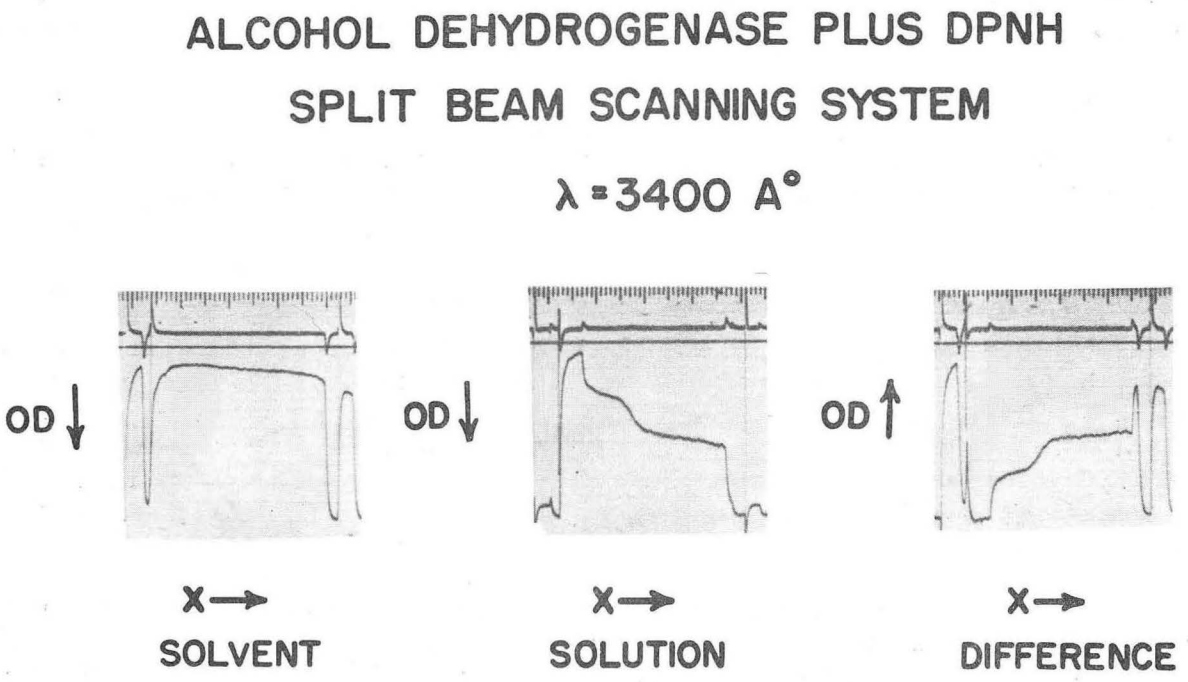

Fig. 37. Visicorder traces illustrating derivative operation in each of three modes. The response is logarithmic, and therefore indicates optical density as shown: (a) A scan recorded with the Mode switch in Reference position. The system responds to reference-cell content, a solvent (0.1 molar phosphate buffer, pH 7.4). The upper trace records the derivative. (b) A repeat scan with the Mode switch in Sample position. The system now responds to sample-cell content--alcohol dehydrogenase plus DPNH dissolved in the solvent indicated above. The radius markers are rejected by the gating circuits. The derivative is inverted for reasons described in the text. (c) A third scan with the Mode switch in Difference position. The system responds to the density difference between cells, compensating for non-uniform illumination. Radius marker amplitudes have no significance in terms of optical density. The sharp spike following the left-hand radius marker results from a disparity between the radial position of the reference and sample cells. The spike adjacent to the right-hand radius marker results from sedimentation in the sample cell. Preceding modification, one double-sector cell. Derivative traces from the modified version are much cleaner.

The Mode switch includes a Reference Transmittance position that bypasses the log amplifier. Such bypassing permits linear recordings of either reference sector and facilitates alignment and focusing of the optics. If one wishes to study the illumination profile or the menisci, he must set the photomultiplier supply for internal regulation. The transmittance modes are useful because they accentuate those changes normally minimized by the logarithmic circuit. The log circuit, on the other hand, is useful in exaggerating changes that occur at input amplitudes that are small relative to normal-amplitude pulses. The Mode switch includes a position for recording Sample Transmittance. The transmittance modes are not truly linear but they are useful for aligning the optics. They also facilitate trouble shooting. The Baseline pushbutton is disabled in the transmittance modes.

The Baseline pushbutton is useful for checking null accuracy. For example, null is generally made at the air space, a position where reference and sample-pulse amplitudes are essentially equal. When nulling, we compensate slight disparities between the reference and sample channels, adjusting their relative gain until the pulses cancel. If both pulses are reduced to zero or disconnected (Baseline depressed), the difference should remain at zero and the function galvanometer should not change position. If it does, the subtraction, or null, was imperfect in the first place. Depressing Baseline indicates the galvanometer position where perfect null prevails. Compare this position with pertinent parts of the Difference trace to ensure that the null was made with the required precision. The Baseline pushbutton is also useful in revealing the influence of switching spikes. If those spikes charge the holding circuits to any appreciable value, the baseline shifts when switching commences; i.e., when the scanner moves from regions of darkness to light and vice versa, even though the Baseline pushbutton is depressed. Null accuracy is related to the amount of shift, with smaller shifts yielding greater accuracy.

Concerning Visicorder galvanometers, it is desirable that the integral galvo be mechanically positioned at the zero optical density (12 cm) position with the Trace Amplitude control at zero. This ensures that the electrical and mechanical zeros coincide, and that the baseline does not move when the mode selector is changed to sample mode.

Reference-pulse regulator performance can be checked in several ways. One is for us to observe reference-pulse amplitude while scanning. The reference pulses should remain essentially constant in amplitude throughout the scan when the photomultiplier supply is set for External regulation. A Visicorder trace in the Reference Transmittance mode is also helpful, especially when compared with a Reference Transmittance trace taken with the photomultiplier supply set for Internal regulation.

Calibrator accuracy can be confirmed if one measures the pulse-amplitude ratio as described in Sec. V.D.

G. Anomalies

Anomalies appear in many forms. Sample traces, for example, should not include a radius marker, but if they do it may be because of an incorrect Delay setting. If the gating circuits switch too soon, the sample hold charges up to that residual level of the radius-marker pulse that exists at the time of switching. This switching error can be corrected by one's advancing the Delay control and adjusting for minimum radius-marker height with stable traces and with the Mode switch in Sample position.

Anomalies sometimes appear also in the reference-cell traces, as shown in Fig. 38. If they do, it may be because of light scattering. Light scattered by the cells or by the radius-marker hole sometimes produces spurious pulses when the scanner is near the radius-marker image. These pulses are displaced in time from the desired pulses and are usually apparent on the oscilloscope. When exaggerated by the logarithmic amplifier, they have appreciable magnitude, as shown in Fig. 39 (center pulse, upper trace). If the traces seem to indicate scattered light, the oscilloscope should be connected to monitor the reference and sample holds. If scattered light is responsible, spurious peaks will appear as shown in Fig. 40(a), lower trace. This effect is apparent only if the holding-circuit discharge-time constant is short enough that its decayed voltage at the time of the spurious pulse is less than the logarithmic amplitude of the spurious pulse arriving.

Scattered light is sometimes evident in the recorded traces of only one cell. It is not evident in both cells because the switching circuits discriminate against it differently with the cell-selector switch at 1 than with the cell selector at 2. The reason becomes more apparent when one refers to Fig. 1. Scattered light pulses from the radius-marker hole follow Cell-2 pulses by 270-deg rotation; they follow Cell-1 pulses by only 90 degrees [the radius-marker (Schlieren) optics is displaced 180 deg from the absorption optics].

Sometimes the difference trace indicates less density at greater radii. This is contrary to the sedimentation process and is usually due to improper illumination. In the event of such traces, record the illumination profile (reference trace, internal regulation) and a sample trace with external regulation. In some cases the light transmitted at greater radii is more although the illumination is less, and optical density within the cell is constant with radius. This phenomenon might be due to light dispersion resulting from nonparallel light within the cell.

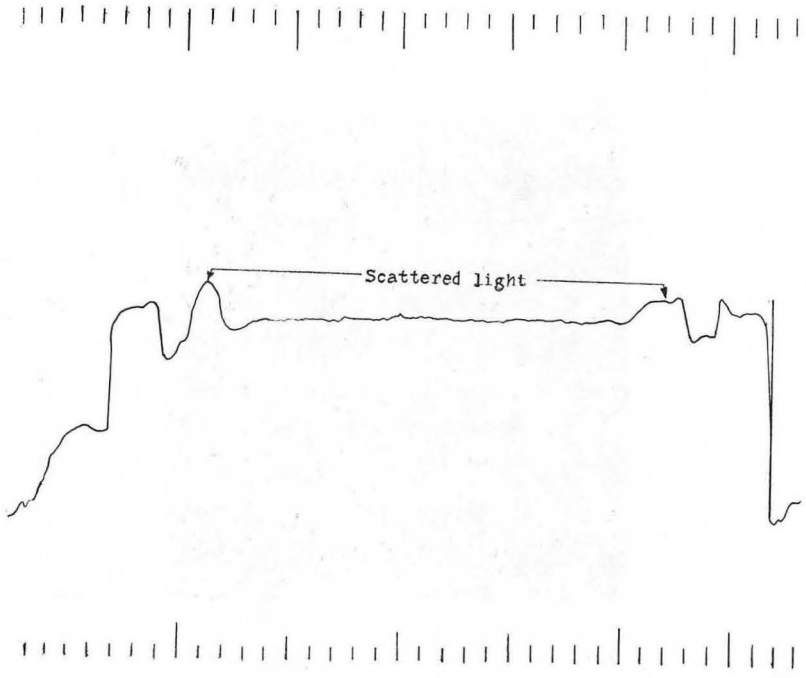

Fig. 38. Visicorder trace showing the reference-cell-profile distortion resulting from scattered light. The holding-circuit discharge-time constant is too short, as shown in Fig. 40. Preceding modification, one double-sector cell.

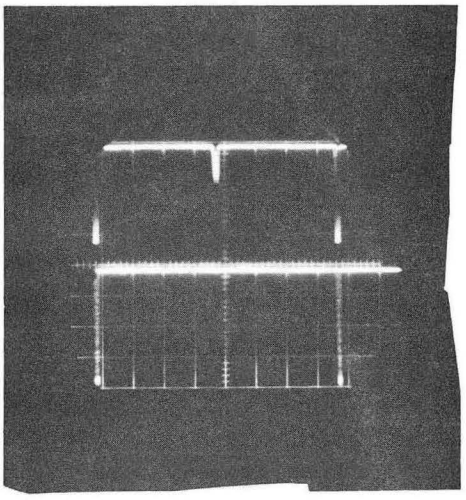

ZN-3606

Fig. 39. Single exposure of an oscilloscope trace, dual-beam, taken with the scanner positioned at one of the radius-marker holes. Scattered light is prevalent, producing spurious pulses when the two sectors (one double-sector cell) appear 180 deg after the radius marker. The upper trace is the log output (inverted), exaggerating the almost invisible pips that appear in the center of the lower trace (the photomultiplier-output pulses). The amplitude of the pulses from the scattered light is approximately 1% that from the radius-marker pulses. Preceding modification one double-sector cell.

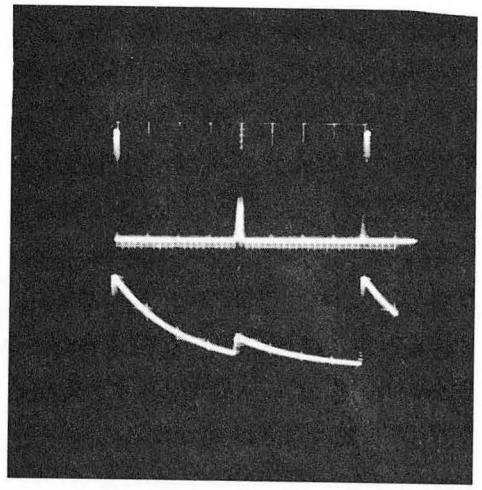

(a)

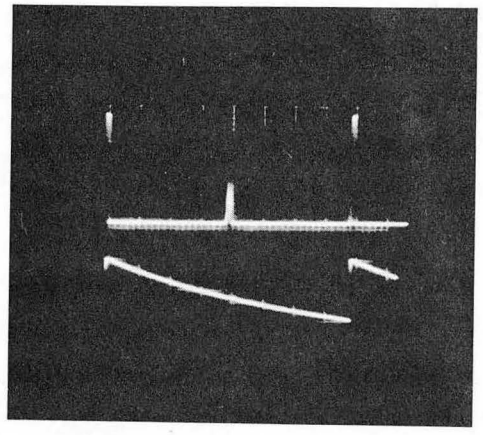

ZN-3605

Fig. 40. Oscilloscope traces, dual-beam, showing the reference-hold response to scattered light pulses: (a) The upper trace is the log output; the lower trace is the reference-hold voltage. The holding-circuit discharge-time constant is short, so the spurious pulses increase the average voltage output. (b) Same as (a) except that the holding-circuit time constant has been increased. The holding circuit no longer responds to the spurious pulses. Preceding modification, one double-sector cell.

VI. MAINTENANCE ADJUSTMENTS

A. Pair and Cell Gates

Refer to Figs. 28 and 60 (Appendix B).

1. Operate the system with two double-sector cells; make sure that the pair and cell gates are switching properly.

2. Turn both Bias controls counterclockwise (zero bias).

3. Set the Null and Reference Amplitude controls to 0, Sector/cell and Cell selector switches to position 2. (Cell-1 setting is also permissible.)

4. Monitor the reference charging-diode input with an oscilloscope; adjust R1 and R2 trimpots for minimum pedestal.

5. Monitor the sample charging-diode input with an oscilloscope; adjust S1 and S2 trimpots for minimum pedestal.

B. Regulating Gate

Refer to Figs. 28 and 63 (Appendix B).

1. Operate the system double sector; make sure that the regulating gate is switching properly.

2. Monitor the regulating-gate charging-diode input with an oscilloscope; adjust R trimpot for minimum pedestal.

3. Adjust the R Gain control to the minimum value producing satisfactory regulation. If gain is excessive, the regulator relay fails to de-energize in dark regions, and the photomultiplier-supply voltage becomes excessive.

C. Holding Circuits

Refer to Figs. 27 and 61 (Appendix B).

1. Complete the gate adjustments as indicated in Sec. VI. A.

2. Set the Null and Reference Amplitude controls to 1000.

3. Monitor the reference hold with an oscilloscope (10-MΩ probe); adjust trimpot G1 until the hold voltage decays to one-half its peak value (dc levels).

4. Monitor the sample hold with an oscilloscope probe; adjust trimpot G2 until the hold voltage decays to one-half its peak value (dc levels).

D. Bootstrap Amplifiers, Bias

Refer to Figs. 27 and 61 (Appendix B).

1. Complete the gate and holding circuit adjustments, Secs. VI. A and VI. C.

2. Set Trace Amplitude to 1000, Trace Position to 500, Null and Reference Amplitude controls to zero.

3. Adjust Reference Bias for 0.15 volt at reference charging-diode input. The function galvanometer should be at least 1 cm to the left of the base-line (zero OD) position (normally at the 12-cm position). If it is not, Reference Bias should be increased until it is; the spot appears at 11 cm if the base line position is at 12 cm.

4. Adjust Sample Bias until the Visicorder spot returns to the base-line position (12 cm).

E. Set-Pulse Adjustments

When making these adjustments, refer to Fig. 62. Set-pulse amplitude is critical, principally because the Schlieren light source is ac operated (60 cps). Such ac operation produces intensity modulation, which causes pulse amplitude to fluctuate more than tenfold. The height of a given pulse is related to the instantaneous line voltage prevailing when the rotor exposes light, and to the total illumination at the photomultiplier.

Light fluctuations are compensated somewhat by the addition of a pulse amplifier (Fig. 32) that raises low-level pulses to a satisfactory magnitude and limits high-level ones to a maximum. Amplification is not the total solution, however. Scattered light pulses from the cell images generally appear at the stationary photomultiplier even though it is not, in theory, positioned to intercept them. These scattered light pulses have an amplitude approaching the minimum set-pulse amplitude. They are displaced in time from a proper set pulse, and they produce erratic switching.

In order to counteract the scattered light we add a removable plate just after the camera lens of the Schlieren optics. This plate intecepts light from the cell images only and permits light from the radius marker to pass unattenuated. Set-pulse-amplitude adjustments are as follows:

1. Operate with two double-sector cells; set cell selector at 1; monitor Set jack (Fig. 25) with an oscilloscope.

2. Remove the yellow filter above the Schlieren light source.

3. Be sure that the stationary photomultiplier is positioned to intercept the radius-marker image. Rotate the photomultiplier until the set pulses are at a maximum and scattered light pulses have no appreciable magnitude.

4. Adjust the Schlieren-light aperture until the minimum set-pulse amplitude is approximately half the maximum value.

5. Adjust the removable plate following the Schlieren camera lens until the scattered light pulses are at a minimum. If the plate is positioned properly genuine set pulses are unaffected and scattered light pulses are reduced to much less than the minimum value of the legitimate set pulses.

6. Record the Difference traces of both cells several times. The traces should be clean and the system should record the same cell every time we scan with the Cell Selector switch at a given position. If it does not, adjust the set control until these conditions are met.

When set-pulse amplitude is satisfactory, a satisfactory radius marker should appear in the Difference trace of both cells. If it doesn't, the scanner-activated switch probably needs adjustment and the following procedure is indicated:

1. Set the selector switches to record cell-2 Difference.

2. Using the oscilloscope, position the scanner at the inner radius of the radius marker.

3. Turn the micrometer adjustment that activates the set-pulse switch (Fig. 19) counterclockwise until the shoulder no longer depresses the switch and the radius marker produces a Visicorder deflection. Record a scan, then examine the trace. If the entire radius marker does not appear, the micrometer should be adjusted counterclockwise until it does. If turned too far (ccw), anomalies appear at the cell bottom, indicating that set pulses have been disconnected too soon.

VII. PERFORMANCE

A number of performance tests were conducted. Many of these involve oscilloscope presentations and some were photographed to convey performance characteristics more accurately. One photographic series reveals pulse separation. Other photographs disclose switching relationships, holding-circuit performance, and logarithmic response. Also included are representative Visicorder tracings and a calibration plot to indicate the range over which the system is linearly responsive to sample optical density. Some tests were conducted preceding conversion, but the results are relevant to the modified version. Tests prior to conversion are so indicated. Some oscilloscope traces are included in Appendix D.

A. Visicorder Traces

Figure 41 is an interesting demonstration of double-sector performance with two cells. Figure 42 records performance when the light source was on the verge of failure, with the light pulsing in amplitude almost periodically. Another series, Fig. 43, illustrates compensation resulting from the difference system when the illumination profile is extremely nonuniform. Figure 44 illustrates regulator performance.

B. Oscilloscope Photographs

Pulse-separation photographs are shown in Fig. 45. With regard to switching, the gating circuits have been very reliable. It is frequently possible to cover the speed range between 1000 and 60 000 rpm without changing the Delay control.

The switching time measures less than 1 μsec, as shown in Fig. 46. This photograph confirms that switching occurs in the time interval between "mates."

Figure 47 shows switching signals applied to the pair gates. The reference and sample cells are gated out-of-phase, as indicated. One-shot duration is five times greater when the centrifuge is operated below 6200 rpm.

Also interesting is the time required for each hold to charge to the input-signal level. This time is related to the RPM setting. When set for 60 000 rpm, the sample-hold charging time measures 2 μsec, as shown in Fig. 48. The discharge time constant is shown in Fig. 49.

Another concern is logarithmic response to pulses, especially at 60 000 rpm. With this in mind, another series was taken to record frequency and amplitude characteristics. One photograph, Fig. 50, shows log amplifier response to a photomultiplier pulse pair. The waveform is clean, and the pulse-amplitude ratio conforms to the value expected from manufacturers' date (Fig. 51).

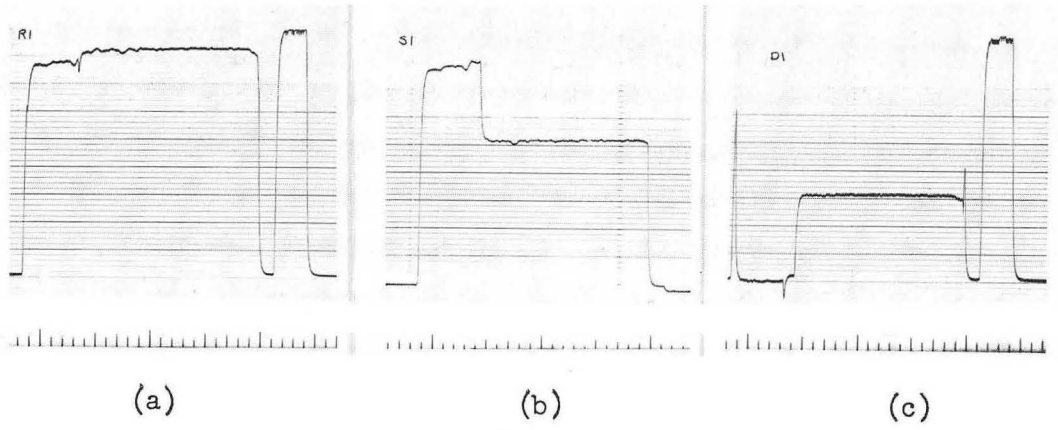

ZN-4904

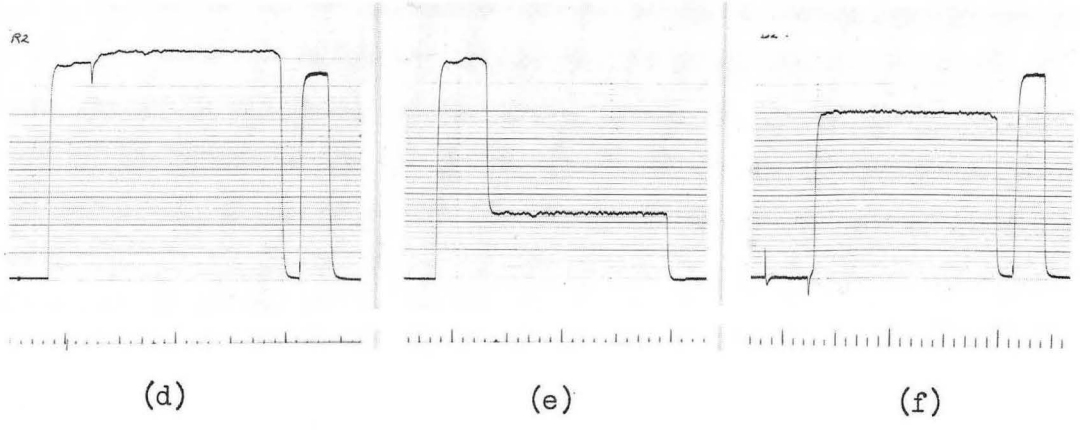

ZN-4905

Fig. 41. Visicorder traces illustrating performance with two double-sector cells. The reference-pulse regulator was disabled in order to indicate the improvement resulting from the difference system. (a) A scan recorded with the Mode selector at Reference, the Cell selector at 1. (b) A repeat scan with the Mode selector at Sample, Cell selector at 1. (c) A third scan with the Mode selector at Difference, Cell at 1. (d) Cell selector at 2, Mode selector at Reference. (e) Cell at 2, Mode selector at Sample, (f) Mode Selector at Difference, Cell at 2.

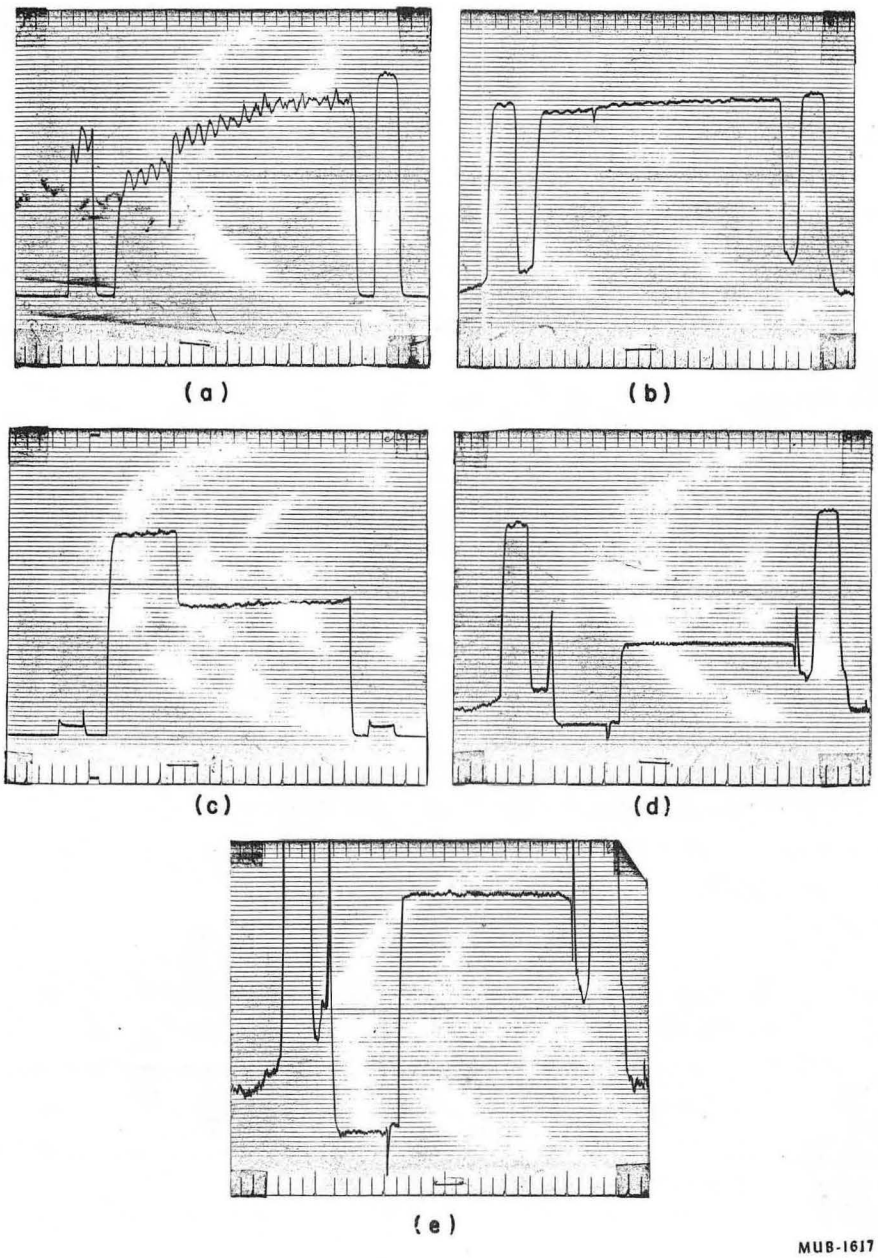

Fig. 42. Visicorder traces recording an experiment in which the light source was on the verge of failure, pulsing in amplitude almost periodically: (a) A scan recorded with the Mode switch at Reference Transmittance. This is a linear response to reference-cell content. (b) A repeat scan with the Mode switch in Reference. Response is logarithmic, so the fluctuations are less apparent. (c) A third scan with the Mode selector at Sample. (d) A fourth scan with Mode at Difference. The light pulsations cancel, excluding radius markers which are expected to fluctuate. (e) An expanded version of (d). The Trace Amplitude control was advanced considerably, moving the upper portion of the radius markers completely off the paper. Preceding modification, one double-sector cell.

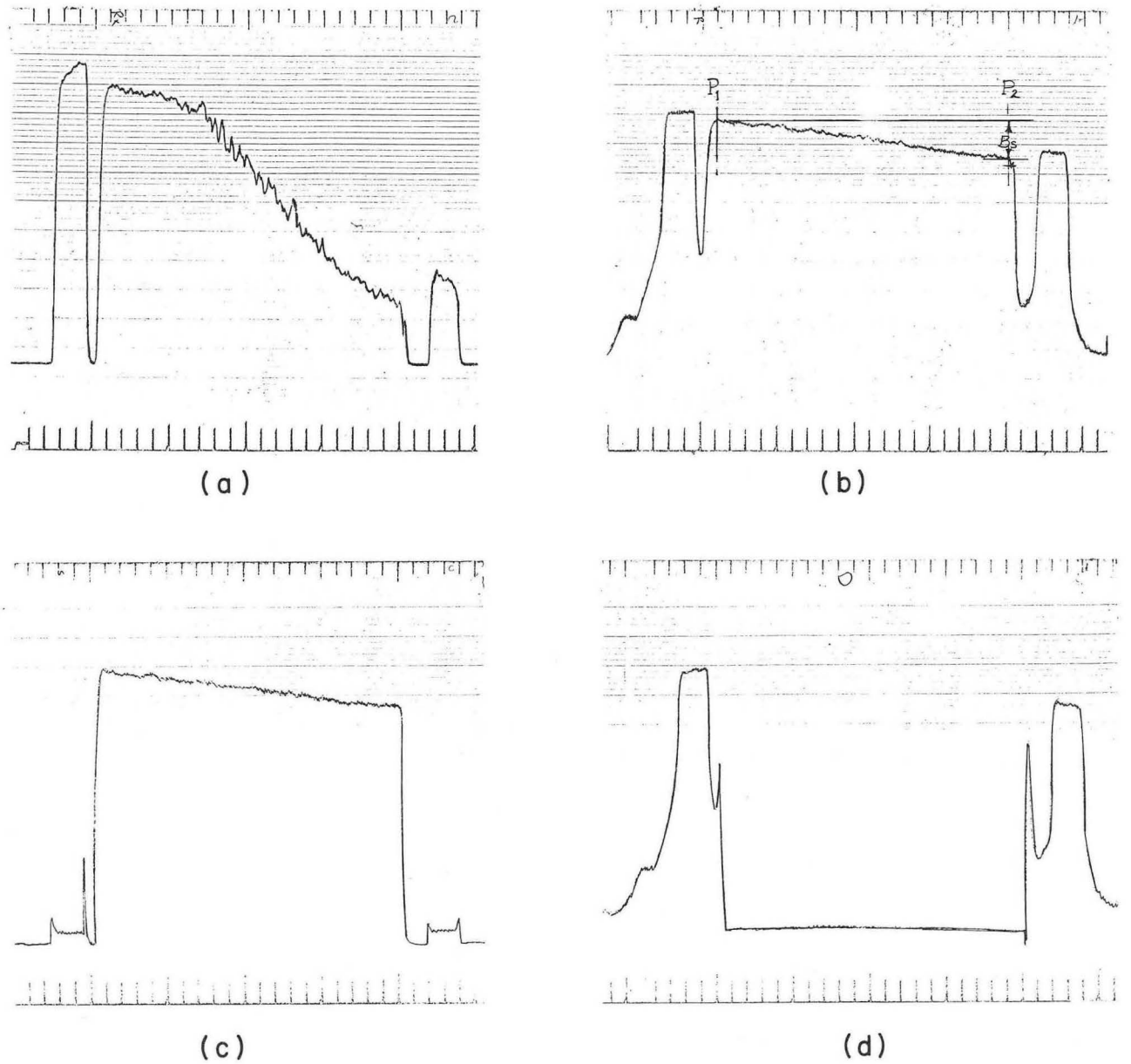

Fig. 43. Visicorder traces illustrating the compensation resulting from subtraction when the illumination profile is extremely nonuniform. Both cells were empty; B_S shows the base-line shift between scanner positions P1 and P2: (a) Mode switch in Reference Transmittance. This is a linear recording to emphasize the degree of nonuniformity. (b) Mode selector at Reference. This is a logarithmic response to the reference cell. (c) Mode switch at Sample. (d) Mode selector in Difference position. Preceding modification, one double-sector cell. Note the fiducial markers.

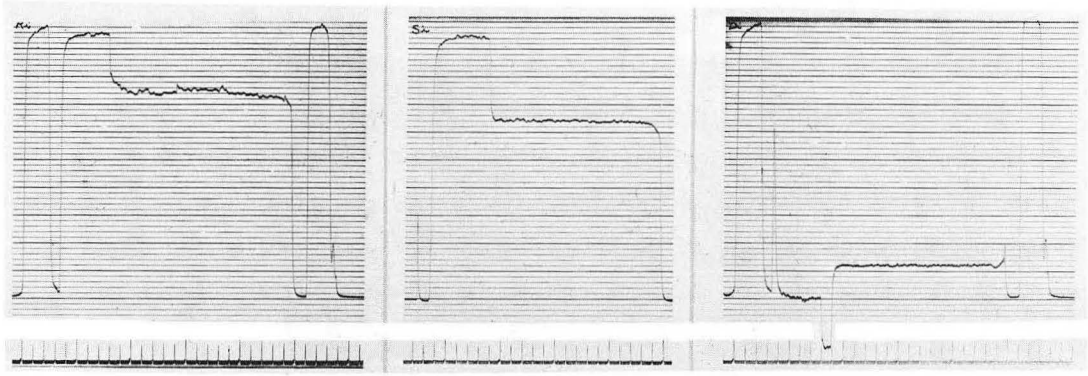

(a) (b) (c)

ZN-4906

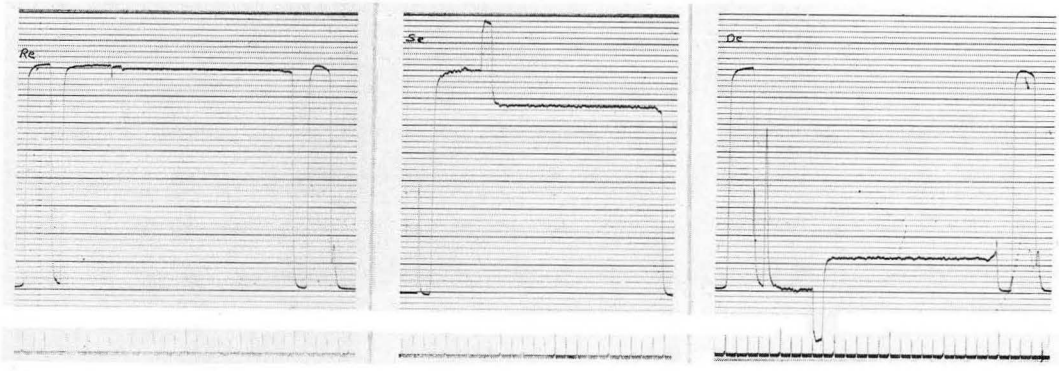

(d) (e) (f)

ZN-4907

Fig. 44. Visicorder traces illustrating regulator performance, one double-sector cell. Solution from the sample sector leaked into the reference sector. (a) Mode selector at Reference, internal regulation. (b) Mode at Sample, internal regulation. (c) Mode at Difference, internal regulation. (d) Mode at Reference, external regulation. Note how the regulator compensates for changes in reference-pulse amplitude [see (a)]. (e) Mode at Sample, external regulation. (f) Mode at Difference, external regulation.

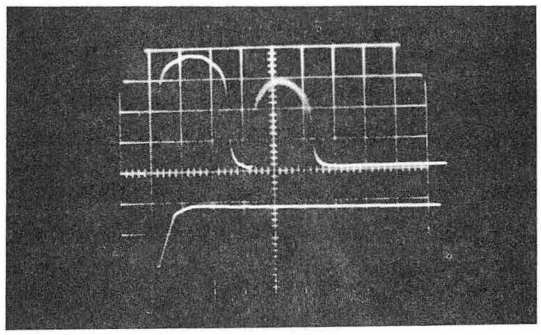

(a)

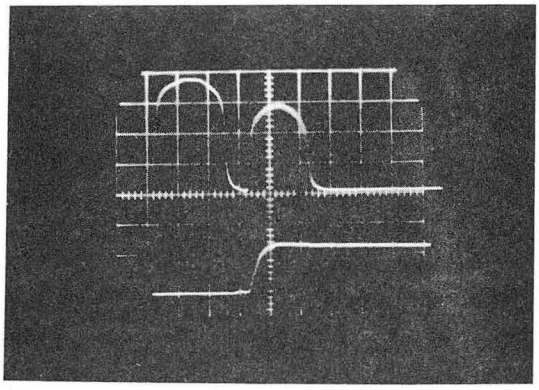

(b)

ZN-3604

Fig. 45. Pulse-separation photographs at 60 000 rpm. Each circle is a single exposure of an oscilloscope trace, dual-beam: (a) The upper trace shows a photomultiplier pulse-pair as it appears at the output of the log amplifier. The trace beneath it shows the reference-hold voltage. (b) Sample-hold response to the same pair of input pulses. Comparison of (a) and (b) shows that the pulses are effectively separated, and that each of the two "mates" is routed to the appropriate holding circuit. Preceding modification, one double-sector cell.

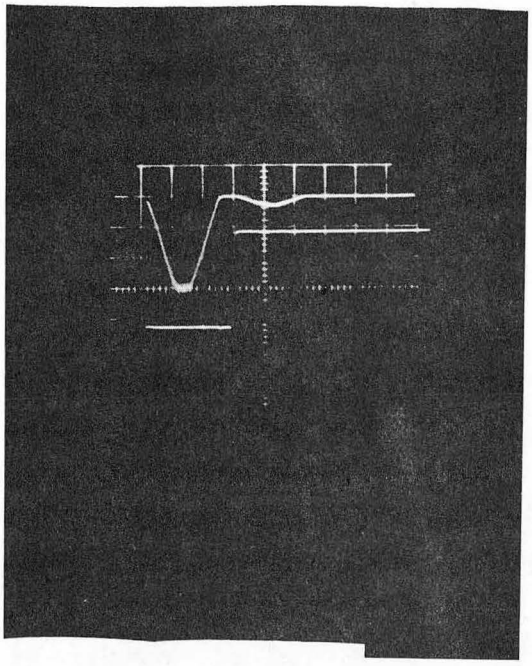

ZN-3603

Fig. 46. Switching photographs at 60 000 rpm--a single exposure of a dual-beam trace. The upper trace shows a photomultiplier pulse pair; the lower trace is the switching signal to the sample-pair gate. The sweep speed is 5 μsec/cm, indicating that the switching time measures less than 1 μsec. This photograph also confirms that switching occurs in the time interval between "mates." Preceding modification, one double-sector cell.

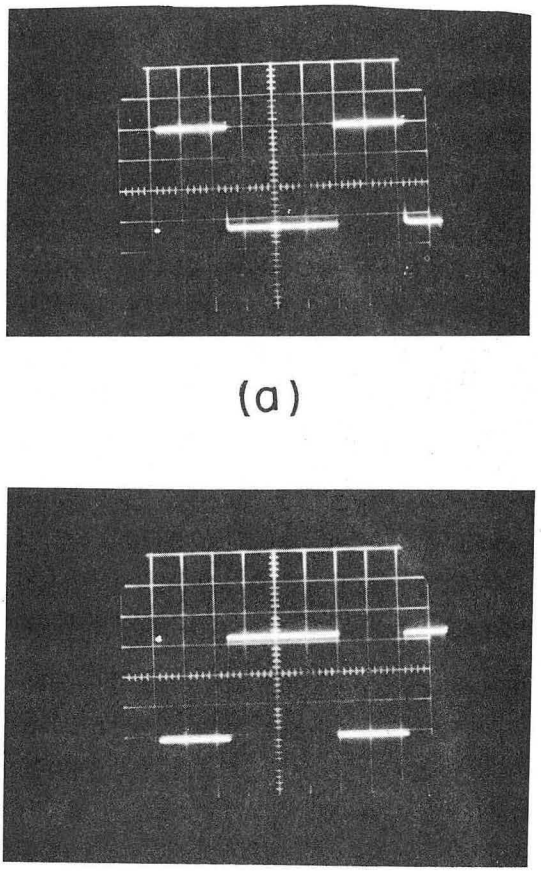

Fig. 47. Switching signals applied to the reference and sample pair-gates. Oscilloscope sweep speed is 200 μsec/cm; vertical sensitivity is 10-V/cm, and zero volts corresponds to the centerline of the reticle: (a) Switching signal applied to the reference-pair gate, open for 720 μsec at the centrifuge speed indicated. (b) Switching signal to the sample-pair gate, open for 440 μsec, the measured duration of the one-shot pulse. One-shot duration is increased to 2 msec when operating below 6200 rpm. Preceding modification, one double-sector cell.

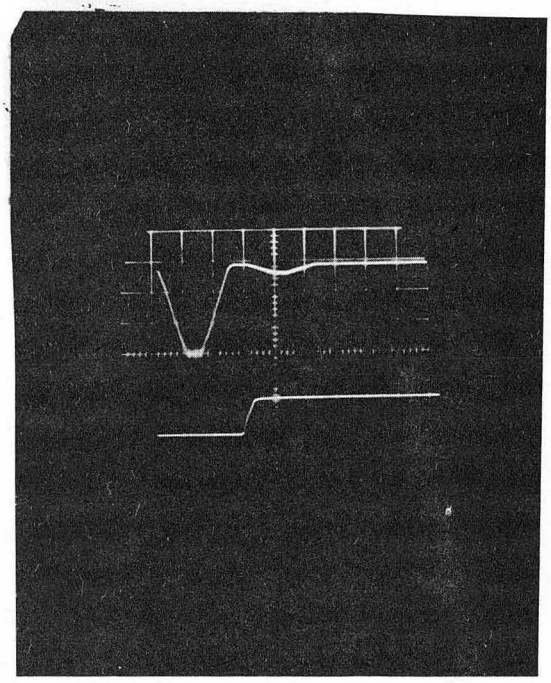

ZN-3601

Fig. 48. A single exposure, dual-trace, for measuring the sample-hold charging time at 60 000 rpm. The upper trace shows a photomultiplier-pulse pair; the lower trace indicates the sample-hold voltage with Mode at Reference and with a 6-V battery connected to the input (pin 9) of the sample gate. When so operated, none of the pulses is applied to the sample-gate input. The sample-hold responds to the 6-V battery, alternately connected and disconnected by the switching circuits. The sweep speed is 5 μsec/cm. The charging time measures 2 μsec with the RPM control set for 60 000 rpm. Preceding modification, one double-sector cell.

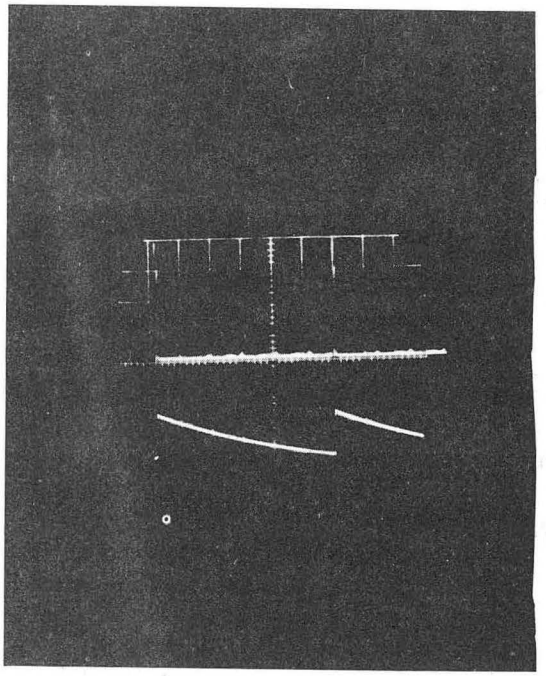

ZN-3602

Fig. 49. Oscilloscope traces illustrating sample-hold discharge-time constant. Oscilloscope sweep speed has been reduced enough to show the sample-hold response to two sets of pulse pairs. The time separation between "mates" is very small compared to the time per revolution, so it is difficult to detect the pulse-pairs which are very prominent in Fig. 45. The decay-time constant is very effective in increasing the average output voltage. With the time constant shown (a representative value), the average output level is approximately 75% of the peak input voltage. Preceding modification, one double-sector cell.

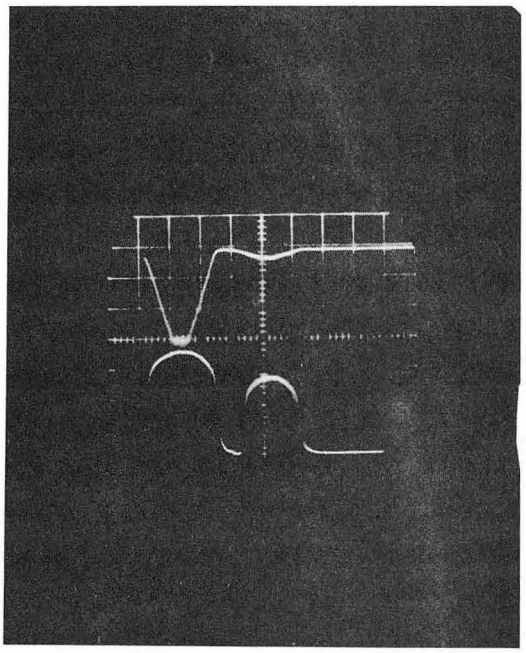

ZN-3600

Fig. 50. Single exposure, dual-trace, showing the logarithmic-amplifier response to a photomultiplier pulse pair at 60 000 rpm. The output waveform from the log amplifier (compressor plus amplifier) is indicated by the lower trace. The log compressor exaggerates the noise superimposed upon low-amplitude pulses (high optical density). The waveform is clean, and the pulse-amplitude ratio conforms to the value expected from manufacturer's data, Fig. 51. Preceding modification, one double-sector cell.

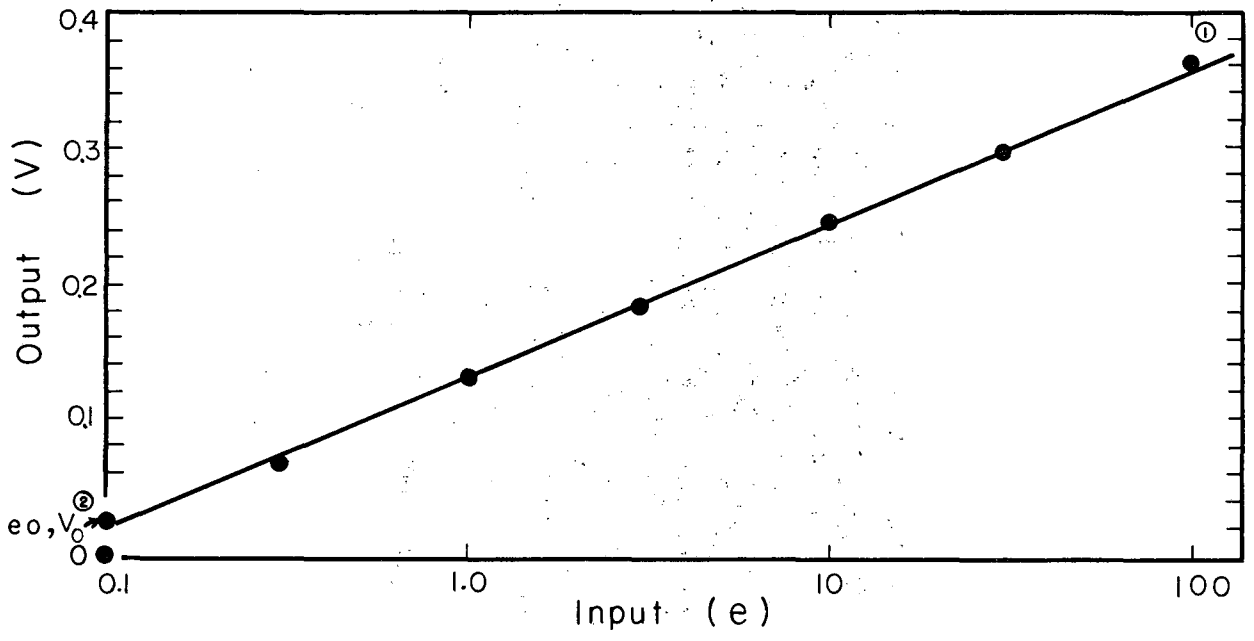

Fig. 51. Logarithmic-compressor amplitude response, manufacturer's data. Test points are at 1 kc. Model C-7A logarithmic voltage compressor (Kane Engineering Laboratories, Palo Alto, California).

At higher optical densities the noise is exaggerated by the properties of the logarithmic compressor. This is more readily apparent if one considers that the same noise is superimposed upon both the reference and sample pulses. If both pulses have large magnitudes relative to the noise, the noise component is minimized by the logarithmic properties. The same noise superimposed upon a pulse of lesser amplitude (higher optical density) produces a greater fluctuation at the compressor output, as shown in Fig. 50.

C. Calibration Curves

Log-compressor amplitude response is shown in Fig. 51. System response to pulse amplitude is also important. Visicorder deflection versus reference-pulse amplitude is indicated in Fig. 52. Data were taken with the scanner positioned at the radius-marker hole. The photomultiplier-supply voltage was adjusted to produce pulses of various heights and the Visicorder deflection was recorded. Switching circuits were disabled for the test. The resulting plot indicates that response is logarithmic over an extended range. Subsequent tests revealed that nonlinearity at the higher input levels can be attributed to the log compressor. The plot does not pass through the origin because the charging diode requires a fractional volt to become conductive.

The most important consideration of performance is system response to solutions of measured optical densities. This is shown in Fig. 53. It represents total response and indicates that the system is linearly responsive (accuracy ± 1% of full-scale deflection) to optical densities between 0 and 1.8.[24] Maximum sensitivity is approximately 20 cm/OD.

Multiple-cell operation expedites calibration, i.e., it permits simultaneous operation with two solutions, one in each cell. The results are consistent with single-cell performance. One run provides two points; if extrapolated, those points should pass through the origin (zero optical density). System performance can be comprehensively tested in a single run.

Optical density measurements are described in Sec. V. D. The calibration resulting appears in Fig. 33.

D. Improvements

Performance of the modified version is considerably better than that of the earlier version, especially with regard to stability, switching, and the derivative. Stability is improved by the bootstrap amplifiers; switching properties are better because of the delay uni and the reference-pulse regulator. The derivative traces are much cleaner due to an improved filter. The reference-pulse regulator sustains switching when illumination is extremely nonuniform or when a solvent of appreciable optical density is used (see Fig. 44).

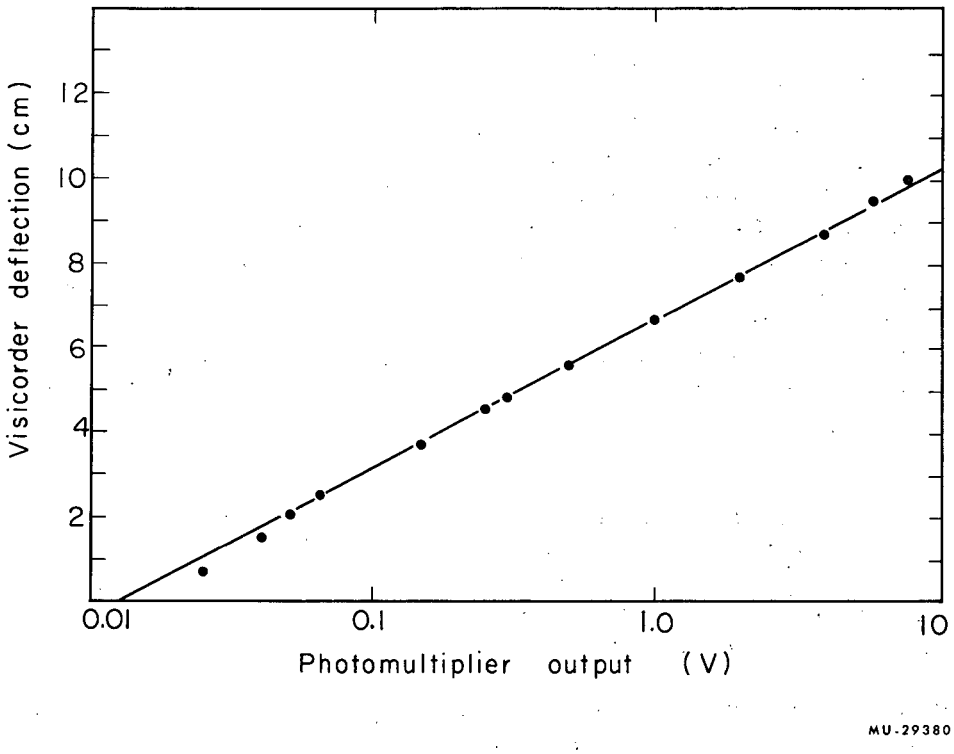

Fig. 52. Visicorder deflection versus reference-pulse amplitude, Mode switch at Reference, and the switching circuits disabled (delay control at 1000). The scanner was positioned to intercept the radius-marker hole (one double-sector cell) and the photomultiplier-supply voltage adjusted to produce pulses of various heights. Preceding modification.

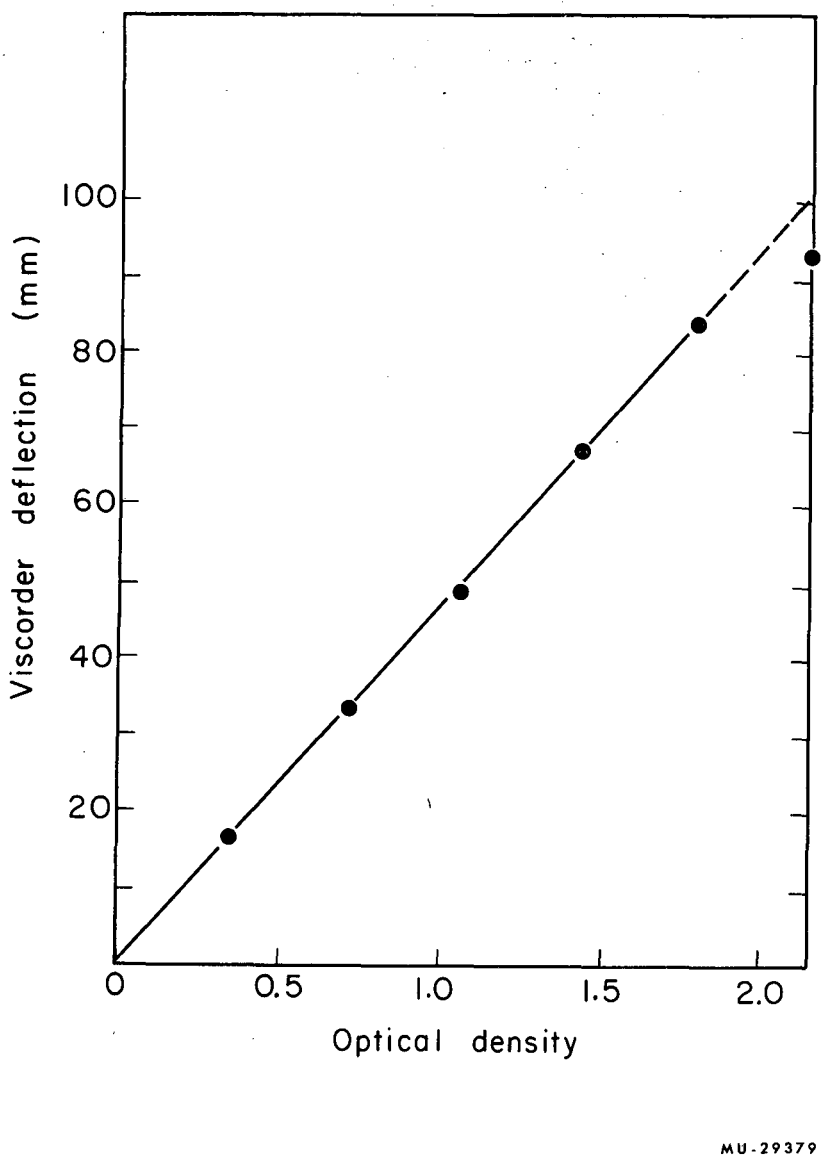

Fig. 53. System response to solutions of measured optical densities, Mode at Difference. The deflections are approximately 25% of those obtainable at maximum gain. The calibration indicates that the system is linearly responsive (accuracy ± 1% of full-scale deflection) to optical densities between zero and 1.8. The photomultiplier supply was adjusted for 2-V reference pulses. Optical density in the centrifuge is 1.2 times the value for a 1-cm path length. Preceding modification, one double-sector cell.

E. Applications

Articles relevant to scanner applications are indicated in references 25 through 27. These articles chronicle scanner evolution and indicate some of the studies that have been made. Future articles will emphasize derivative performance, spectral analysis techniques, and calibration applications.

VIII. FUTURE CONSIDERATIONS

The opportunities for extending scanner performance appear to be unlimited. Among them are:

1. Operation with a greater number of cells.

2. Operation with two single-sector cells, each cell approaching a sector angle of 90 degrees. Circular slits could provide the resolution necessary. This approach is less practical if ultraviolet light sources of higher intensity become available.

3. A servo arrangement for synchronizing the scanning mechanism with the recorder-chart drive. Recorder traces, in that event, would have a magnification factor independent of scanning speed.

4. A printer for recording such information as run number, time, and date on each recorded trace. This could prevent confusion should the traces be filed erroneously.

5. Computer techniques for extending accuracy. Recording techniques could permit data processing subsequent to scanning.

ACKNOWLEDGMENTS

The photoelectric scanner was sponsored by the Molecular Biology and Virus Laboratory, University of California, Berkeley. The work was under the direction of Professor Howard K. Schachman who conceived the application of double-sector cells to centrifuge work, and is responsible for most of the optics relevant to the transition from photographic recording. The scanning mechanism was designed by Messrs. Frederick H. Bierlein, Robert K. Johnson, George Lauterbach, and Franz X. Plunder. Messrs. Charles G. Dols and Paul Salz contributed useful suggestions. Miss Boihon Chin conducted many of the experiments.

This work was done under the auspices of the U. S. Atomic Energy Commission.

APPENDICES

A. Derivations

The primary requirement of any system is that its response be linearly related to the optical density OD of the sample, or by definition,

$$OD = \log I_o/I, \tag{1}$$

where OD is the optical density of the sample, I_o is the light intensity entering the sample, and I is the attenuated value after absorption.

The ratio I/I_o is termed transmittance. With regard to the sample, the term I/I_o may be designated ν, or:

$$\nu = I/I_o . \tag{2}$$

Substituting (2) into (1) we obtain

$$OD = \log 1/\nu. \tag{3}$$

The next procedure is to develop an expression for the system response in order to ascertain that it does conform to Eq. (3). With this in mind a derivation follows:

Figure 54(a) is a simplified diagram of the reference-cell optics, consisting of a light source, the reference cell, and a photomultiplier. If we assume that the photomultiplier is linearly responsive to light intensity, it develops a peak pulse amplitude proportional to its sensitivity P_r, the light intensity L_r, the light-fraction intercepted f_r, and the transmittance of the reference cell R (cell window plus solvent). Expressed as an equation, this gives us

$$e_r = P_r L_r f_r R \qquad (e_r = \text{PM output voltage}). \tag{4}$$

Referring to Fig. 54(b) the sample path includes the sample cell of transmittance S(cell window plus solvent) and a virus[28] concentration of transmittance ν:

$$e_s = P_s L_s f_s S \nu. \tag{5}$$

The subscripts to P, L, and f have been introduced to account for differences between each channel. If the time interval between sample and reference pulses is short, and if the scanning mechanism moves only a short distance during that time, the ratios P_r/P_s, L_r/L_s, and f_r/f_s can be considered to be 1. Their individual values may vary throughout the scan, but their ratios do not.

If we take the log of Eqs. (4) and (5), and then subtract,

$$\log e_r - \log e_s = \log R/S - \log \nu. \tag{6}$$

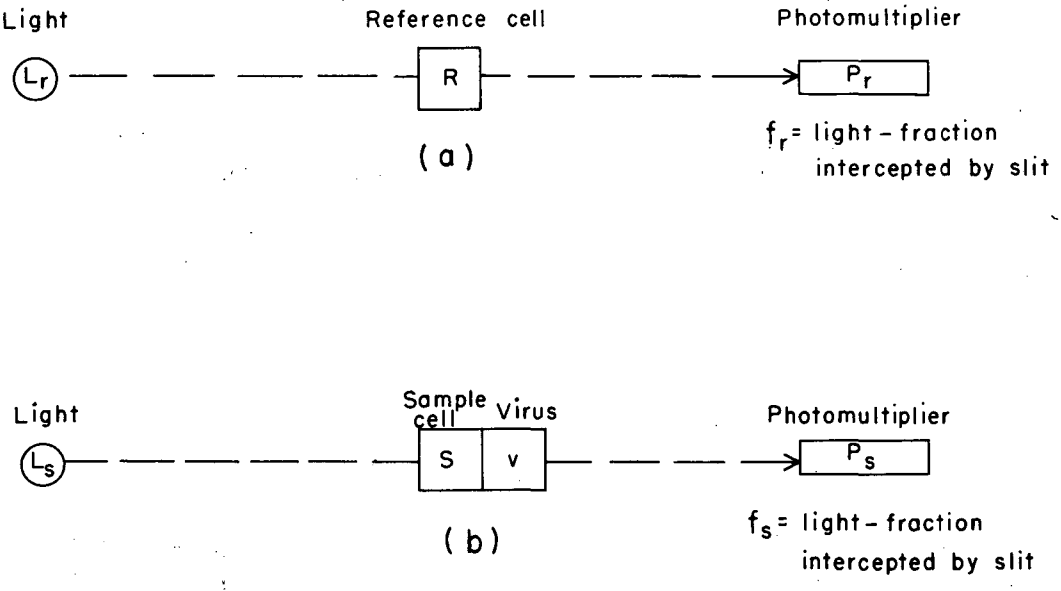

Fig. 54. Optical system, simplified diagram, for purposes of derivation: (a) Reference-cell light path, and (b) sample-cell light path.

If the ratio R/S is constant, Eq. (6) indicates that the log difference varies with virus density, and that it is displaced from zero by some amount related to the ratio R/S. If R/S is 1, there is no displacement, and the output level is directly proportional to virus optical density.

The preceding discussion indicates that a log operation is necessary, but does not provide for the fact that the log amplifier is logarithmic over a limited range. It also fails to consider channel disparities, such as channel gain differences. With this in mind, a derivation involving the additional parameters follows:

Referring to Fig. 32, we find that each channel produces a holding circuit voltage H proportional to the log-amplifier output voltage V, channel gain A, and holding-circuit gain constant T. Writing the expression for each channel, we obtain

$$H_r = V_r A_r T_r, \tag{7}$$

and

$$H_s = V_s A_s T_s. \tag{8}$$

Let us assume that the log amplifier is common to both channels, that its response is similar to that shown in Fig. 51, and that operation is confined to the linear region between 1 and 2. An examination of the figure reveals that the peak pulse amplitude appearing at the log amplifier output may be described by an equation of the form, $V = V_0 + m(\log e - \log e_0)$. Elaborating, the log output voltage V is equal to some constant V_0, plus the slope m, (which depends upon log-amplifier gain), times the difference between the logs of the input voltage e and the voltage corresponding to the abscissa of V_0, or e_0. Expressed as an equation for each channel, we have

$$V_r = V_0 + m(\log e_r - \log e_0), \tag{9}$$

and

$$V_s = V_0 + m(\log e_s - \log e_0). \tag{10}$$

In practice, the log output voltage from each channel is routed to a different holding circuit, and so the gain constants T_r and T_s are not exactly equal. This is corrected with the Null adjustment so that the gain ratio A_r/A_s compensates for their difference.

Substituting the values of (9) and (10) into (7) and (8) respectively, the holding circuit voltages, H, may be expressed

$$H_r = A_r T_r (V_0 + m \log e_r/e_0) \tag{11}$$

$$H_s = A_s T_s (V_0 + m \log e_s/e_0). \tag{12}$$

With regard to recorder deflection D, the amplitude is proportional to the voltage difference across the holding circuits multiplied by the gain constant G that follows the difference amplifier input. Rewriting and substituting the values of Eqs. (11) and (12), we get

$$D = G[A_r T_r (V_0 + m \log e_r/e_0) - A_s T_s (V_0 + m \log e_s/e_0)]. \quad (13)$$

The null adjustment is normally made in the air space where the transmittance ν is equal to 1. When D is adjusted for zero, the gain ratio has been adjusted so that

$$A_r T_r = A_s T_s \left[\frac{V_0 + m \log e'_s/e_0}{V_0 + m \log e'_r/e_0}\right]. \quad (14)$$

The primes have been added to represent photomultiplier output voltages when positioned in the air space at both cell ($\nu = 1$).

If Eqs. (4) and (5) are substituted into Eq. (14), and if it is assumed that the quantities P, L, and f, do not change in the time interval between the reference and sample pulses, and that the values of R and S are equal and constant, then

$$A_r T_r = A_s T_s. \quad (15)$$

Substituting the values of Eqs. (4), (5), and (15) into Eq. (13), the recorder deflection D becomes

$$D = G A_s T_s m \log 1/\nu. \quad (16)$$

Equation (16) indicates that the recorder deflection is proportional to virus concentration. The amount of deflection for a given virus transmittance is controlled by adjusting the value of G. This is done with an adjustable attenuator (Trace Amplitude), which determines the output level applied to the Visicorder galvanometer. This equation also indicates that the system response is independent of variations appearing in the illumination profile.

The previous derivation was made on the assumption that R and S are equal. Equation (16) shows that non-uniform illumination is not important, provided that we stay within the linear region of Fig. 51. Let us now assume that R and S are not equal, then deduce the errors resulting from nonuniform illumination profiles that are considered acceptable to system performance.

Substituting Eq. (14) into Eq. (13), we have

$$D = G A_s T_s \left[\left(\frac{V_0 + m \log e'_s/e_0}{V_0 + m \log e'_r/e_0}\right)(V_0 + m \log e_r/e_0) - (V_0 + m \log e_s/e_0)\right]. \quad (17)$$

The quantity in the first parentheses is a constant K_1. Referring to Eq. (14), it represents the ratio $A_r T_r / A_s T_s$ after the null adjustment has been made. Its exact value depends upon the absolute magnitude of P, L, and f which existed at the time of nulling, or

$$K_1 = \frac{V_0 + m \log e_s'/e_0}{V_0 + m \log e_r'/e_0} . \tag{18}$$

If we assume that P, L, and f are constant in the time interval between pulses, substituting Eqs. (4), (5), and (18) into Eq. (17):

$$D = G A_s T_s [K_1(V_0 + m \log P L f R/e_0) - (V_0 + m \log P L f S v/e_0)]. \tag{19}$$

This may be rewritten:

$$D = G A_s T_s [K_1 V_0 + K_1 m \log R/e_0 - V_0 - m \log S/e_0 + K_1 m \log P L f - m \log P L f - m \log \nu]. \tag{20}$$

The first four terms are constant if we call K_2

$$K_2 = (K_1 - 1) V_0 + K_1 m \log R/e_0 - m \log S/e_0. \tag{21}$$

Substituting Eq. (21) into (20), and rewriting, we have

$$D = G A_s T_s [K_2 + (K_1 - 1) m \log P L f - m \log \nu]. \tag{22}$$

Equation (22) reveals that if R and S are not equal, the virus profile will be modified by the illumination profile. The degree of modification is related to the percentage variation of the quantity (P L f) and to the magnitude of $(K_1 - 1)$. Referring to Eq. (18), when R and S are equal, both pulses, e_s' and e_r', are equal, and so K_1 is equal to 1. In that case, K_2 and the illumination term, $(K_1 - 1)$ m log P L f, fall out of Eq. (22), as expected.

Let us now consider the practical case to find out the extent to which this split-beam system compensates for non-uniform illumination profiles. The Visicorder tracings of Fig. 43 are a good example. Both cells were empty, offering negligible attenuation, and so the reference and sample cell profiles are practically identical. The difference trace shows that the illumination profile is cancelled out, and so the baseline is very flat. The values of R and S are very closely matched, but this is not surprising since both cells are enclosed by a common window material.

The values of R and S are usually equal, but it is useful when they are not to have an equation formulating the magnitude that the baseline shifts. Referring to Eq. (22), we see that nonuniform illumination produces a baseline shift B_d equal to the change in value of the quantity $G A_s T_s (K_1 - 1)$ m log P L f from the value that it assumes at the position where the null

is made. This deviation from the true baseline B_d changes with scanner position, and it may be expressed as

$$B_d = G A_s T_s (K_1 - 1) m (\log P' L' f' - \log P L f), \quad (23)$$

where P', L', and f' represent the magnitudes of P, L, and f at the time when the null adjustment was made.

The absolute magnitude of B_d can be computed, if desired, but there is another quantity related to it which is more interesting. For example, it is useful to know how a baseline shift with the difference system compares with the shift of single-beam, assuming the illumination profile is the same in both cases. Referring again to Fig. 43(b), reference optical density prior to taking the difference, the illumination profile changes by a magnitude B_s when the scanner is moved from P_1 to P_2. This is equivalent to a shift in the baseline, and we wish to know the extent to which the magnitude of B_s is reduced by the difference system when R and S are not equal. In essence, we wish to know the ratio of B_d/B_s.

The magnitude of B_s can be deduced from Eq. (13). When the Mode switch is in Reference position, the holding circuit voltage H_s of Eq. (12) does not appear in the output, and so the deflection in this mode, D_s, becomes

$$D_s = G A_r T_r (V_0 + m \log e_r/e_0). \quad (24)$$

The baseline shift in this mode, B_s, is equal to the difference between the values that D_s assumes when the scanner is moved from position 1 to position 2 of Fig. 43(b). Assuming that the null is made at position 1, substituting Eqs. (4) and (5) into (24), we obtain the value of D_s for positions 1 and 2:

$$D_s 1 = G A_r T_r (V_0 + m \log P' L' f' R/e_0) \text{ (position 1)}, \quad (25)$$

and

$$D_2 2 = G A_r T_r (V_0 + m \log P L f R/e_0) \quad \text{(position 2)}, \quad (26)$$

The baseline shift B_s is equal to the difference between Eqs. (25) and (26). Subtracting and simplifying, we obtain

$$B_s = G A_r T_r m(\log P' L' f'/P L f) \quad (27)$$

Substituting Eq. 14 into 27, we get

$$B_s = G A_s T_s m \left(\frac{V_0 + m \log e'_s/e_0}{V_0 + m \log e'_r/e_0} \right) \log P' L' f'/P L f. \quad (28)$$

Substituting Eq. (18) into (28), we have

$$B_s = G A_s T_s m K_1 \log P' L' f'/P L f. \quad (29)$$

We wish to find the ratio B_d/B_s. Substituting the values of Eqs. (23) and (29), and simplifying, we get

$$B_d/B_s = (K_1 - 1)/K_1. \tag{30}$$

If Eq. (30) is to be of value, we must determine some typical values of K_1. Equation (18) formulates its magnitude, but we need to know the magnitude of m. Referring to Fig. 51 and Eq. (9), and substituting arbitrary values, we have

$$0.36 = 0.02 + m (\log 100 - \log 0.1). \tag{31}$$

Solving for m, we obtain

$$m = 0.11. \tag{32}$$

Referring now to Eq. (18) and Fig. 51, assume a mismatch between the reference and sample pulse voltages. A 20% mismatch would typically represent values of 2 and 2.4 volts for e'_s and e'_r respectively. Substituting the appropriate values from Fig. 51 into Eq. (18), we obtain

$$K_1 = \frac{0.02 + 0.11 \log 2/0.1}{0.02 + 0.11 \log 2.4/0.1} = 0.954. \tag{33}$$

Substituting the value of K_1 from Eq. (33) into (30), we get

$$B_d/B_s = (0.958 = 1)/0.958 = -0.048. \tag{34}$$

The negative sign indicates an overcompensation when the value of $e'_s < e'_r$. If their values are interchanged to become 2 V for e'_r and 2.4 V for e'_s, Eq. (34) assumes a value of +0.051.

Equation (34) indicates that if the cells are mismatched in the ratio of 2/2.4, the difference system reduces the magnitude of the baseline shift to 5.1% of the value that it would have in the absence of the difference scheme.

B. Schematics and Index

Titles	Figure number
Operational unit, simplified schematic for trouble shooting	55
Scanning-photomultiplier and emitter follower	56
Linear amplifier and clamp	57
Log amplifier	58
Gate drivers and calibrator	59
Pulse separators	60
Holding circuits, bootstrap and derivative amplifiers	61
Gating Chain	62
Reference-pulse regulator	63
Stationary photomultiplier	64
Set-pulse amplifier	65
Marker generator	66
Scan control	67
Scan-speed selector	68
Galvanometer control, two ultracentrifuges	69
Operational-unit power supply	70
Log compressor power supply	71
Scanning-photomultiplier power supply	72

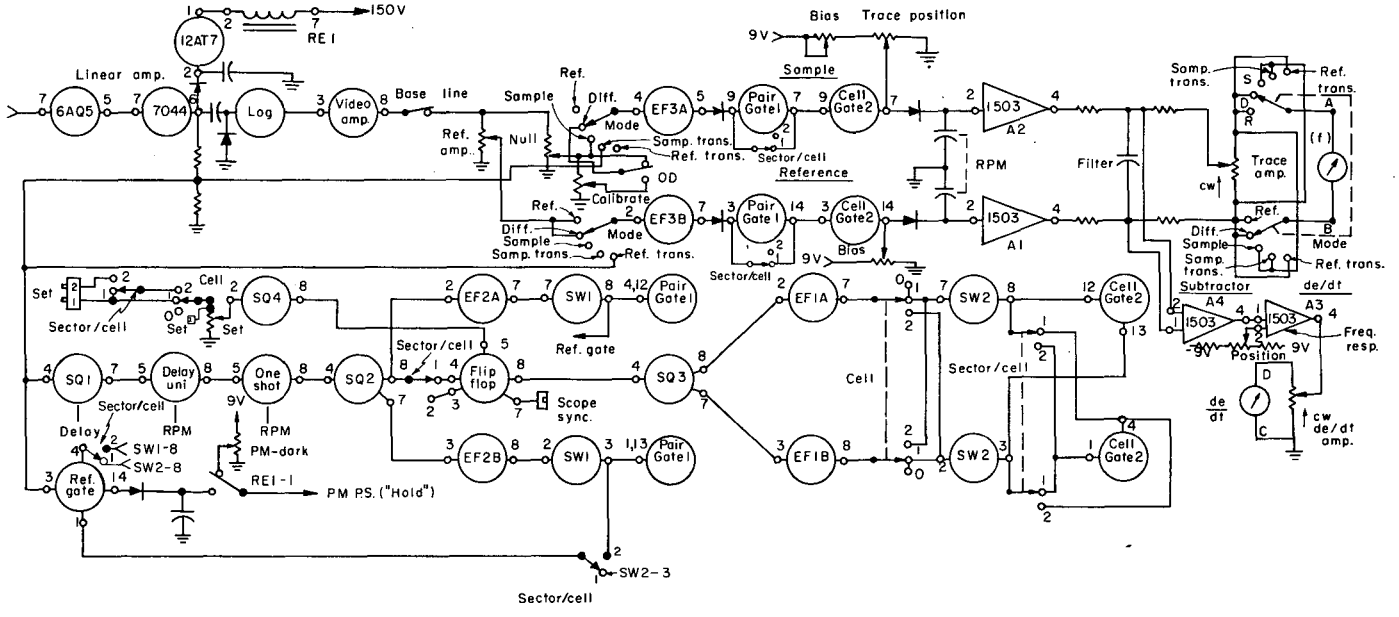

MUB-5883

Fig. 55. Operational unit, simplified schematic for trouble-shooting.

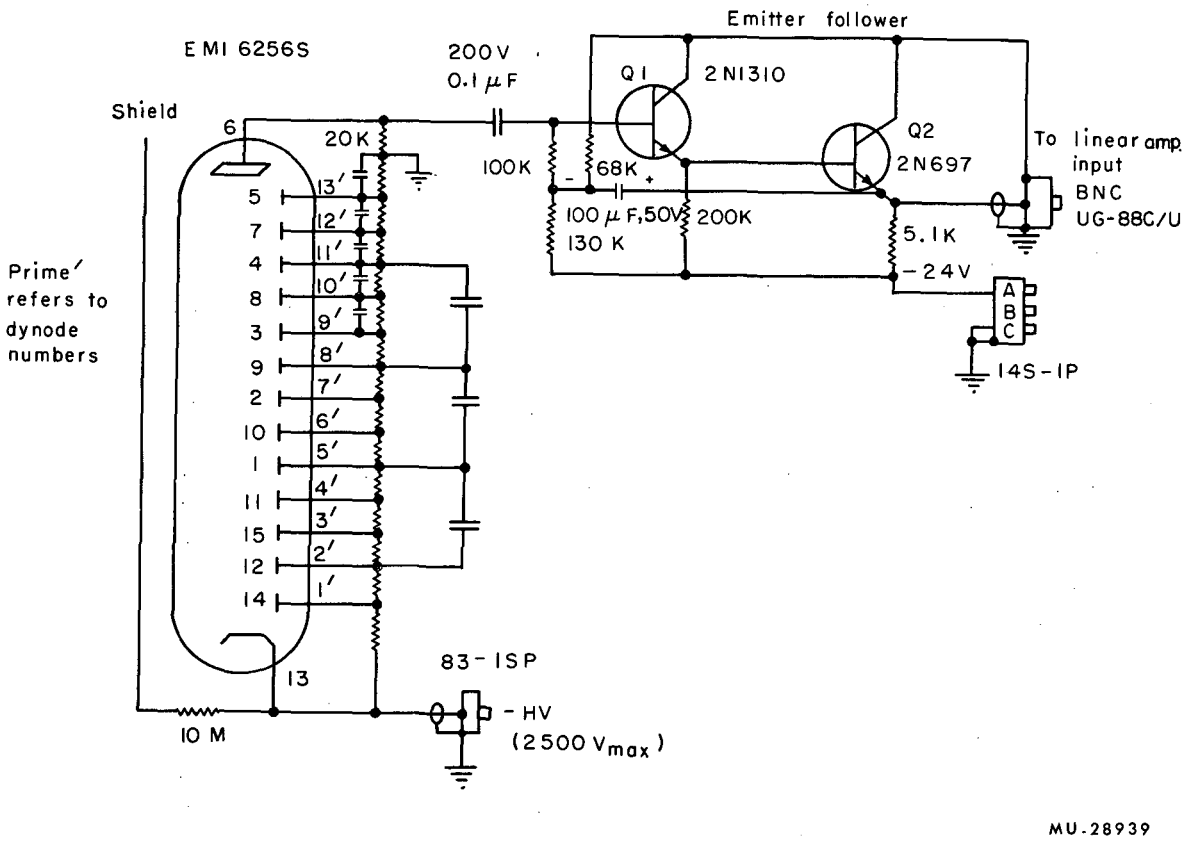

Fig. 56. Scanning photomultiplier and emitter follower. All photomultiplier resistors are 100k, 0.5W, 5%, unless otherwise noted. Capacitors are 0.02 μF, 1kV ceramic. All emitter follower resistors are 0.5W.

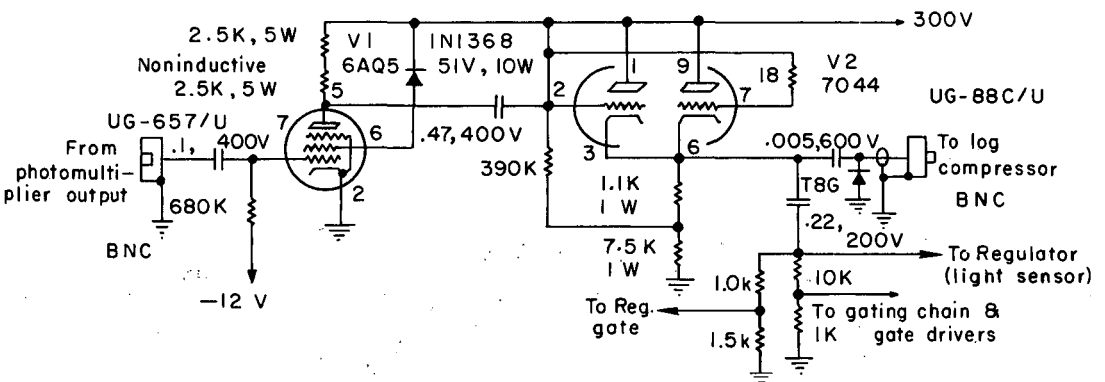

Fig. 57. Linear amplifier and clamp. All resistors are 0.5W unless otherwise noted. The amplifier output is clamped previous to driving the log compressor. Attenuated outputs drive the gating chain, the gate driver, and the reference-pulse regulator gate. Amplifier output, unattenuated, also drives the relay-activating circuit at the reference-pulse regulator. (V1 grid resistor, 680k, is rather high).

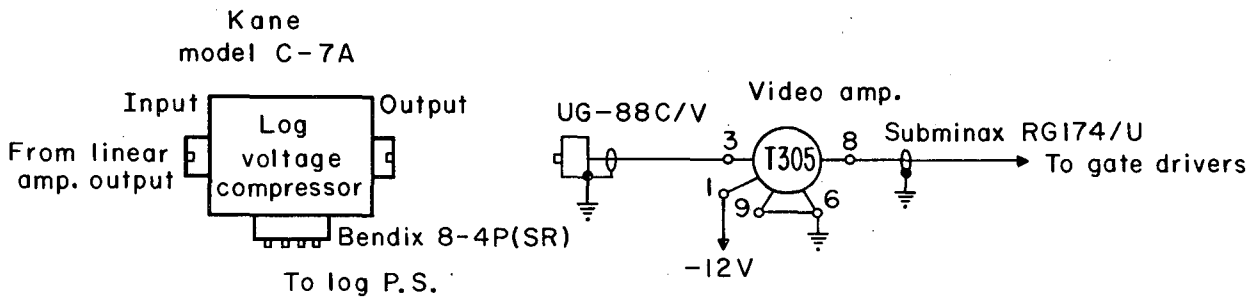

MUB-5838

Fig. 58. Logarithmic amplifier. All resistors are 0.5W unless otherwise indicated. The circled unit is a packaged circuit, Engineered Electronics Company. The log compressor is battery operated when supplied by the manufacturer, but the batteries have been replaced by a power supply (Fig. 71). Adjust compressor bias to value recommended by manufacturer.

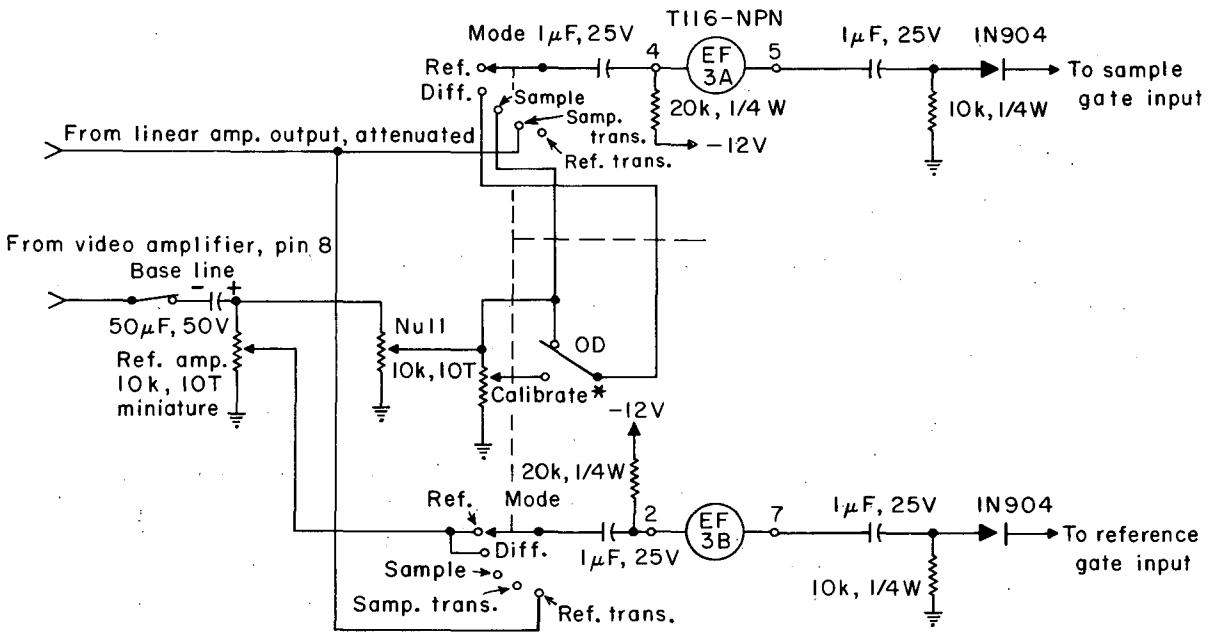

Fig. 59. Gate drivers and calibrator. The circled units are packaged circuits manufactured by EECO. Pin 1 connects to -12V, pins 6 and 9 connect to ground. The Calibrate potentiometer is a 10k, 10-turn helipot. It seems to be frequency (speed) insensitive, but further tests are contemplated. Mode switch is 6-pole, 5-position, Central Lab 2525 nonshorting.

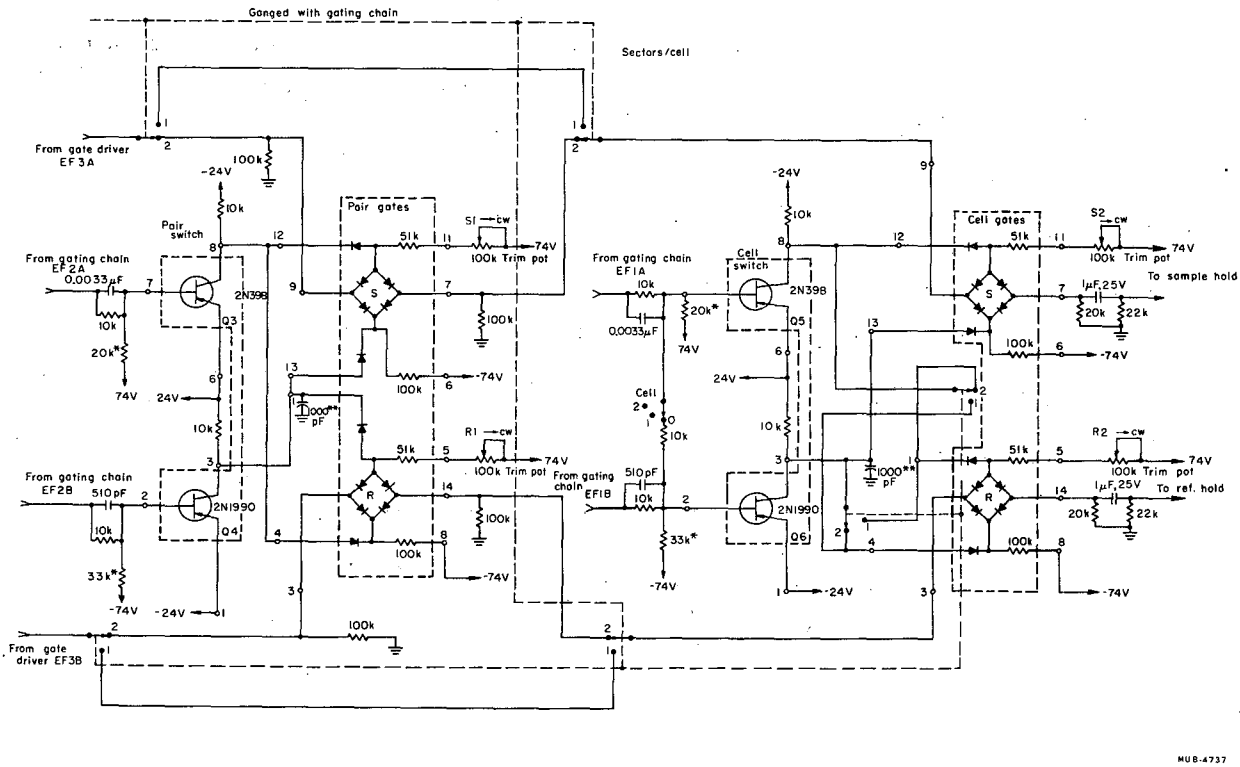

Fig. 60. Pulse separators. The switches and 6-diode gates are fabricated into EECO containers (Fig. 31). All diodes are 1N643, all resistors are $\frac{1}{4}$W. *Indicates that the resistor is selected for the proper switching waveform. **Indicates that the capacitor is selected to reduce the influence of switching spikes (selecting 2N1990's sometimes helps). The adjustments for R1, S1, R2, and S2 are indicated in the text.

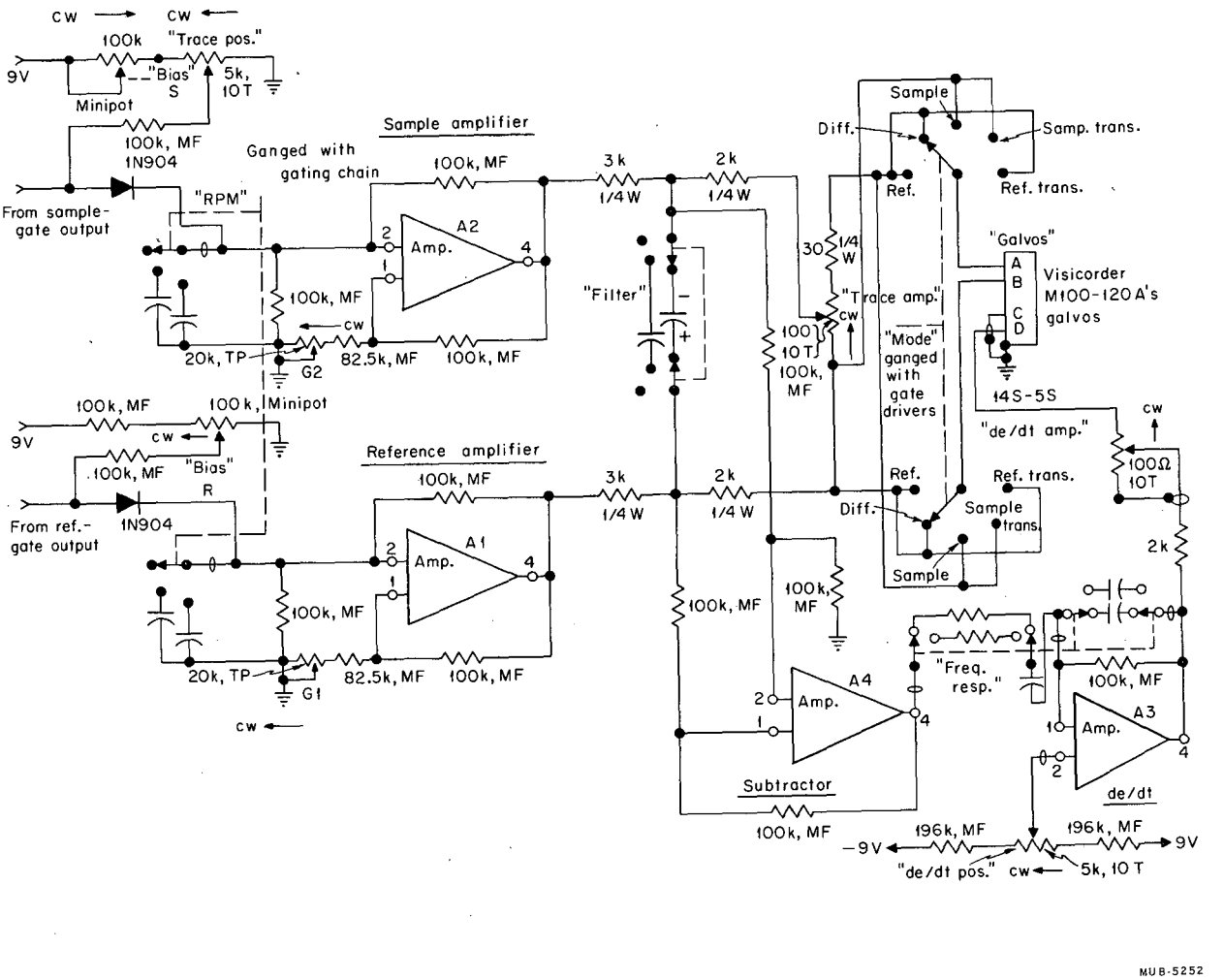

Fig. 61. Holding circuits, bootstrap and derivative amplifiers. The amplifiers, Burr-Brown model 1503, obtain power from ± 12-V power supplies. Shielded coax to each amplifier is grounded at the relative amplifier only (avoids ground loops). Component values subject to selector switch settings are indicated by the accompanying table. All resistors indicated by $\frac{1}{4}$W are carbon; those indicated by MF are metal film, also $\frac{1}{4}$W. Adjustments for G1, G2, and Bias are indicated in text. The diodes (1N904) are matched, but this may not be necessary. The reference and sample amplifiers are bootstrap type. The RPM switch is a 6 pole, 12 position, fabricated from two Centralab PA2013 (4 pole, 12 pos., 4 wafers). The Filter switch is 2 poles, 12 position, Leeds Northrup 31-3-0-2. The Frequency Response switch is 4 poles, 12 position, Centralab PA2013.

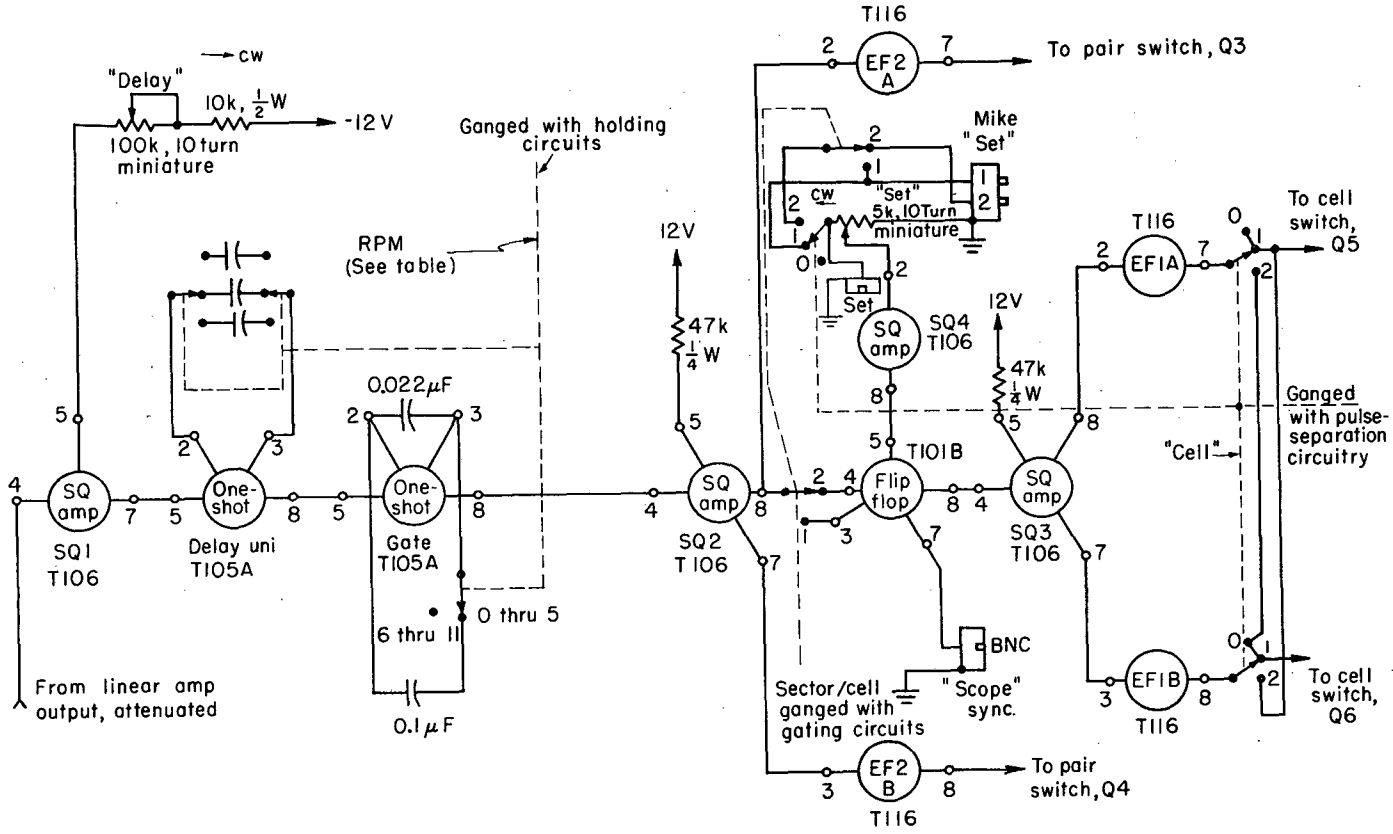

Fig. 62. Gating chain. The circled units are packaged circuits manufactured by EECO. Pin 1 connects to -12-V, pins 6 and 9 connect to ground. The Sector/cell switch is 8 poles, 2 position. It is fabricated from 2 Centralab PA2015 wafers (5 poles, 3 positions per wafer). The Cell switch is 4 poles, 12 position, Leeds Northrup 31-3-04. RPM table appears in Fig. 61. The RPM switch is ganged with holding circuits (Fig. 61); cell and Sector/cell switches are ganged with pulse separators (Fig. 60).

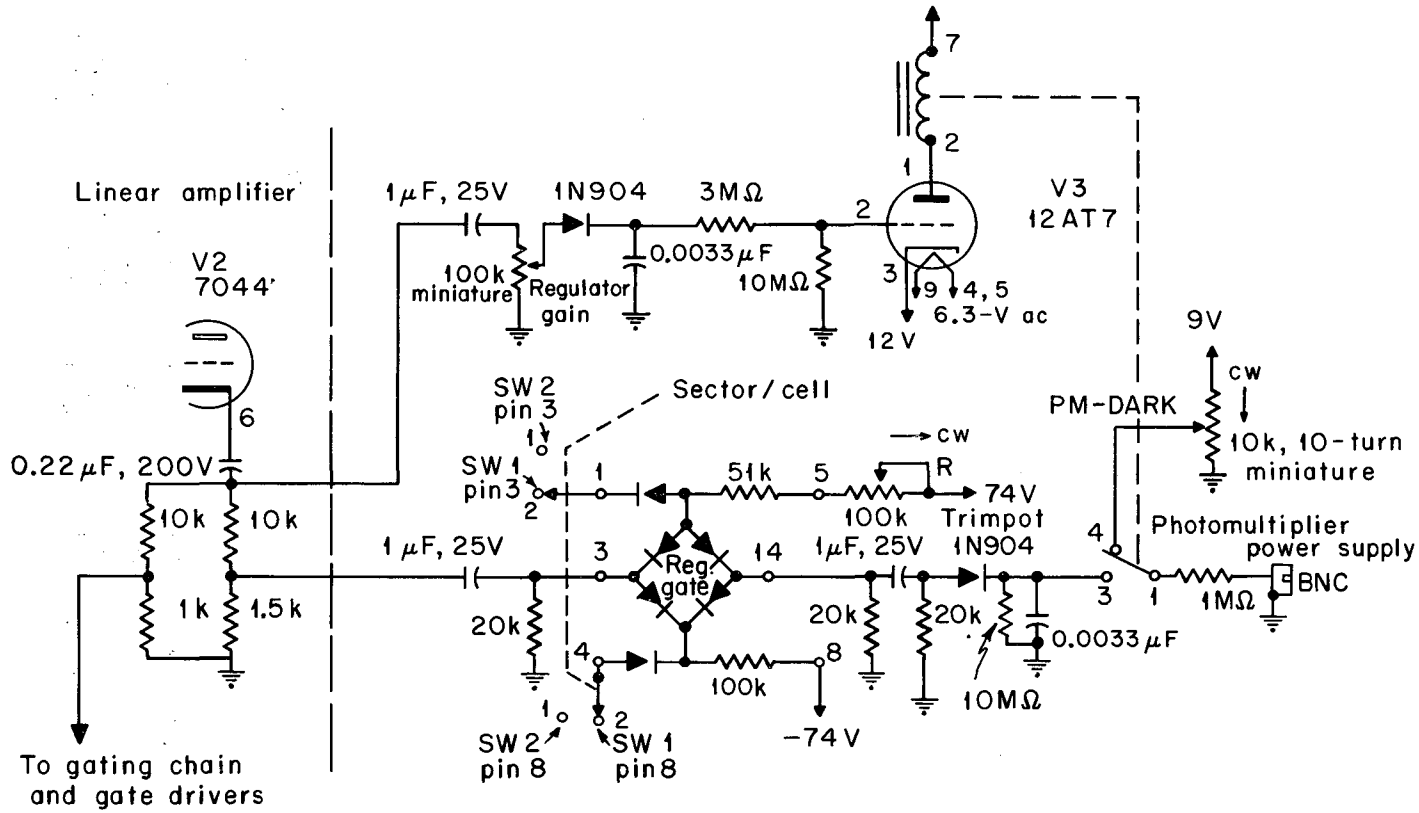

MUB-4734

Fig. 63. Reference-pulse regulator. All resistors are $\frac{1}{4}$W. Reference-gate diodes are 1N643. Relay is Potter Brumfield, KCP11, 10k; pin 7 connects to 225-V (150-V is sufficient in some cases).

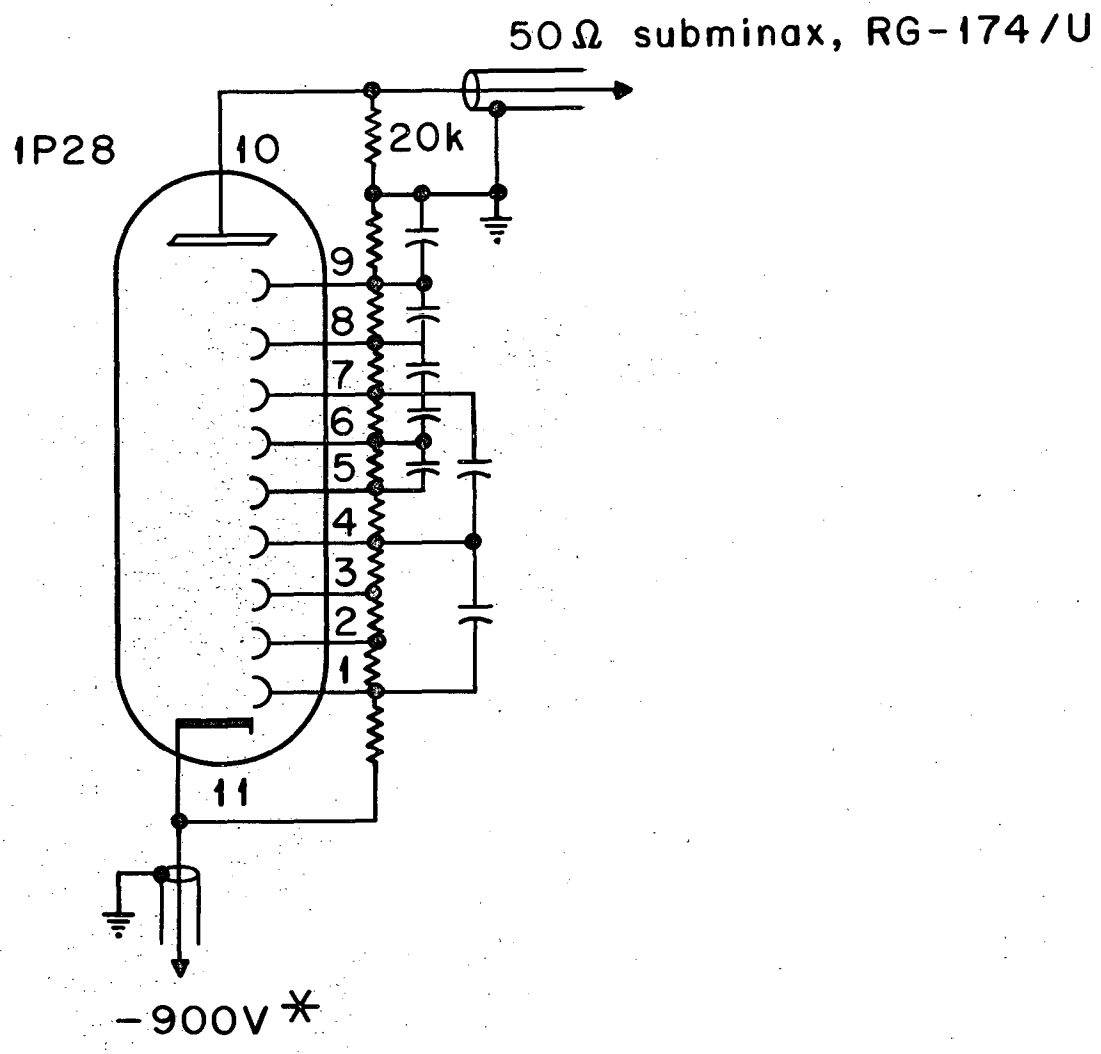

Fig. 64. Stationary photomultiplier. *Derived from Plasticap Power Supply, Model HV20-502M, 2kV, 5 ma, dropped to 900-V with a divider. The output coax connects to the set-pulse amplifier input. Resistors in dynode chain are 100k, $\frac{1}{2}$W; capacitors are 0.02 μfd, 1kV ceramic.

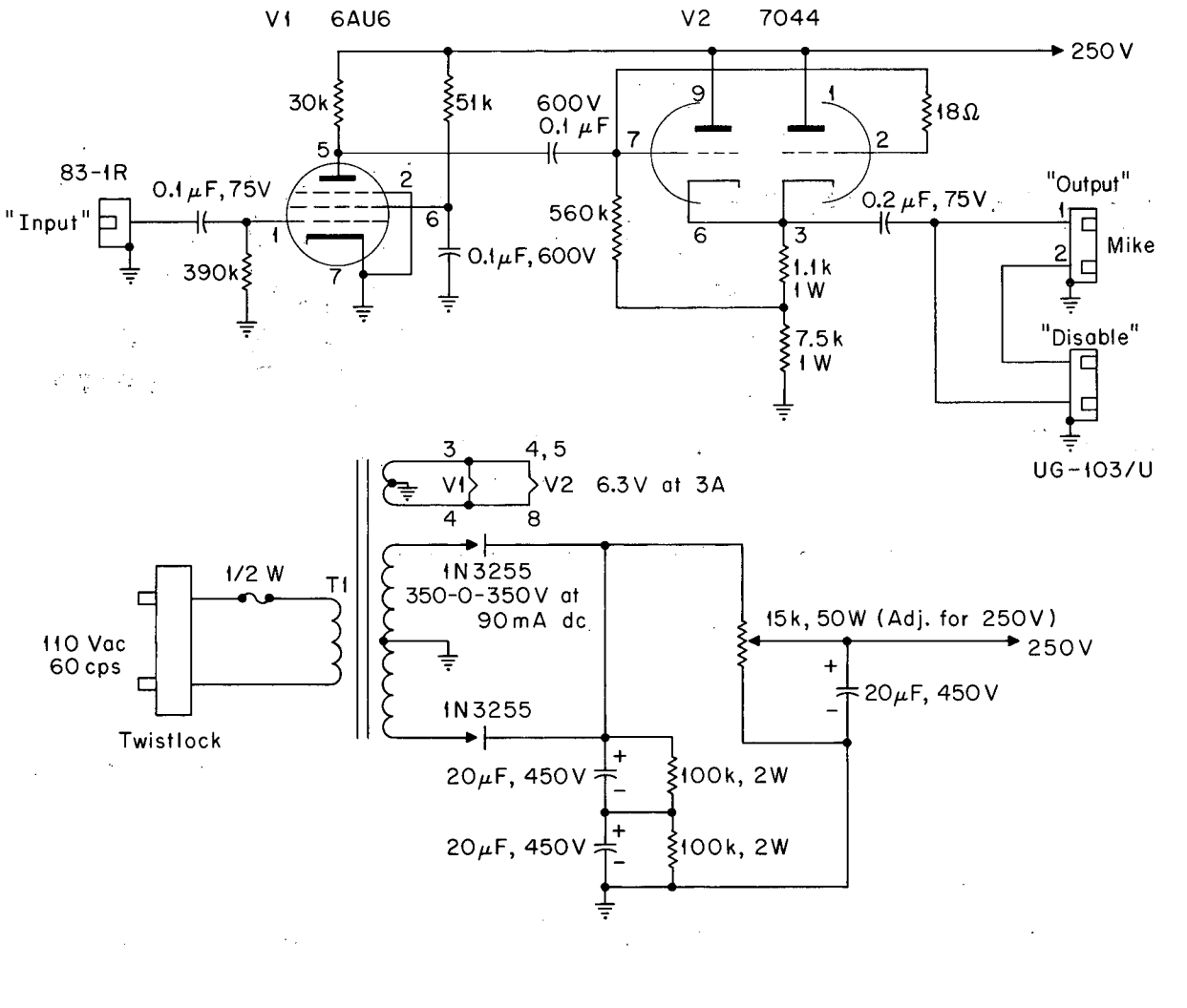

Fig. 65. Set-pulse amplifier. All resistors are $\frac{1}{2}$W unless otherwise noted. Transformer T1 is Stancor PC 8409.

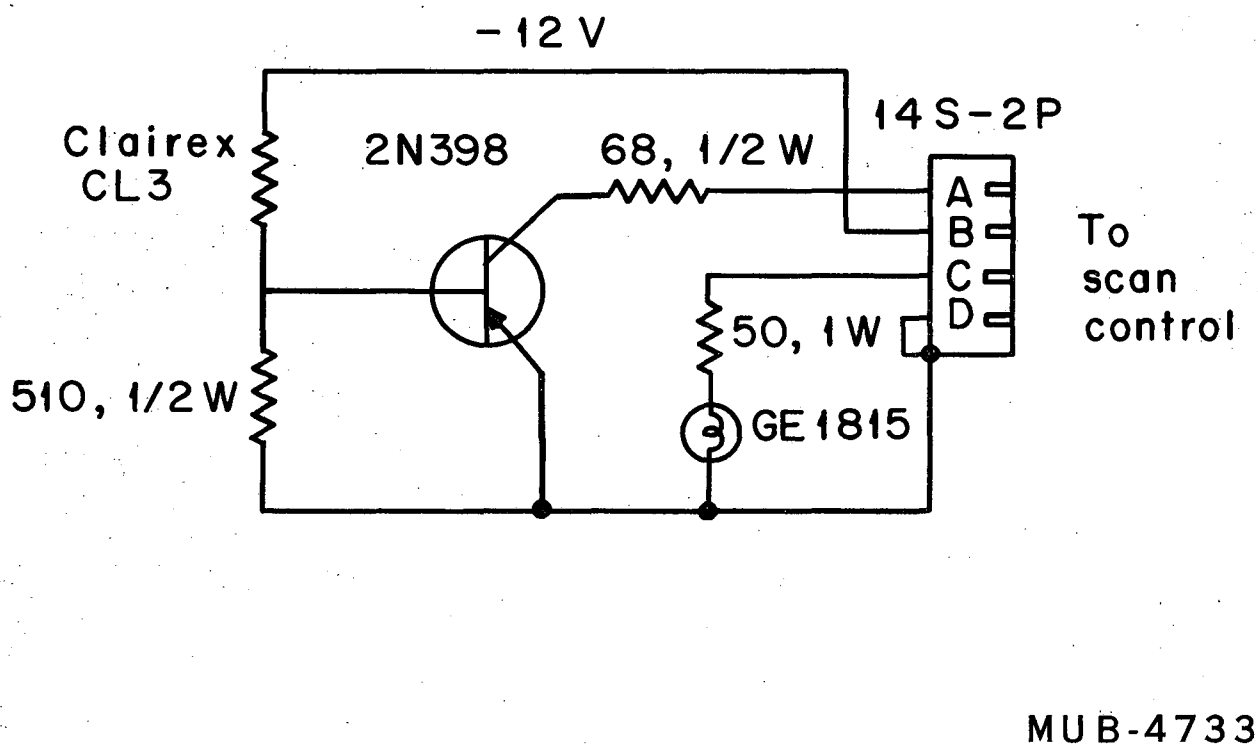

Fig. 66. Marker generator. Clairex CL3 is a photosensitive element.

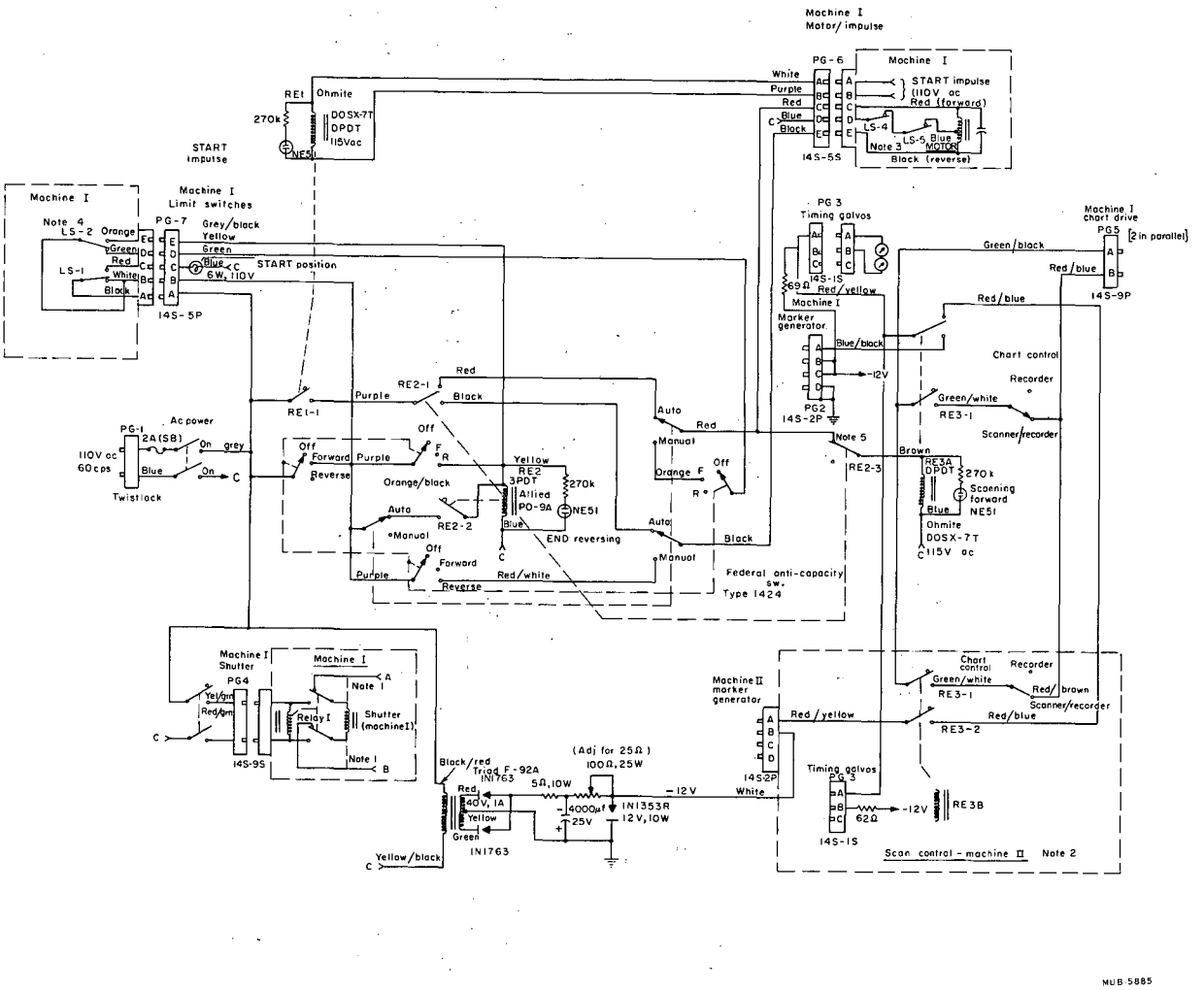

Fig. 67. Scan control. Note 1. Manufacturer connects A and B to shutter (dashed lines). Relay 1 (DPDT, 115 V ac) is added and circuit modified to that shown. Note 2. Includes circuitry for two centrifuges--schematic shows machine I only. Machine II circuitry is identical except for differences indicated. The machines share a Visicorder; Relays RE3A and RE3B connects its chart control and timing galvos to the machine that is scanning. If both machines scan simultaneously the timing galvos are connected to machine I. Note 3. LS-4 and LS-5 are safety limit switches at each end of travel. Note 4. LS-1 at START position, LS-2 at END position. Note 5. RE2-3 prevents RE3 from operating through motor capacitor when scanning in reverse. Plug in relays are preferable to those shown.

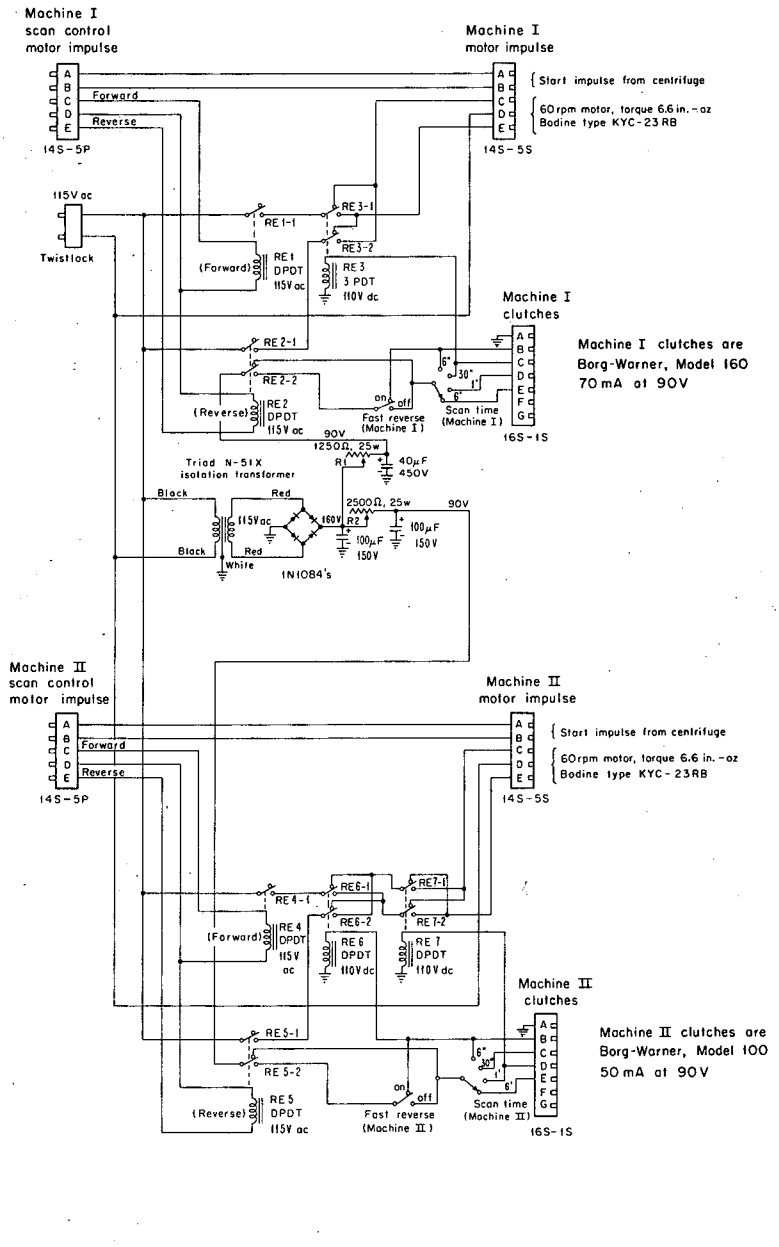

Fig. 68. Scan-speed selector. The circuitry will be modified so that the power supply is energized only if either machine is scanning.

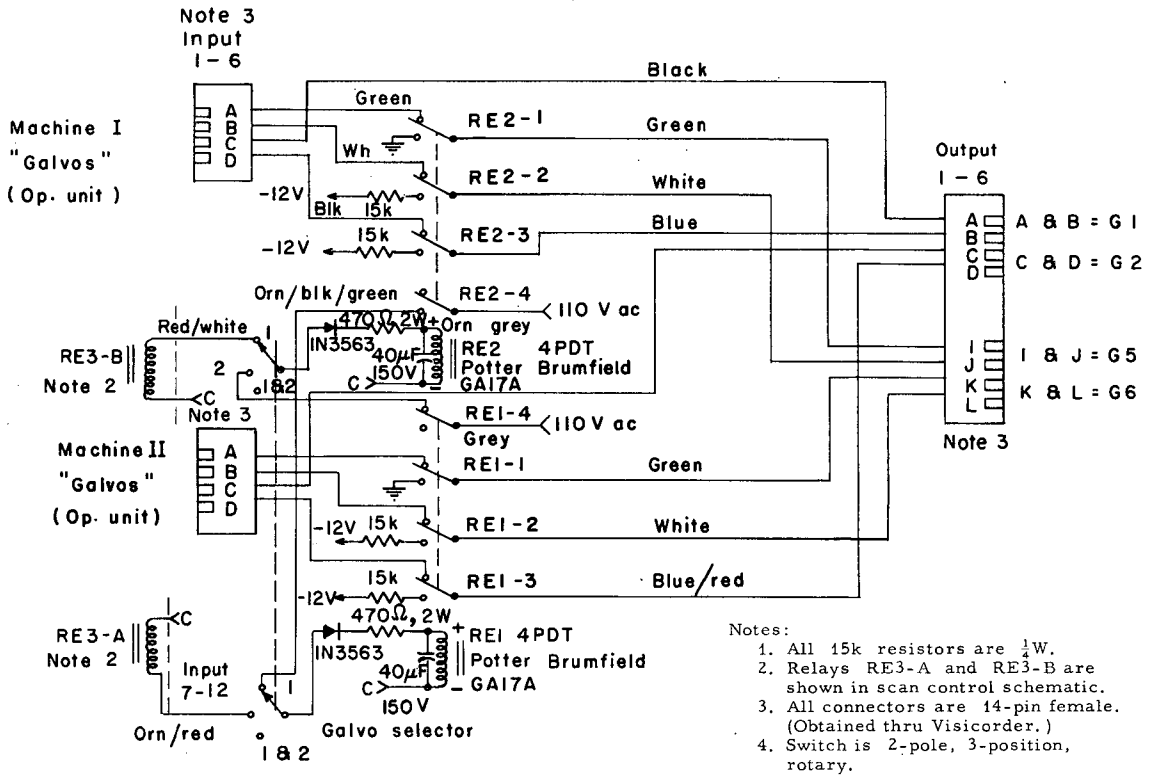

MUB-5843

Fig. 69. Galvanometer control, two ultracentrifuges.

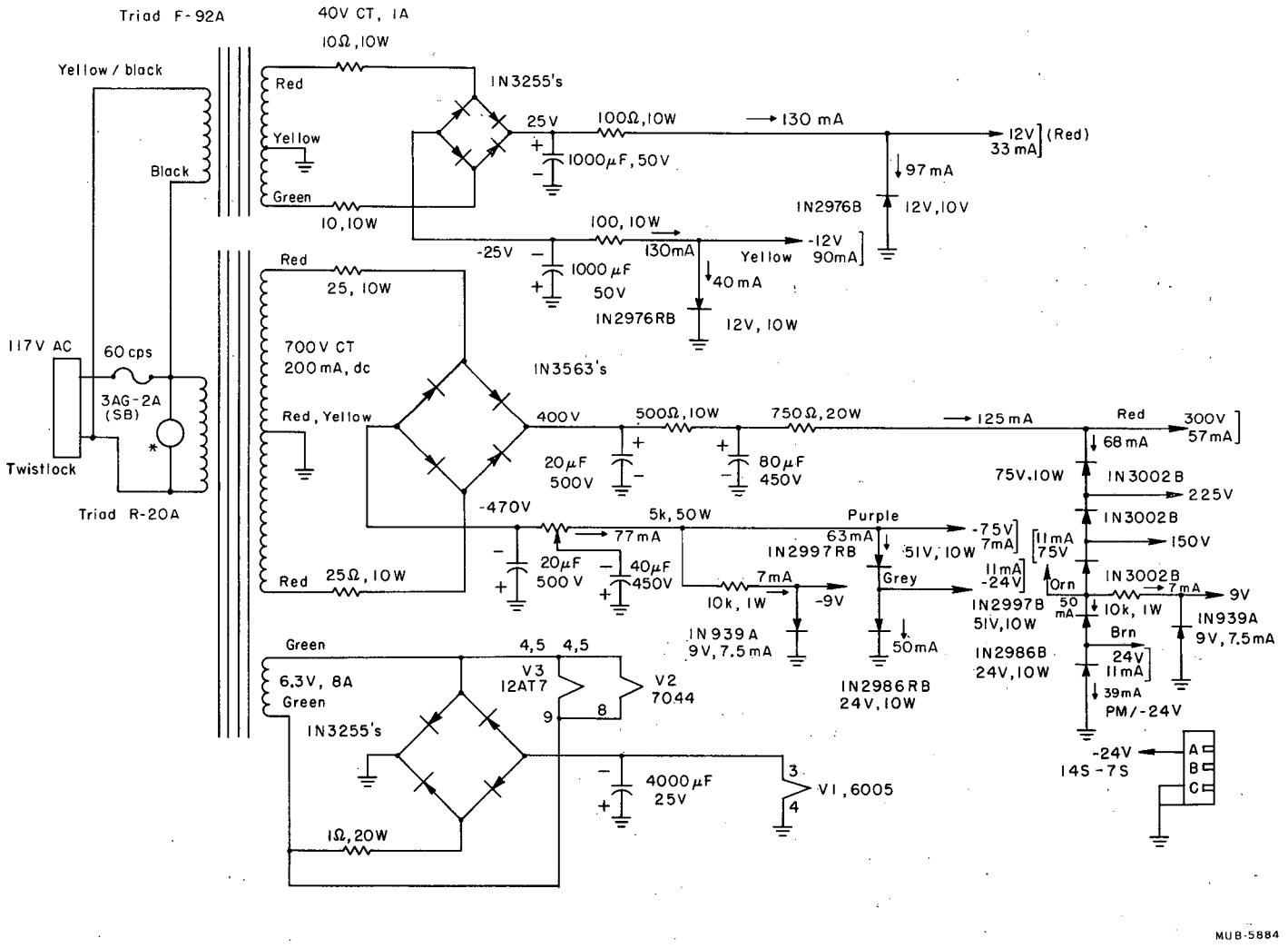

Fig. 70. Operational-unit power supply. *Rotron Muffin Fan, 14W, polarized for least pickup. All currents are measured in the absence of light (nonswitching). A 0.1-μF Mylar bypass capacitor has been added between -24V and ground.

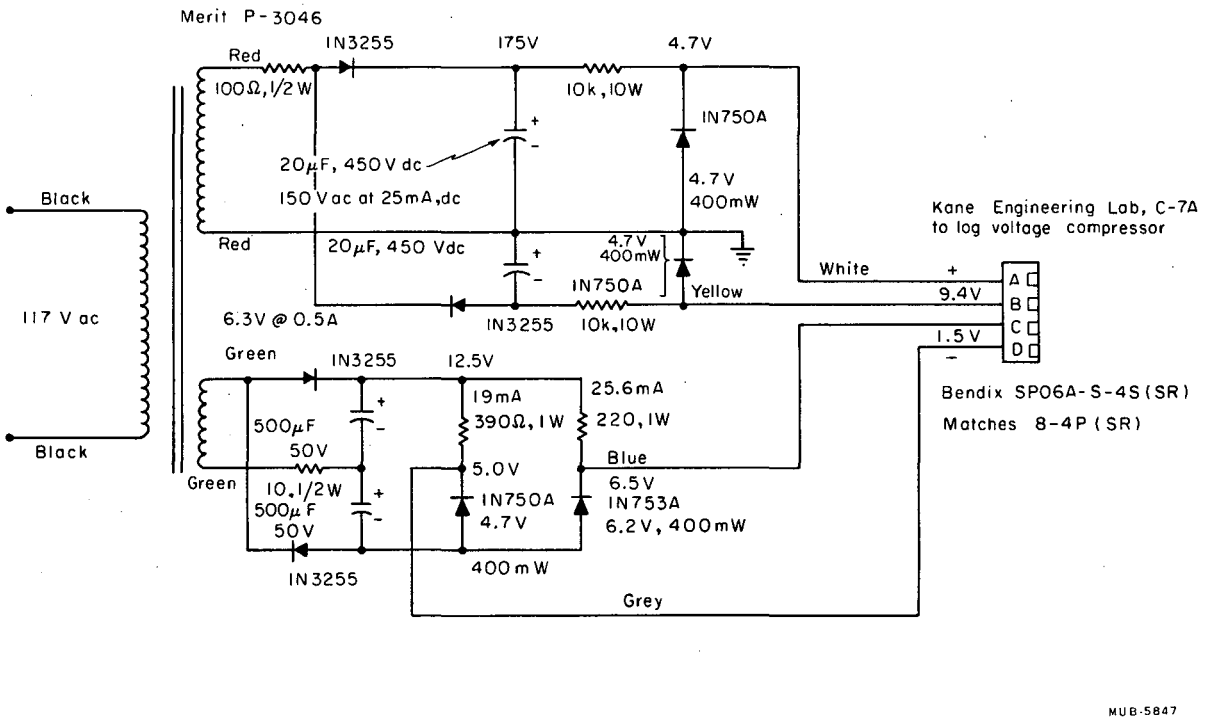

Fig. 71. Log-compressor power supply. All currents and voltages are measured at no-load.

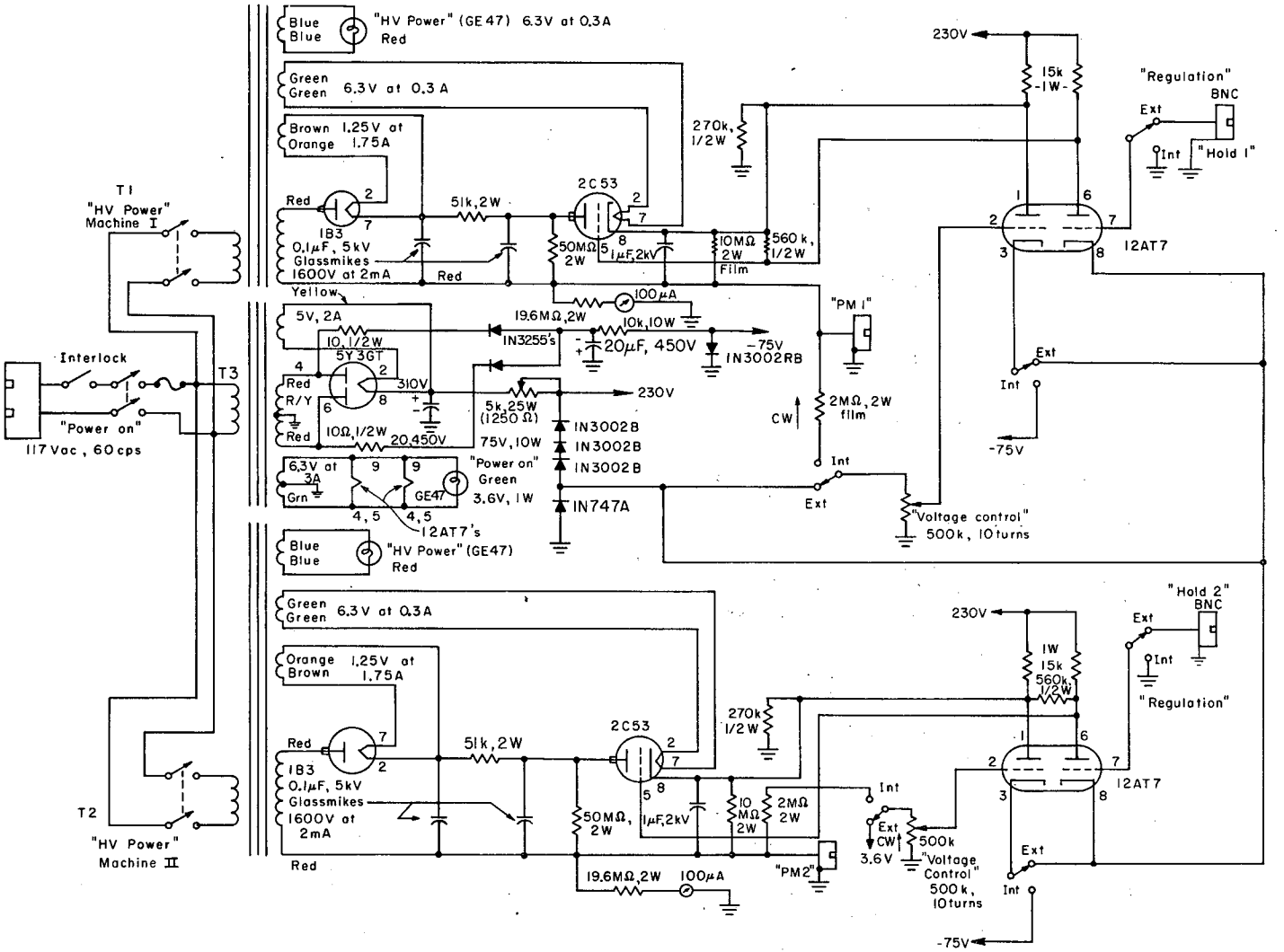

Fig. 72. Scanning-photomultiplier power supply. Transformers T1 and T2 are Thordarson 24R28. Transformer T3 is a Thordarson 22R02, 300-0-300, 70 mAdc. PM1 and PM2 are Cannon connectors, type MS3102A-18-16S(C).

C. Tables of Switching Properties and Frequency Characteristics

Table II. Filter and derivative frequency response parameters.

Filter Parameters	
Filter switch position	Filter capacity (μF)
0	none
1	none
2	none
3	none
4	1
5	2
6	3.3
7	5
8	10
9	25
10	40
11	100

Derivative "Frequency Response" Parameters		
Frequency response switch position	Shunt capacity (μF)	Resistance (kΩ)
0	none	none
1	0.1	10
2	0.15	15
3	0.2	20
4	0.3	30
5	0.4	39
6	0.47	47
7	0.57	56
8	0.67	68
9	1.0	100
10	1.47	150
11	2.0	200

Centrifuge speed (rpm)			rpm Switch position	Holding capacitors
600	to	720	0	0.03 μF
720	to	1 100	1	0.02 μF
1 100	to	2 200	2	0.01 μF
2 200	to	3 100	3	0.007 μF
3 100	to	4 300	4	0.005 μF
4 300	to	6 200	5	0.0035 μF
6 200	to	11 000	6	0.002 μF
11 000	to	15 000	7	0.0015 μF
15 000	to	22 000	8	0.001 μF
22 000	to	29 000	9	750 pF
29 000	to	43 000	10	500 pF
43 000	to	60 000	11	360 pF

NOTE: Holding capacitors are either Mylar or mica.

Table III. Gating chain–Delay time versus Centrifuge speed (calculated values).

RPM	RPM Switch position	Delay uni C (μF)	T delay[a] (μsec)	T/deg[b]	Delay (deg)
600 to 720	0	0.01	200	280 to 230	0.73 to 0.87
720 to 1 000	1	0.01	200	230 to 150	0.87 to 1.30
1 100 to 2 200	2	0.0068	140	150 to 75	0.91 to 1.80
2 200 to 3 100	3	0.0033	68	76 to 54	0.87 to 1.20
3 100 to 4 300	4	0.0022	46	54 to 39	0.85 to 1.20
4 300 to 6 200	5	0.0022	46	39 to 27	1.20 to 1.70
6 200 to 11 000	6	0.001	22	27 to 15	0.81 to 1.50
11 000 to 15 000	7	0.000510	12	15 to 11	0.81 to 1.0
15 000 to 22 000	8	0.000510	12	11 to 7.6	1.0 to 1.6
22 000 to 29 000	9	0.000250	7	7.6 to 5.8	0.92 to 1.2
29 000 to 43 000	10	0.0002	6	5.8 to 3.9	1.0 to 1.5
43 000 to 60 000	11	0.0001	4	3.9 to 2.8	1.0 to 1.4

[a] T delay = $\left(\frac{C}{50} + 2\right)$ μsec (C in pF) T is the delay time introduced by delay uni.

[b] T/deg is the time required for the rotor to turn one degree = $10^6/6$ rpm(μsec).

Table IV. Filter-frequency characteristics and influence on resolution (calculated values).

Switch position (filter)	Capacity (μF)	Rise time (msec)	70% Frequency (cps)	Resolution = Ts/Tr[a] 6 min	1 min	30 sec	6 sec (scan rate)
0	none						
1	none						
2	none						
3	none						
4	1	5.3	66	69 000	10 000	5 700	1 100
5	2	11	32	34 000	5 600	2 800	560[b]
6	3.3	17	21	20 000	3 400	1 700	340
7	5	27	13	13 000	2 200	1 100	220
8	10	53	6.6	6 900	1 100	570[b]	110
9	25	130	2.7	2 800	460[b]	230	46
10	40	210	1.7	1 700	280	140	28
11	100	530	0.66	690[b]	110	57	11

[a]Ts represents time required for a complete scan; Tr the rise time indicated by this table. Resolution values are theoretical. In order to confirm these numbers, one should obtain a deflection on Visicorder, press Baseline button, operate recorder chart at 100 mm/sec, then release Baseline button. The rise time is related to Filter setting, and can be deduced from the slope and chart speed.

[b]Recommended setting. If noise is a problem, resolution is not critical, the Filter switch can be set to a higher position.

Table V. Derivative-Frequency response characteristics, calculated values.

Switch position[a] (freq. response)	Shunt capacity (μF)	Series resistance (kΩ)	Break frequency (cps)	Switch position[a] (filter)
0	none	none		
1	0.1	10	16	5
2	0.15	15	11	7
3	0.2	20	8.0	8
4	0.3	30	5.3	
5	0.4	39	4.0	
6	0.47	47	3.4	
7	0.57	56	2.8	9
8	0.67	68	2.4	
9	1.0	100	1.6	10
10	1.47	150	1.1	
11	2.0	200	0.80	11

[a]Frequency-response position must be compatible with filter. The table indicates the recommended settings for the filter positions normally used. If noise is a problem and if the boundaries are not steep, frequency response can be set to a position higher than indicated.

Table VI. Scan-speed selector, trouble-shooting table.

Centrifuge	Scan time	Relays energized (forward)	Motor terminals energized	Relays energized (reverse)	Motor terminals energized	Relays energized (fast reverse)	Motor terminals energized
I	6 sec	RE1	C, D	RE2	E, D	RE2	E, D
I	30 sec	RE1, RE3	E, D	RE2, RE3	C, D	RE2	E, D
I	1 min	RE1	C, D	RE2	E, D	RE2	E, D
I	6 min	RE1	C, D	RE2	E, D	RE2	E, D
II	6 sec	RE4, RE6	C, D	RE5, RE6	E, D	RE5, RE6	E, D
II	30 sec	RE4	E, D	RE5	C, D	RE5, RE6	E, D
II	1 min	RE4, RE7	C, D	RE5, RE7	E, D	RE5, RE6	E, D
II	6 min	RE4	E, D	RE5	C, D	RE5, RE6	E, D

Table VII. Scan control - galvanometer displacing circuitry.

Galvanometer selector position	Function	Relay status
1	Machine I galvanometers on paper unless Machine II scanning forward	RE1 energized, RE2 de-energized. If Machine II scans, reverse is true
2	Machine II galvanometers on paper unless Machine I scanning forward	RE2 energized, RE1 de-energized. If Machine I scans, the reverse is true
1, 2	Both galvanometers on paper at all times	No relays energized.

If one wishes to bypass the galvanometer displacing circuitry he can connect Machine I "Galvanometers" (operational unit) to plug 1-6, Machine II "Galvanometers" (operational unit) to plug 7-12. Transfer galvanometers 5 and 6 to positions 7 and 8. Galvanometers become:

Machine I	G1 = Integral	G2 = Derivative
Machine II	G7 = Integral	G8 = Derivative

D. Pulse Relationships Shown by Oscilloscope Photographs

1. Two Double-Sector Cells

Oscilloscope traces indicating time relationships between outputs from the scanner, set-pulse amplifier, delay uni, one-shot, flip-flop, SW1, SW2, reference and sample holds at 20 410 rpm, sweep speed 500 μsec/ cm shown here.

a. Scanner positioned at cell images (Figs. 73–76) (See page 116).

b. Scanner positioned at radius-marker image (Figs. 77 and 78) (see page 116).

Fig. 73. Cell selector at 1; (a) scanner (b) set-pulse amplifier (c) one-shot, 5V/cm (d) flip-flop, 5V/cm (e) SW1, pin 3, 20V/cm (f) SW2, pin 3, 20V/cm.

Fig. 74. Cell selector at 2; (a) scanner (b) set-pulse amplifier (c) one-shot, 5V/cm (d) flip-flop, 5V/cm (e) SW1, pin 3, 20V/cm (f) SW2, pin 3, 20V/cm.

Fig. 75. Holding circuits, cell selector at 1 and 2; (a) scanner (b) set-pulse amplifier (c) reference hold, Cell selector at 2, 0.5 V/cm (d) sample hold, Cell selector at 2, 0.5V/cm (e) reference hold, Cell at 1, 0.5V/cm (f) sample hold, Cell at 1, 0.5V/cm. (Illustrates how the holding circuits accept alternate pulse-pairs--which pairs depends upon the cell selector position). The straight line below each hold indicates the dc output level when Baseline is depressed.

Fig. 76. Delay uni and one-shot duration versus RPM control setting; (a) scanner (b) set-pulse amplifier (c) delay uni, RPM at 8 (d) one-shot, RPM at 8 (e) delay uni, RPM at 5, (f) one-shot, RPM at 5. (The one-shot duration of (f) is too long because the centrifuge is running too slow for RPM at 5).

Fig. 77. Cell selector at 1; (a) scanner (b) set-pulse amplifier (c) one-shot, 5V/cm (d) flip-flop, 5V/cm (e) SW1, pin 3, 20V/cm (f) SW2, pin 3, 20V/cm.

Fig. 78. Cell selector at 2; (a) scanner (b) set-pulse amplifier (set-pulses disconnected) (c) one-shot, 5V/cm (d) flip-flop, 5V/cm (e) SW1, pin 3, 20V/cm (f) SW2, pin 3, 20V/cm. (The flip-flop spends more time in each state than it does in Fig. 77 because there are no set pulses).

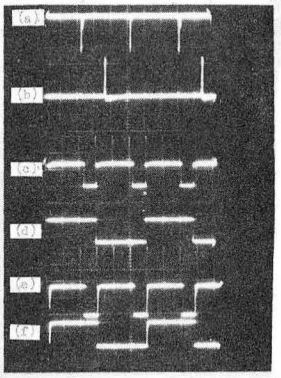

Fig. 73

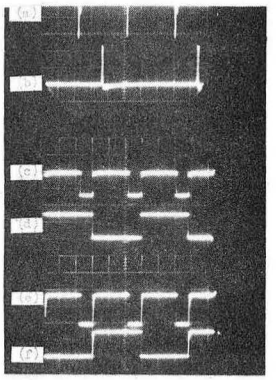

Fig. 74

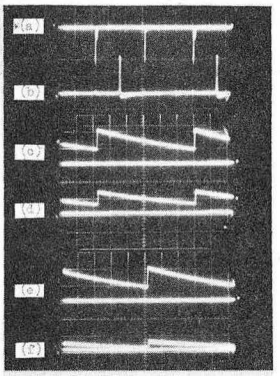

Fig. 75

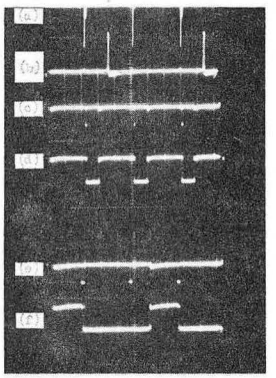

Fig. 76

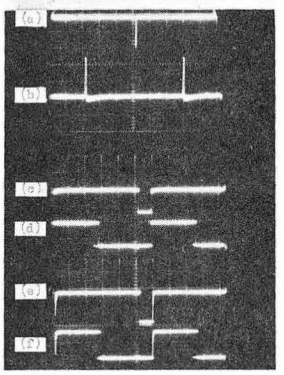

Fig. 77

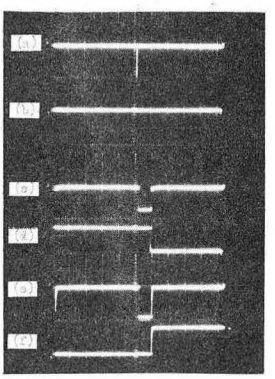

Fig. 78

ZN-4868

2. Two Single-Sector Cells

Oscilloscope traces indicating time relationships between outputs from the scanner, set-pulse and linear amplifiers, SO-1, delay uni, one-shot, flip-flop, SW1, SW2, SO-4, reference and sample holds at 20 410 rpm, oscilloscope sweep-speed at 400 μsec/cm unless otherwise indicated. Scanner positioned at cell images.

Fig. 79. One-shot, flip-flop, and holding circuits; (a) scanner (b) set-pulse amplifier (c) one-shot (d) flip-flop (e) reference hold, 0.5V/cm (f) sample hold, 0.5V/cm. The straight lines below (e) and (f) indicate the dc output level when Baseline is depressed.

Fig. 80. SW1 and SW2 waveforms; (a) scanner (b) set-pulse amplifier (c) SW1, pin 3 (d) SW1, pin 8 (e) SW2, pin 3 (f) SW2, pin 8. Vertical sensitivity is 20V/cm for SW1 and SW2 waveforms.

Fig. 81. SO-4 response to set-pulse overshoot; (a) scanner (b) set-pulse amplifier (c) scanner (d) SO-4, 10V/cm (e) scanner (f) flip-flop.

Fig. 82. Linear amplifier, SO-1, and one-shot, 10 μsec/cm; (a) scanner (b) linear amplifier (SO-1 input) (c) scanner (d) SO-1, 5V/cm (e) scanner (f) one-shot.

Fig. 83. Linear amplifier, SO-1, and delay uni, 10μsec/cm (a) scanner (b) linear amplifier (SO-1 input) (c) scanner (d) SO-1 (e) scanner (f) delay uni, RPM at 8.

Fig. 84. Delay uni versus RPM control setting, 40 μsec/cm; (a) scanner (b) delay uni, RPM at 0 or 1 (c) scanner (d) delay uni, RPM at 2 (e) scanner (f) delay uni, RPM at 3.

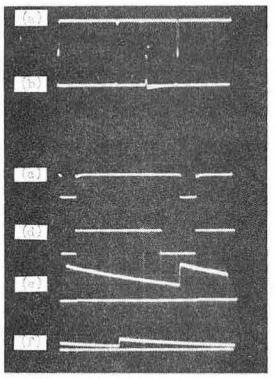

Fig. 79

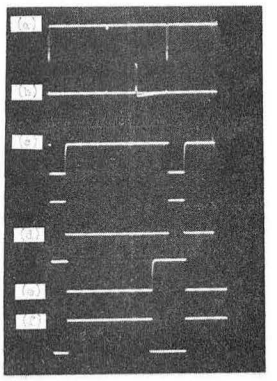

Fig. 80

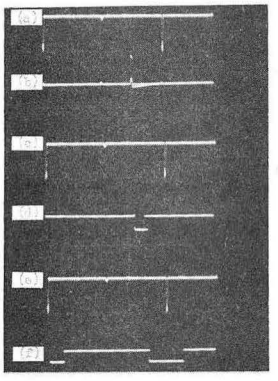

Fig. 81

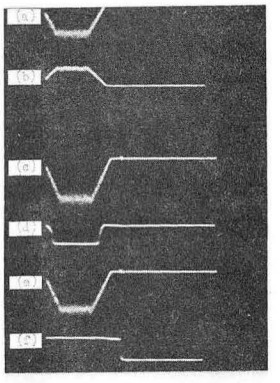

Fig. 82

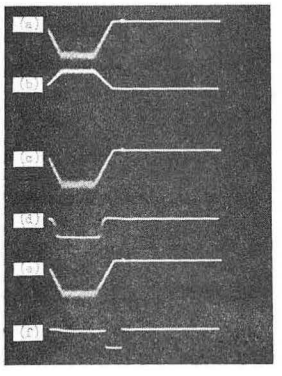

Fig. 83

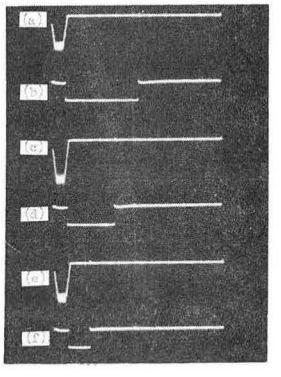

Fig. 84

ZN-4869

REFERENCES AND FOOTNOTES

1. Howard K. Schachman, Ultracentrifugation in Biochemistry (Academic Press, New York, 1959).

2. Kenneth W. Lamers, Ultracentrifuge Photoelectric Scanner, Split-Beam, UCRL-10499, 1962.

3. The slit scans the images in a radial direction with its length perpendicular to the direction of travel.

4. The secondary optical system, Schlieren type, is standard equipment for this centrifuge; it is used for diffraction-type measurements. The Schlieren optical system is displaced one-half revolution from the absorption optical system. The stationary photomultiplier could have been positioned to intercept light from part of the radius-marker image projected by the absorption system. The absorption images projected change position with wavelength (lens must be moved), however, so we chose to use the Schlieren optical system which operates at a fixed wavelength.

5. A rotary head permits selection of one of six slits. The slit dimensions presently used are (1) 0.00099 by 0.4 inch (2) 0.003 by 0.093 inch (3) 0.00133 by 0.081 inch (4) 0.00617 by 0.107 inch (5) 0.00150 by 0.4 inch (6) 0.00354 by 0.4 inch. The slit most commonly used for double-sector operation is number (2).

6. Four scanning rates are available. The image is scanned in 6, 30, 60 or 360 seconds. The scanner returns to the start position in 6 seconds unless the fast return is disabled.

7. The slit length must be shorter than the projected size of the dividing rib between sectors.

8. The cells are loaded with regard to rotation.

9. Eliahu I. Jury, Sampled Data Control Systems (John Wiley and Sons, Inc., New York, 1958), p. 48.

10. J. Millman and H. Taub, Pulse and Digital Circuits (McGraw-Hill Book Company, Inc., New York, 1956), p. 174.

11. J. Millman and H. Taub, Pulse and Digital Circuits (McGraw-Hill Book Company, Inc., New York, 1956), p. 140.

12. One gate would be adequate if the gating signal were conditioned differently. The method used was chosen for expediency.

13. A slight delay, added in order to improve pulse separation, is subject to speed.

14. We could have disconnected set pulses at the radius marker with the Cell selector at "1", also. In that event, the cell gates pass every other pulse in both cell positions (1 and 2). We chose not to disconnect set pulses in both cell positions because it is easier to determine set-pulse performance with the scanner positioned at the radius marker and with set-pulses effecting switching each and every revolution. Figure 13 indicates that the flip-flop spends equal time in each state when the scanner is positioned at the radius marker and when the cell selector is at position "2." When the cell images are being scanned, the flip-flop spends unequal time in each state (see Fig. 12).

15. The flip-flop, when operated by appropriate impulses, is more readily adaptable to different speeds.

16. Visicorder is the commercial name for a recording oscillograph, Honeywell, employing an ultraviolet beam and selfdeveloping paper. The maximum writing speed is greater than 10 000 inches per second. The galvanometers used are M100-120A with a sensitivity of 10 μA per inch and a frequency response (flat ± 5%) of 0 to 60 cps.

17. The ultracentrifuge used is manufactured by Spinco (Model E). The speed range is 600 to 67 000 rpm, which corresponds to 260 000 g's at 60 000 rpm.

18. J. Millman and H. Taub, Pulses and Digital Circuits (McGraw-Hill Book Company, Inc., New York, 1956), p. 445.

19. F. Goulding, The Series-Parallel Transistor Switch as a Linear Gate, in Instrumentation Techniques in Nuclear Pulse Analysis, National Academy of Sciences-National Research Council Publication 1184.

20. Handbook of Operational Amplifier Applications, Burr-Brown Research Corp., Tucson, Arizona, (1963), p. 57.

21. Loop gain is approximately 20.

22. Long term calibration accuracy would be improved if we monitored the linear amplifier output pulses instead of those appearing at its input. In that event, photomultiplier dynode voltage is adjusted to produce 25-V pulses to the log compressor input. Long term changes in linear amplifier gain are therefore nullified.

23. Reference mode traces are optional. If desired, we can record the difference traces only.

24. The instrument can be operated at higher densities if the photomultiplier dynode voltage is increased to produce reference pulses of greater amplitude (5V maximum). In that event, the system might become nonlinear, and calibration accuracy is less (unless recalibrated).

25. S. Hanlon, K. Lamers, G. Lauterbach, R. Johnson, and H. K. Schachman, Ultracentrifuge Studies with Absorption Optics, I. An Automatic Photoelectric Scanning Absorption System, Arch. Biochem. Biophys. 99, 175 (1962).

26. H. K. Schachman, L. Gropper, S. Hanlon, and F. Putney, Ultracentrifuge Studies with Absorption Optics, II. Incorporation of a Monochromator and its Application to the Study of Proteins and Interacting System, Arch. Biochem. Biophys. 99, 175 (1962).

27. K. Lamers, F. Putney, I. Z. Steinberg and H. K. Schachman, Ultracentrifuge Studies with Absorption Optics, III. A Split-Beam Photoelectric, Scanning Absorption System.

28. The sample is not always virus, but it will be treated as such here, for purposes of derivation.

This report was prepared as an account of Government sponsored work. Neither the United States, nor the Commission, nor any person acting on behalf of the Commission:

A. Makes any warranty or representation, expressed or implied, with respect to the accuracy, completeness, or usefulness of the information contained in this report, or that the use of any information, apparatus, method, or process disclosed in this report may not infringe privately owned rights; or

B. Assumes any liabilities with respect to the use of, or for damages resulting from the use of any information, apparatus, method, or process disclosed in this report.

As used in the above, "person acting on behalf of the Commission" includes any employee or contractor of the Commission, or employee of such contractor, to the extent that such employee or contractor of the Commission, or employee of such contractor prepares, disseminates, or provides access to, any information pursuant to his employment or contract with the Commission, or his employment with such contractor.